Classe di Scienze - Perfezionamento in Fisica

Ph.D. Thesis

A natural Higgs boson: models and phenomenology

Candidate
Andrea Tesi

Supervisor
Prof. Riccardo Barbieri

Contents

Acknowledgments

I feel I cannot settle the debts I have with Riccardo Barbieri. His constant advice, his inspiring way of asking questions and to filter the relevant information, his taste as theoretical physicist have been a unique source of inspiration to me. I thank him for all this and for the patience he showed me. I cannot do anything else than noticing that I have been lucky to have been one of his students.

I would like to thank Stefania De Curtis for having encouraged me to begin studying particle physics, for her support during, and after, my master degree and for everything she has done for me.

I thank Michele Redi, for the interesting discussions, for the infinite number of mails, for his constant support and help. I really enjoyed to collaborate with him.

Thanks to Dario Buttazzo and Filippo Sala with whom I shared the first two years of my PhD. It has been a good time discussing about physics and much more.

Thanks to all the others I collaborated with, Kristjan Kannike, Giuliano Panico, David Straub and Andrea Wulzer, from each of them I learned many and different things.

Thanks to all the people of the high energy physics group at the Scuola Normale that contributed to create a unique environment: Paolo Campli, Oleksii Matsedonskyi, David Pirtskhalava, Enrico Trincherini and Caterina Vernieri.

Finally I thank Leda.

Abstract

After a brief description of the Standard Model of Particle Physics, we introduce the Hierarchy Problem and its possible resolutions. Among several possibilities we choose two protection mechanisms that realize a Natural Fermi scale: Composite Higgs and Supersymmetry. Our aim is to consider realistic natural models for the Fermi scale and compare them with the experimental data coming (mainly) from precision measurements.

In the case of Composite Higgs, we discuss the fine tuning needed to realize a successful electro-weak symmetry breaking and accommodate a 125 GeV Higgs. Composite Higgs can naturally explain such light mass if new coloured fermions with the same quantum numbers of the top are below or at 1000 GeV. Direct searches are starting to probe the natural region of this kind of models. However, there are strong constraints on this picture coming from electro-weak and flavour tests. Although non trivially, it is possible to satisfy the bounds if appropriate representations of the composite fermions are chosen and an approximate $U(2)^3$ flavour symmetry is at work.

The Minimal Supersymmetric Standard Model (MSSM) experiences a significant fine-tuning because a 125 GeV Higgs boson is too heavy to be obtained naturally. After a brief review of the MSSM and a discussion of its Higgs sector, we consider the Next-to-Minimal Supersymmetric Standard Model (NMSSM). The NMSSM provides a 125 GeV Higgs boson with milder tuning and it also mitigates naturalness upper bounds on stops and gluinos, which start to be strongly constrained from below by direct searches. Another relevant aspect of the NMSSM is the suggestion that the lightest new particles could be the CP-even scalars of its extended Higgs sector. This possibility can be efficiently constrained from the measurements of the Higgs mass and branching ratios at LHC. In many cases the Higgs fit is an important constraint, competitive with direct searches. When these constraints are absent we outline possible strategies for future experimental searches.

We conclude with a brief summary and comment on the relative importance of electro-weak and Higgs precision measurements in the models discussed in the thesis.

This thesis is mainly based on the papers [1], [2], [3], [4], [5] and [6] published during my three years of PhD.

Part I

What we know and what we do not understand

Chapter 1

Introduction

Neglecting all the masses, Nature at short distances is invariant under $G_{\rm SM} = SU(3)_c \times SU(2)_L \times U(1)_Y$, with helicity ± 1 particles G^a_μ, W^a_μ, B_μ and couplings g_s, g, g'. Matter, in the form of spin-1/2 particles, is a set of Weyl fermions, each of them appearing in three copies (generations), classified according to their quantum numbers,

spin-1/2	$SU(3)_c$	$SU(2)_L$	$U(1)_Y$
q_L	**3**	**2**	$1/6$
u_R	**3**	**1**	$2/3$
d_R	**3**	**1**	$-1/3$
l_L	**1**	**2**	$1/2$
e_R	**1**	**1**	-1

Table 1.1. Quantum numbers of Weyl fermions in the SM.

Together, $G_{\rm SM}$ and table 1.1 define the minimal gauge lagrangian of the SM. The use of gauge-invariance can be thought of as an artefact to keep manifest locality and Lorentz invariance. Interaction vertices among spin-1 and spin-1/2 particles (and among the vectors themselves) are precisely described by this theory.

The inclusion of masses for vector bosons (and fermions) is a relevant deformation of the theory in the infra-red (IR). The massive and massless theories show two radically different behaviours. The whole difference resides in the fact that a massive vector has three degrees of freedom, while massless vectors only two. To underline the difference we can restore the gauge invariance including explicitly a scalar mode in addition to the two massless $\pm$ helicity states, by promoting the gauge parameters to scalar degrees of freedom, with their own gauge transformation. The minimal lagrangian gets an additional gauge-invariant piece,

$$\mathcal{L} \supset v^2 \mathrm{Tr}[D_\mu U (D_\mu U)^\dagger]. \tag{1.1}$$

This is a non-linear σ model of $SU(2) \times SU(2)/SU(2)$, where $U(x) = \exp i\pi^a \sigma^a / v$ is the exponentiation of the Goldstone bosons (GBs), π^a, *i.e.* the longitudinal components of the vector bosons. The very presence of a non-linear sigma model suggests that the theory undergoes a regime in which scattering amplitudes have a bad behaviour with energy. A

theory with massive weak bosons has an internal *physical* cut-off at $\sim 4\pi v$, as one can infer from $\pi\pi$ scattering.

This argument was the true theoretical motivation (a theorem in a sense) to expect new particles/dynamics before $4\pi v$: a "discovery" of something new at those energies was unavoidable. Now that a scalar resonance of mass 125 GeV has been found [7,8], thanks to the incredible efficiency of the LHC, we know that the "new physics" needed before $4\pi v$ is weakly-coupled to a high degree and it is seems nothing else than the Higgs model [9,10].

The SM is simply the minimal gauge lagrangian supplemented by the Higgs model, and it is defined by

$$\mathcal{L}_{\rm SM} = |D_\mu H|^2 + \mu^2|H|^2 - \lambda|H|^4 + (Y_u^{ij}\bar{q}_L^i u_R^j H^c + Y_d^{ij}\bar{q}_L^i d_R^j H + Y_e^{ij}\bar{l}_L^i e_R^j H + h.c.) + \text{kin. terms}, \tag{1.2}$$

where H is a $(\mathbf{1},\mathbf{2},1/2)$ under $G_{\rm SM}$. It can be conveniently parametrized as

$$H = \frac{1}{\sqrt{2}}\begin{pmatrix} \sqrt{2}\pi^+ \\ v + h + i\pi_3 \end{pmatrix}.$$

If $\mu^2, \lambda > 0$, H develops a Vacuum Expectation Value (VEV) $v^2 = \mu^2/\lambda \neq 0$, such that $\langle |H|^2 \rangle = v^2/2 \sim (174\text{ GeV})^2$, that breaks the original gauge symmetry in the desired way,

$$SU(2)_L \times U(1)_Y \xrightarrow{v} U(1)_{\rm em}. \tag{1.3}$$

This Introduction consists of two main parts reflecting the dichotomy of its title.

In the first part (sections 1.1-1.3) we describe the above lagrangian (1.2) in several limits. As it is well known one of the reasons why the SM is so successful in describing fundamental physics not only relies on its manifest global symmetries but also on its partially hidden accidental symmetries (exact or approximate). We will discuss them but also other less evident facts stemming from (1.2) in three "sectors": 1) Electro-weak sector, 2) Flavour sector, 3) Higgs sector. Of course none of them is isolated from the rest, as manifest from the leading role played by the Higgs field. Given the notorious overall success of the SM, any deformation is bounded to energies higher than those currently under experimental scrutiny. While discussing these three "sectors", we will comment on a few basic consequences derivable from present data, as an anticipation of what will be discussed in this thesis.

In the second part (sections 1.4,1.5) we introduce the Hierarchy Problem and comment on the possible solutions. We describe how the naturalness principle suggests the presence of relatively light New Physics (NP) and conclude in section 1.6 with a detailed outline of the project.

1.1 The Electro-weak sector

The scalar potential has an accidental symmetry $SU(2)_L \times SU(2)_R$ where the right-handed $SU(2)$ is manifest upon writing (1.2) in terms of the real components of H. In the vacuum it is spontaneously broken to $SU(2)_c$, its diagonal combination. If exact it would have implied a spectrum classified according to $SU(2)_c$ multiplets. $SU(2)_L \times SU(2)_R$ is explicitly broken by the hyper-charge interaction and by the SM Yukawas, while it is preserved by $SU(2)_L$

gauge interactions. The leading source of breaking is the top-bottom sector, where t_R and b_R can hardly be thought of being in the same $SU(2)_R$ doublet given the hierarchy between the top and bottom masses. At tree level $SU(2)_c$ notoriously implies degeneracy of $W^{\pm}$and Z in absence of g'.

The approximate custodial symmetry of the electro-weak sector can be systematically analysed in terms of gauge boson vacuum polarization amplitudes, which encode a large part of electro-weak effects accurately measured at LEP, not only the custodial preserving ones.

1.1.1 Oblique corrections

LEP [11] has provided electro-weak observables measured to a great accuracy and there is a common way used since early '90s to present its findings. The three parameters of the weak sector (g, g', v) can be fixed in terms of the three most precise observables α, G_F, M_Z, which are called the input parameters, all the other derived observables depend on these three quantities. The derived observables relevant to us are the Z width into leptons, asymmetries at the Z-pole and the W-mass measured at the TeVatron.

We can define three quantities [12] directly related to $\Gamma(Z \to l^+ l^-)$, A^l_{FB} (hence to the axial and vector couplings of the Z, $g_{A,V}$) and M_W

$$\Delta r = 1 - s^2 c^2 [(1 - \frac{M_W^2}{M_Z^2})\frac{M_W^2}{M_Z^2}]^{-1}, \tag{1.4}$$
$$\Delta \rho = -2(1 + 2g_A), \tag{1.5}$$
$$\Delta k = (1 - g_V/g_A)/(4s^2) - 1, \tag{1.6}$$

which are often traded, via a triangular system, for the famous ε-parameters,

$$\varepsilon_1 = \Delta\rho, \tag{1.7}$$
$$\varepsilon_2 = c^2\Delta\rho + s^2/(c^2 - s^2)\Delta r - 2s^2\Delta k, \tag{1.8}$$
$$\varepsilon_3 = c^2\Delta\rho + (c^2 - s^2)\Delta k, \tag{1.9}$$

where $c^2 = 1 - s^2$ and s is the sine of Weinberg's angle. These measurable quantities can be exactly computed as [13]

$$\begin{aligned}
\varepsilon_1 &= e_1 - e_5 - \delta G_{V,b}/G_F - 4\delta g_A, \\
\varepsilon_2 &= e_2 - s^2 e_4 - c^2 e_5 - \delta G_{A,b}/G_F - \delta g_V - 3\delta g_A, \\
\varepsilon_3 &= e_3 + c^2 e_4 - c^2 e_5 + (c^2 - s^2)/(2s^2)\delta g_V - (1 + 2s^2)/(2s^2)\delta g_A.
\end{aligned} \tag{1.10}$$

The e_i encode the so-called oblique corrections defined in terms of vacuum polarization amplitudes

$$\begin{aligned}
e_1 &= \frac{\Pi_{33}(0) - \Pi_{WW}(0)}{M_W^2}, & e_4 &= F_{\gamma\gamma}(0) - F_{\gamma\gamma}(M_Z^2), \\
e_2 &= F_{WW}(M_W^2) - F_{33}(M_Z^2), & e_5 &= M_Z^2 F'_{ZZ}(M_Z^2), \\
e_3 &= \frac{c}{s} F_{30}(M_Z^2),
\end{aligned} \tag{1.11}$$

Adimensional form factors	operators	custodial	$SU(2)_L$
$g^{-2}\widehat{S} = \Pi'_{3B}(0)$	$(H^\dagger\tau^a H)W^a_{\mu\nu}B_{\mu\nu}/gg'$	+	−
$g^{-2}M_W^2\widehat{T} = \Pi_{33}(0) - \Pi_{WW}(0)$	$\lvert H^\dagger D_\mu H\rvert^2$	−	−
$-g^{-2}\widehat{U} = \Pi'_{33}(0) - \Pi'_{WW}(0)$		−	−
$2g^{-2}M_W^{-2}V = \Pi''_{33}(0) - \Pi''_{WW}(0)$		−	−
$2g^{-1}g'^{-1}M_W^{-2}X = \Pi''_{3B}(0)$		+	−
$2g'^{-2}M_W^{-2}Y = \Pi''_{BB}(0)$	$(\partial_\rho B_{\mu\nu})^2/2g'^2$	+	+
$2g^{-2}M_W^{-2}W = \Pi''_{33}(0)$	$(D_\rho W^a_{\mu\nu})^2/2g^2$	+	+

Table 1.2. The 7 coefficients from the expansion of Π_{ij} at $O(q^4)$ as discussed in [14].

where

$$\Pi^{\mu\nu}_{ij}(q^2) = -i\eta^{\mu\nu}[\Pi_{ij}(0) + q^2 F_{ij}(q^2)] + (q^\mu q^\nu \cdots). \tag{1.12}$$

The non-oblique contributions to ε_i are box corrections to vector and axial couplings $\delta G_{V,A}$, and vertex corrections $\delta g_{V,A}$. Hence, the ε_i parameters are not vanishing in the SM and receive both oblique and direct corrections. However, as far as universal theories are considered, NP contributions always enter the above parametrization via oblique corrections.

If NP is decoupled from the weak scale, it is often sufficient to expand the above e_i at small external momenta q^2 in an effective field theory (EFT) approach. Then, an expansion up to $(q^2)^2$ of the four polarization amplitudes gives a total of 12 coefficients. Three of them are fixed in terms of the input parameters, whereas other two combinations are constrained by gauge invariance. At $O(q^4)$ a total of seven coefficients appears, see table 1.2. Each coefficient can be mapped to one or more higher dimensional operators classified according to their custodial and weak isospin quantum numbers, thus providing a useful catalogue of sources of breaking of the above symmetries, which is not manifest in (1.10).

The relations between the new physics contributions to e_i (ε_i), called Δe_i ($\Delta\varepsilon_i$), and the 7 coefficients are the following

$$\begin{aligned}
\Delta e_1 &= \widehat{T}\,, \\
\Delta e_2 &\simeq \widehat{U} - V - \frac{s^2}{c^2}W\,, \\
\Delta e_3 &\simeq \widehat{S} + \frac{X}{sc}\,,
\end{aligned}
\qquad
\begin{aligned}
\Delta e_4 &\simeq -\frac{s^2}{c^2}W - \frac{2s}{c}X - Y\,, \\
\Delta e_5 &\simeq W - 2\frac{s}{c}X + \frac{s^2}{c^2}Y,
\end{aligned}
\qquad
\begin{aligned}
\Delta\varepsilon_1 &\simeq \widehat{T} - W + 2X\frac{s}{c} - Y\frac{s^2}{c^2}, \\
\Delta\varepsilon_2 &\simeq \widehat{U} - W + 2X\frac{s}{c} - V\,, \\
\Delta\varepsilon_3 &\simeq \widehat{S} - W + \frac{X}{sc} - Y.
\end{aligned}$$

These formulae clarify the difference among the ε-parameters and the properly normalized Peskin-Takeuchi parameters $\widehat{S}, \widehat{T}, \widehat{U}$ [15] . The latter cannot be identified directly with the former for at least two reasons: 1) if the NP is not confined to sufficiently high energies the EFT expansion is meaningless; 2) even if NP is decoupled, there is no dimensional argument to expect W and Y be suppressed with respect to $\widehat{S}$ and $\widehat{T}$.

Having in mind this difference, on which we shall return later in the thesis, the latest electro-weak fit after the Higgs discovery [16] shows a remarkable agreement of the SM with

the Electro-Weak Precision Tests (EWPTs),

$$S = 0.03 \pm 0.10, \quad T = 0.05 \pm 0.12, \quad U = 0.03 \pm 0.10. \tag{1.13}$$

On the other hand the values of ε_i determined by the fit are [17]

$$\varepsilon_1 = (5.6 \pm 1.0)\ 10^{-3}, \quad \varepsilon_2 = (-7.8 \pm 0.9)\ 10^{-3}, \quad \varepsilon_3 = (5.6 \pm 0.9)\ 10^{-3}. \tag{1.14}$$

1.1.2 Electroweak sector of NP

Taking the outcome of the electro-weak fit we can try to infer some generic aspects of NP in the electro-weak sector. Working with only $\widehat{S}$ and $\widehat{T}$, keeping in mind that it is often insufficient as discussed above, we should pay particular attention to the following kind of NP: tree-level and log-enhanced 1-loop contributions.

i) Tree-level contributions to $\widehat{T}$ can arise in models with extended Higgs sectors with scalars in higher representation of $\mathrm{SU}(2)_L$ (like triplets). A tree-level contribution to $\widehat{S}$ is a robust prediction of models with additional weak bosons. A lower bound of about 3 TeV on their masses can be derived.

ii) Log-enhanced contributions arise if the Higgs couplings to vectors deviate from the SM values. In fact, from an incomplete cancellation between GBs and Higgs contribution in bosonic self-energies, we get the famous result [18]

$$S \simeq +\frac{1}{12\pi t_w^2}(1-c_V^2)\log\frac{\Lambda^2}{m_h^2} + \cdots, \quad T \simeq -\frac{3}{16\pi c_w^2}(1-c_V^2)\log\frac{\Lambda^2}{m_h^2} + \cdots, \tag{1.15}$$

where c_V is the coupling of the Higgs to vectors and Λ is the cut-off of the theory where new degrees of freedom will enter the game. The dots represent finite (Λ^0) and decoupling terms ($1/\Lambda^2$) that can be computed once the model is specified. We will consider later in the thesis the effect coming from additional Higgses coupled to the SM one. The presence of IR-logs due to the Higgs boson shows once more the interplay of the Higgs and ElectroWeak Symmetry Breaking (EWSB) sectors.

1.2 The Flavour sector

The non-trivial flavour structure of the SM arises entirely from the Yukawa sector

$$\mathcal{L}_{\rm SM} \supset Y_u^{ij}\bar{q}_L^i u_R^j H^c + Y_d^{ij}\bar{q}_L^i d_R^j H + Y_e^{ij}\bar{l}_L^i e_R^j H + h.c., \tag{1.16}$$

where we have assigned the index $i = 1, 2, 3$ to the three families in the quark and in the lepton sector. $Y_{u,d,e}^{ij}$ are generic 3×3 complex matrices for a total of 27 complex parameters. We can get rid of many of them by going to the basis defined by

$$Y_u = V^\dagger \hat{y}_u, \quad Y_d = \hat{y}_d, \quad Y_e = \hat{y}_e. \tag{1.17}$$

The following notation has been introduced:

- $\hat{y}_u = \text{diag}(y_u, y_c, y_t)$, $\hat{y}_d = \text{diag}(y_d, y_s, y_b)$ and $\hat{y}_e = \text{diag}(y_e, y_\mu, y_\tau)$, are the (real) Yukawa couplings. The fermion masses are $m_{ij} = \frac{v}{\sqrt{2}}\hat{y}_{ij}$.
- V is the Cabibbo-Kobayashi-Maskawa (CKM) matrix [19,20]. It can always be written with 3 real and 1 imaginary parameters ($\delta_{\rm KM}$).

Eq. (1.17) allows to derive many consequences for the Flavour sector of the SM. Given the large $U(3)^5$ symmetry of the fermionic kinetic terms together with the fact that only V allows for flavour transition, a few basic facts can be summarized: *i*) Individual lepton numbers are conserved, $U(1)_e \times U(1)_\mu \times U(1)_\tau$; *ii*) The total baryon number $U(1)_B$ is conserved (at the perturbative level); *iii*) Flavour Changing Neutral Currents (FCNCs) are absent at tree-level in the SM; *iv*) CP violation (CPV) is governed by the sole δ_{KM} complex phase in V [20].

A useful convention for the CKM matrix is provided by the Wolfenstein parametrization [21],

$$V = \begin{pmatrix} 1-\frac{1}{2}\lambda^2-\frac{1}{8}\lambda^4 & \lambda & A\lambda^3(\rho-i\eta) \\ -\lambda+\frac{1}{2}A^2\lambda^5[1-2(\rho+i\eta)] & 1-\frac{1}{2}\lambda^2-\frac{1}{8}\lambda^4(1+4A^2) & A\lambda^2 \\ A\lambda^3[1-(1-\frac{1}{2}\lambda^2)(\rho+i\eta)] & -A\lambda^2+\frac{1}{2}A\lambda^4[1-2(\rho+i\eta)] & 1-\frac{1}{2}A^2\lambda^4 \end{pmatrix}. \quad (1.18)$$

Experiments have shown a remarkable agreement with the CKM picture of flavour and CP violation. Very likely, the SM model Yukawa couplings are the *dominant* source of flavour and CP violations observed so far, as we are going to discuss.

1.2.1 Overall success of the CKM picture

A recent fit to CKM [22] confirms the success of the CKM picture

$$A = 0.823 \pm 0.014, \;\; \bar{\rho} = \rho(1-\lambda^2/2) = 0.142 \pm 0.020, \;\; \bar{\eta} = \eta(1-\lambda^2/2) = 0.341 \pm 0.012 \quad (1.19)$$

and the fitted value of λ is given to an excellent precision by the input $|V_{us}| = 0.2249(8)$ [23]. The inconsistency of $\bar{\eta}$ with zero shows that the mechanism of CPV is at work. Another striking success of the CKM picture is the agreement of several constraints in the famous plot of the unitarity triangle [24].

It can be shown that the CKM picture of CPV is not only at work but also dominant. A quantitative approach in order to quantify possible deviations from this picture consists in assuming that NP affects only loop observables such as $B_0 - \bar{B}_0$ mixing. For ΔB_d, NP can be parametrized as

$$h_d e^{i2\sigma_d} = \mathcal{A}_{NP}/\mathcal{A}_{SM}. \quad (1.20)$$

Fitting tree-level decays and ΔB, one can show that $\bar{\eta}$ is inconsistent with zero and $h_d \lesssim 0.2 \div 0.3$. This suggests that CKM is certainly at work but possible deviations of $20 \div 30\%$ from that picture could be possible in some scenarios of NP [22].

Flavour physics can set bounds on the scale of NP. Given the accuracy of the CKM picture, generic NP effects are likely constrained to very high scales. A very useful tool consists in equipping the SM with a tower of irrelevant $G_{\rm SM}$-invariant operators constructed with the low-energy particle content [25],

$$\mathcal{L}_{\rm eff} = \mathcal{L}_{\rm SM} + \sum_i \frac{c_i}{\Lambda^{d_i}}\mathcal{O}_i. \quad (1.21)$$

Assuming that the dimensionless coefficients c_i's have no particular structure and are $O(1)$, we can derive lower bound on the scale Λ. Observable like ϵ_K put the strongest constraint: $\Lambda_{\epsilon_K} \gtrsim 10^5$ TeV. Even removing the strongest one, several others are of the order $\Lambda \gtrsim 10^{3\div 4}$ TeV [26].

Such strong bounds on Λ can have two possible explanations. The first is that flavour violations are confined to very short distances. The second is that, if NP is present at a scale accessible to present experiments, it has to be highly non-generic. Requiring a NP scale of order TeV, these bounds reflect themselves into very small dimensionless coefficients c_i [26]. Such bounds can be relaxed only assuming a non-trivial NP structure, which makes the c_i naturally suppressed.

1.2.2 Flavour symmetries

As done for part of the observables in the electro-weak symmetry breaking sector, it is also possible to understand the mechanism of suppression of FCNCs and why the CKM picture works well in terms of approximate symmetries. Indeed, the presence of a symmetry will naturally suppress higher dimensional operators in (1.21) thanks to some selection rules, simultaneously allowing for a reduction of the NP scale Λ.

However, differently from the case of custodial symmetry, there is no unique compelling candidate for describing the absence of NP flavour effects and the hierarchy of masses and mixing of the flavour sector. Different mechanisms/symmetries are distinguished by the different way the Yukawa couplings Y_u and Y_d are thought of. Clearly when $Y_{u,d} \to 0$ a $U(3)^3$ symmetry arises from the kinetic terms. However the use of such symmetry to approximately describe the quark spectrum via a small breaking is questionable due to the largeness of y_t. Anyhow, no matter what the actual symmetry is, its role is to select a series of effective operators (in the mass basis), generally made of the following fermion bilinears

$$\bar{q}_L^i \gamma^\mu K_{LL}^{ij} q_L^j, \quad K_{LR}^{ij} \bar{q}_L^i \sigma^{\mu\nu} d_R^j. \tag{1.22}$$

Notice that in the SM only K_{LL} and K_{LR} are different from zero, while symmetries different from $U(3)^3$ can deviate from these minimal terms. It is interesting to understand what are the predictions of a few mechanisms and/or symmetries: in the rest of this section we will be discussing three of them as relevant for this thesis.

$\mathbf{U(3)^3}$

A flavour symmetry $U(3)^3$ is also called Minimal Flavour Violation (MFV), because the only source of flavour transition is V. Formally it amounts to consider Y_u and Y_d as spurions of such symmetry transforming as

$$Y_u \sim (3, 3^*, 1), \quad Y_d \sim (3, 1, 3^*). \tag{1.23}$$

In this case, the only relevant fermion bilinears are indeed the ones of (1.22) and, more specifically,

$$K_{LL}^{ij} = \xi_{ij}, \quad K_{LR}^{ij} = y_d^j \xi_{ij} \tag{1.24}$$

where

$$\xi_{ij} = V_{ti}^* V_{tj}. \tag{1.25}$$

Notice that eq.s (1.22)-(1.24) are the ingredients of Flavour Violation in the SM itself. MFV predicts correlated effects in $b \to s$, $b \to d$ and $s \to d$ both in $\Delta F = 2$ and $\Delta F = 1$ amplitudes and possible new sources of CPV in $\Delta F = 1$ chirality breaking operators.

$\mathbf{U(2)^3}$

As already discussed, $y_t \simeq 1$ can hardly be thought of as a small parameter. A better motivated approximate symmetry of the quark spectrum is $U(2)^3$ acting on the two lightest generations and minimally broken [27, 28]. The spurions of are

$$\Delta Y_u \sim (2, 2^*, 1), \Delta Y_d \sim (2, 1, 2^*), \boldsymbol{V} \sim (2, 1, 1), \tag{1.26}$$

which give rise to the following Yukawas,

$$Y_u = y_t \left(\begin{array}{c|c} \Delta Y_u & x_t \boldsymbol{V} \\ \hline 0 & 1 \end{array}\right), \quad Y_u = y_b \left(\begin{array}{c|c} \Delta Y_d & x_b \boldsymbol{V} \\ \hline 0 & 1 \end{array}\right). \tag{1.27}$$

$\Delta Y_u, \Delta Y_d$ are the analogues of Y_u, Y_d in the first two generation sector, whereas $\mathbf{V}$ is the minimal way to describe the communication of the 1-2 generations with the third one, while keeping the breaking of $U(2)^3$ at a few 10^{-2} level. Eq. (1.22) in the $U(2)^3$ case has the same suppression of ξ_{ij} of MFV but new phases can appear. As an example

$$K_{LL}^{ij} = (c_B \delta_{j3} + c_K \delta_{j2}) e^{i\phi_B \delta_{j3}} \xi_{ij}, \tag{1.28}$$

where c_K and c_B are real and of similar order. In this framework some relevant predictions are

i) correlated effects in $\Delta B = 2$ with a possible new source of CPV. Differently from MFV, $\Delta B = 2$ and $\Delta S = 2$ are not correlated, with the latter aligned in phase with the SM.

ii) Correlated effects in $\Delta B = 1$ with a possible new phase, both in chirality breaking and conserving operators, and $\Delta S = 1$ uncorrelated.

The virtues of $U(2)^3$ are several. As shown in [22, 28], this symmetry can reconcile a NP scale close to the weak scale in a natural way: the scale Λ can be as light as ~ 3 TeV, with $c_i \sim .2 \div 1$. Moreover, treating differently the first two generations and the third one, it works closer to the hierarchy in the quark masses and mixings than MFV.

Anarchy

The anarchic paradigm assumes that the Yukawas are $O(1)$ structureless matrices, Y_*, suppressed by small parameters, whose hierarchy can reproduce both masses and mixings,

$$Y_{u,d}^{ij} = \epsilon_L^i Y_* \epsilon_{Ru,d}^j. \tag{1.29}$$

The fact that Anarchy is in the section of Flavour symmetries is explained by noticing that it acts as a $U(1)^9 = U(1)_{q_i, u_i, d_i}$ symmetry with ϵ_i playing the role of spurions. This leaves

aside the breaking of $U(1)^9$ by Y_*, necessary to avoid that only one generation peaks up a mass. Assuming a hierarchical structure of the ϵ_i one can reproduce the CKM matrix with

$$V_{ij} \sim \epsilon_L^i/\epsilon_L^j, \quad i<j. \tag{1.30}$$

The main consequences of Flavour anarchy is that beside K_{LL}, K_{LR}, which are almost MFV-like but with new complex phases, one expects the presence of the K_{RR}^{ij} structure absent in the SM, most notably

$$\frac{O(1)}{\epsilon_{L3}^2}\frac{y_{d_i}y_{d_j}}{\xi_{ij}}\bar{d}_R^i\gamma^\mu d_R^j, \tag{1.31}$$

which, contracted with K_{LL} in eq.s (1.22) and (1.24), gives a large contribution to the Kaon system.

1.3 The Higgs sector

While the Higgs mass cannot be predicted within the SM, its couplings to matter are uniquely determined. We can ask if the data from LHC7-8 can already constraint such values. In order to do that it is useful to slightly modify the SM Higgs lagrangian to take into account possible deviations,

$$\mathcal{L} \supset 2m_W^2\, W_\mu^+ W^{-\mu} c_W \frac{h}{v} + m_Z^2\, Z_\mu Z^\mu c_Z\, \frac{h}{v} - \sum_{\psi=u,d,l} m_\psi\, \bar{\psi}\psi c_\psi \frac{h}{v}. \tag{1.32}$$

The SM Higgs boson has all the coefficients c_i equal to one. A fit to $c_V = c_W = c_Z$ and $c_f = c_u = c_d = c_l$ suggests that $|c_V - 1| \lesssim 15\%$, while $|c_f - 1| \lesssim 25\%$ at 95%CL [29, 30]. The main observables are the rates $\mu_{i\to j}$ normalized to SM,

$$\mu_{i\to j} = \frac{\sigma(i\to h)\mathrm{BR}(h\to j)}{\sigma(i\to h)_{\mathrm{SM}}\mathrm{BR}(h\to j)|_{\mathrm{SM}}}. \tag{1.33}$$

The initial state depends on the production mechanism. The most relevant channel for a 125 GeV Higgs boson is gluon fusion. Final states can be $WW^*, ZZ^*, b\bar{b}, \tau^+\tau^-$ and $\gamma\gamma$. Assuming no NP in loops implies that gluon fusion and $h\to\gamma\gamma$ are indirect probes of the $ht\bar{t}$ coupling.

1.3.1 The Higgs boson and Perturbativity

The check of perturbativity of scattering amplitudes is often the right place to test a given theory and consequently to look for NP. It should be stressed that the loss of perturbativity is not by itself an inconsistency of the theory, as quantum field theory exists even in the non-perturbative regime. However, in many cases the potential loss of perturbativity pointed to the existence of NP. Ancestors of the SM like the Fermi theory of β-decay and old-Intermediate Vector Boson theory were known to be valid up to m_Z and $4\pi v$ respectively simply by looking at amplitudes with a bad behaviour at high energy. We can try to apply the same argument to the (elastic) scattering of GBs (longitudinal component of W's) and also to $hh\to hh$ scattering.

Deviations from standard couplings to matter

Using the lagrangian (1.32) to compute $\pi\pi$ elastic scattering we get

$$\mathcal{A}(\pi\pi \to \pi\pi) \simeq \frac{E^2}{v^2}(1-c_V^2) + O((\frac{E}{v})^0, (\frac{v}{E})^2). \tag{1.34}$$

Any deviation of c_V from unity will induce a physical cut-off of order $\sim 4\pi v/\sqrt{1-c_V^2}$. We have already discussed that a bound related to EWPTs appears if $c_V \neq 1$ (1.15), as expected from the appearance of a strongly coupled regime. This inconsistency of the model (1.32) when extrapolated to higher energy can be addressed in two ways:

- The theory becomes strongly coupled at $E \sim 4\pi v/\sqrt{1-c_V^2}$.
- Additional particles appear before the cut-off. In this case (1.32) is no more appropriate. Very likely this kind of UV completion is an extended (renormalizable) Higgs sector. In this case a sum rule $\sum_i c_{V_i}^2 = 1$, extended to all scalar particles coupled to vectors, forces to vanish all the energy-growing terms in $\pi\pi$ elastic scattering (see e.g. [31] for the impact of the finite term). Moreover, the constraint coming from (1.15) can be quite easily satisfied.

The last realization, *i.e.* the appearance of *more than one* Higgs, even as replicas of the SM Higgs sector, deserves the highest attention. There are no strong motivations to stick to the minimal case with only one Higgs, and partial difficulties induced by the presence of extra scalars can be controlled. We shall return to this point later in this thesis.

The role of $m_h = 125$ GeV

There is an upper bound on the quartic coupling λ coming from the request of perturbativity. This translates to $m_h < 180$ GeV, if we require perturbativity up to $M_{\rm Pl} \sim 10^{19}$ GeV.

A lower bound comes from the request of vacuum stability. Refined calculations including uncertainties on Higgs and top mass show that $m_h = 125$ GeV destabilizes the potential (*i.e.* negative quartic) at large scales, even close to Planckian energies, as shown in [32], although with a large uncertainty.

The actual value of the Higgs mass lies in the window which satisfies both lower and upper limits, with a slight preference for meta-stability [32]. Hence we cannot infer from this argument any relatively close NP threshold. However, at energies comparable to $M_{\rm Pl}$ non-renormalizable gravitational interactions suppressed by $G_N = 1/M_{\rm Pl}^2$ can turn relevant. The exchange of a graviton, coupled through $\sim h_{\mu\nu}T^{\mu\nu}/M_{\rm Pl}$, will spoil unitarization of $hh \to hh$ scattering by terms of order $\mathcal{A} \simeq E^2/M_{\rm Pl}^2$. Hence at $E \sim M_{\rm Pl}$ it is likely that NP will enter the game.

1.4 Hierarchy Problem

Fundamental Physics is solidly based on the Standard Model of particle physics as the experiments carried out in the last decades have confirmed to an increasing accuracy, as

summarized in the previous sections. This, however, should not let the reader think that there are no open issues, both experimental and theoretical.

Indeed a series of possible manifestations of New Physics is easily derived from few basic facts.

1. **Neutrino masses**. Neutrino oscillations imply massive neutrinos.

2. **Strong CP problem**. Besides the complex phases in V, the SM lagrangian can be extended with a renormalizable CP-odd operator,

$$\frac{\theta}{16\pi^2}\epsilon^{\mu\nu\rho\sigma}G^a_{\mu\nu}G^a_{\rho\sigma}, \tag{1.35}$$

   which has physical effects in spite of being a total divergence. In fact, the neutron electric dipole moment bounds the coefficient of this operator to be extremely small, $\theta < 10^{-10}$. Why is it so small? This could be explained by axions.

3. **Baryon asymmetry**. Barring asymmetric and very peculiar initial conditions, the observed asymmetry between baryons and anti-baryons can not be explained by the sole SM. The SM does not completely satisfy at least two of the three Sakharov conditions [33] necessary for baryogenesis: the size of CPV in the SM is too small and the ElectroWeak phase transition (which is a cross-over, rather than first order, given the actual Higgs mass) cannot provide an efficient departure from thermal equilibrium.

4. **Dark Matter**. If it is a particle, none of the SM ones could play this role.

5. **Charge quantization**. Within the SM we cannot explain why $|Q_e + Q_p| < 10^{-21}$, that is why the electric charges of electron and proton are equal and opposite.

6. **Landau pole of hyper-charge**. $U(1)_Y$ is not asymptotically free. This is an established signal for NP. However the Landau pole appears at $\Lambda_Y \sim m_W e^{1/\alpha} \gg M_{\rm Pl}$, which may confine this aspect to a purely academic problem. Given that gravitational effects become strong many orders of magnitude before Λ_Y, NP should be already at work well before Λ_Y.

* * *

It looks difficult to explain why particle physicists strongly expect the (abundant) presence of NP near the TeV scale, even if none of the possible new phenomena in the previous list is strictly correlated to this scale. This common expectation is related to a possible solution of the so-called *Hierarchy Problem*.

At the risk of simplifying too much, the Hierarchy Problem derives from the question: why is m_h^2 so much smaller than $M_{\rm Pl}^2$? A related question could be why we do not care of the even greater smallness of $\Lambda_{\rm QCD}$ relative to $M_{\rm Pl}$. In the latter case we *know* that $\Lambda_{\rm QCD}$ is exponentially suppressed from UV scale by dimensional transmutation, making $\Lambda_{\rm QCD}$ naturally much smaller than $M_{\rm Pl}$, whereas in the former we simply *do not know* why there is that hierarchy.

In fact we would have expected a different situation. In any effective field theory (EFT) valid up to some scale Λ, where new particles show up, scalar masses are of the order $O(1)\Lambda$, unless some specific mechanism protects them. Differently from chiral fermions or gauge fields, scalars, by themselves, do not have any particular symmetry that keeps their mass small (or even zero). In the SM, given that $M_{\rm Pl}$ is likely to represent such a scale, the Higgs mass is expected to be $m_h^2 \sim M_{\rm Pl}^2$.

To make the previous statement more concrete, the following example could be useful.

1.4.1 Scalar masses and Effective Field Theory

Let us consider a toy-model with two mass scales,

$$\mathcal{L} = \frac{1}{2}(\partial\varphi)^2 - \frac{1}{2}m^2\varphi^2 + \bar{\psi}i\partial\psi - M_\psi\bar{\psi}\psi - y\varphi\bar{\psi}\psi \tag{1.36}$$

and suppose masses are hierarchical, $m \ll M_\psi$. Integrating-out the massive fermion from the UV theory (1.36), we get an IR-theory with just one scalar field. Given the approximate Z_2-symmetry of the UV theory, only broken by the Yukawa coupling y, the IR can be thought of as a quasi-free theory (interaction terms φ^n are suppressed by y^n).

The two theories describe the same low energy physics as long as the parameters are matched order by order in the perturbative expansion. For our purpose, we shall consider only the 1-loop matching of the 2-point function. As discussed in [34,35] it is better to work in a mass independent scheme such as $\overline{\rm MS}$. From the UV theory we get

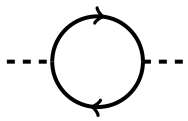

$$\Big|_{\overline{\rm MS}} = -i\frac{4y^2}{16\pi^2}M_\psi^2\left(1 - 3\int_0^1 dx\log\frac{D}{\mu^2}\right) + i\frac{4y^2}{16\pi^2}p^2\int_0^1 dx x(1-x)\left(1 - 3\log\frac{D}{\mu^2}\right),$$

where $D = M_\psi^2 - x(1-x)p^2$. The presence of large-logarithms, $\log M_\psi^2/\mu^2$, and the non-decoupling limit of the $\overline{\rm MS}$ scheme are automatically cured by the EFT approach, as the boundary $\mu = M_\psi$ distinguishes between the two theories with and without the fermion.

The IR theory is approximatively free (no running of the mass). Matching the two theories at the boundary $\mu = M_\psi$ (after an expansion in momenta of the 1-loop ampitude) we get a large matching correction,

$$m^2(\mu = M_\psi) = m^2 + \frac{4y^2}{16\pi^2}M_\psi^2. \tag{1.37}$$

This very equation is at the basis of the Hierarchy Problem. It would be highly unnatural to have a mass much lighter that M_ψ, as this can happen only for a special, although perfectly defined, cancellation between the $\overline{\rm MS}$ mass parameter $m^2(M_\psi)$ and the 1-loop matching correction, the relative accuracy being

$$\Delta^{-1} = \frac{4\pi^2}{y^2}\frac{m^2}{M_\psi^2}. \tag{1.38}$$

This explains that in EFT scalar masses are naturally of order of the cut-off scale. Several examples can be studied, the case of two scalars, together with the one presented here, is discussed for instance in [35].

In the case of fermions, we never experience fine-tuning in renormalized mass terms. This can be traced back to the chiral symmetry, which implies that quantum corrections to fermion masses are always proportional to the bare mass parameter, *i.e.* quantum corrections are multiplicative rather than additive.

What has been shown in this subsection can be summarized as follows. *In an EFT a relevant operator which is a global singlet of the theory, has its dimensionful coefficient of the order of the cut-off of the EFT.*

1.4.2 Tuning in the SM

The SM seen in isolation is clearly free from any fine-tuning, the top mass being the highest threshold. However, nobody can really defend the absence of the fine tuning problem when Gravity is taken into consideration. The non-renormalizable nature of Gravity strongly suggests that the ultimate cut-off of the SM be $M_{\rm Pl}$. Above this threshold, very likely new degrees of freedom appear to UV complete GR and they will affect the Higgs mass through radiative corrections,

$$\delta m_h^2 \sim M_{\rm Pl}^2. \tag{1.39}$$

If we quantify the fine-tuning as $\Delta = \delta m_h^2/m_h^2$, we learn that the SM has a tuning of 10^{32}. This is the precision to which we have to know the initial condition at M_{Pl} to end up at low energy with the observed m_h.

Comment on quadratic divergences

In all the discussion we tried to avoid any mention to the "problem" of quadratic divergences. It is known that if we regulate with an hard momentum cut-off Λ the top-loop we have

$\delta m_h^2 \sim$ 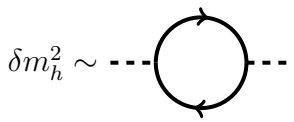 $\sim \frac{3y_t^2}{4\pi^2}\Lambda^2.$

As summarized by eq. (1.37), mass thresholds are the real sources of the Hierarchy Problem. Nonetheless, quadratic divergences roughly give the same estimate of fine-tuning if Λ is considered as a particle mass, coupled to the Higgs with unit strength $y_t \sim 1$. It is true that quadratic divergences are unphysical (indeed vanishing in dimensional regularization), but they are not meaningless.

In fact, the presence of power divergences in the computation of a given observable tell us that that quantity is *not calculable* in the theory under consideration, because too much sensitive to what is going on in the UV. From this perspective, power divergences become extremely useful, as they can give us a suggestion of what can be done to remove the UV-sensitivity. As an example of this, let us compute the Coleman-Weinberg 1-loop effective potential [36] for a scalar h in a theory with massive particles,

$$V_{\rm eff}(h) = \text{const.} + \frac{\Lambda^2}{32\pi^2}\text{STr}M(h)^2 + \frac{1}{64\pi^2}\text{STr}\left[M(h)^4 \log\frac{M(h)^2}{\Lambda^2}\right], \tag{1.40}$$

where $M^2(h)$ is the squared mass matrix and the super-trace is taken over all the indices. This expression, on which we shall return, suggests that the spectrum of particles *coupled to the Higgs* is essential in screening the UV-sensitivity of the Higgs mass term.

More in detail, the way the particle spectrum screens UV sensitivity consists in making $\mathrm{STr}M(h)^2$ a constant independent of h. The case where this constant is zero is related to Supersymmetry, but in general the constant does not need to be vanishing.

Comment on the Cosmological Constant

An even more relevant operator is the trivial one: a constant Λ^4. Such cosmological constant term is known to be experimentally very small if compared to particle physics thresholds: $\Lambda_{cc}^4 \simeq (1 \text{ meV})^4$. The tuning experienced in this case is $10^{120} \simeq M_{\rm Pl}^4/\Lambda_{cc}^4$! Given that models that aim to solve the Cosmological Constant problem are often modifications of General Relativity (at least at large distances), we are not going to discuss anymore this problem.

1.4.3 Possible solutions of the Hierarchy Problem

There is a finite number of "solutions" of the Hierarchy Problem, here ordered according to our taste.

- **Natural Fermi scale**. Here we make the assumption that there is some protection mechanism for the Higgs mass, which screens its sensitivity to Planckian scales or to any other existing high energy threshold, no matter what they are.

  It means that at some scale $\Lambda_{\rm NP}$ new symmetries and/or new dynamics occur, such that

  $$\delta m_h^2 \sim \#\Lambda_{\rm NP}^2 + \cdots \tag{1.41}$$

  from which we can derive a natural upper bound on $\Lambda_{\rm NP}$, if we require that quantum corrections to m_h^2 do not exceed the physical value by a factor $\Delta \equiv \delta m_h^2/m_h^2$,

  $$\Lambda_{\rm NP} \lesssim 450 \text{ GeV}\sqrt{\Delta}. \tag{1.42}$$

  In this scenario we can compute low-energy observables just neglecting what is going on at very high energies. A situation which is always welcome in physics and up to now realized in many different circumstances.

- **Physical Naturalness**. Here we make some assumptions on UV physics. We have to assume that gravity can be UV completed without new particles and does not affect the Higgs mass. Moreover, one has to specify the physics at *any* scale in order to explain the actual Higgs mass as a consequence of any possible threshold encountered along the way [37]. In this picture one can then apply Naturalness to constrain NP suggested by experiments (neutrino masses, dark matter, etc.), and likely it will be again near the TeV scale (or higher if its coupling to the Higgs boson is sufficiently small). At last, also the Landau pole of hyper-charge has to be avoided. To find a model that fulfils all these aspects seems an hard task.

- **Anthropic principles**. Applied to $\Lambda_{c.c.}$, the anthropic principle explains that it is close to a critical value above which galaxy formation cannot occur [38, 39]. If applied to the SM, it suggests that the weak parameter v is close to the upper bound $\sim 5v$, beyond which atoms cannot be formed [40]. The problem is how to verify/falsify this idea.

1.5 Naturalness from symmetries

The aim of this thesis is to present realistic scenarios where the Higgs mass is naturally light thanks to some symmetry argument. The use of a symmetry to realize a protection mechanism for m_h seems a more robust approach than considering dynamical assumptions to keep m_h light. Notoriously, at least two symmetries can play this role:

- **Shift symmetry - Composite Higgs Models** (CHM). A shift symmetry of the Higgs field, $h \to h + \text{const.}$, provides a theory of a massless scalar with only derivative interactions. The vanishing of the scalar potential is ensured by the Goldstone theorem to all order in perturbation theory. This scenario also assumes that the Higgs is part of a strong/composite sector. The UV-sensitivity of the Higgs is thus screened by the compositeness scale even when the shift symmetry is necessarily broken by the Higgs couplings. This kind of modesl goes under the name of Composite Higgs Model.

- **Supersymmetry** (SUSY). In its simplest realization it implies the existence of pairs of fermions and bosons degenerate in mass with highly constrained interactions. We will reserve a more detailed illustration of its principles later in the thesis. Roughly speaking, SUSY attaches a "notion of chirality" also to scalar fields, thus obtaining multiplicative renormalization of their masses.

As long as these two symmetries are exact, the Higgs mass receives quantum corrections proportional to its bare mass (it remains zero in the case of shift symmetry). Of course these cannot be exact symmetries of Nature. There will be a scale $m_{\rm NP}$ where the symmetry is broken: this can be the scale of SUSY breaking or the compositeness scale. The breaking will spoil the multiplicative renormalization leading to quantum corrections of the order

$$\delta m_h^2 \sim c \cdot m_{\rm NP}^2 + \cdots \tag{1.43}$$

from which we can derive a natural upper bound in the same way of eq. (1.42), pointing to a NP testable at current experiments. The coefficient c takes different forms in different models. However, even without entering specific model building, some of its generic aspects can be discussed. Given that we are considering quantum corrections, the parametric form of c is

$$c = \frac{N_c y_t^2}{4\pi^2} F(\Lambda_{\rm UV}, m_{\rm NP}). \tag{1.44}$$

The presence of the colour factor and the Yukawa coupling is easily understood: the largest SM coupling will give the biggest radiative contribution, showing that naively it is the NP associated to the top that controls the naturalness of the weak scale. The function

$F(\Lambda_{\rm UV}, m_{\rm NP})$ represents the sensitivity to the UV physics of the models so extended: the invoked protection mechanism would like to minimize it. As evident from (1.40)

$$F(\Lambda_{\rm UV}, m_{\rm NP}) = a_1 \frac{\Lambda^2_{\rm UV}}{m^2_{\rm NP}} + a_2 \log \frac{\Lambda^2_{\rm UV}}{m^2_{\rm NP}} + a_3 + O(\frac{m^2_{\rm NP}}{\Lambda^2_{\rm UV}}). \tag{1.45}$$

SUSY and CHM differ in the way the screening is achieved: in terms of the above (1.45) they differ by the values of the coefficients a_i, in principle of $O(1)$. Clearly they both have vanishing a_1, however in standard supersymmetric models the coefficient a_2 is non-zero while in Composite Higgs it is practically zero. The physical interpretation of $\Lambda_{\rm UV}$ in SUSY coincides with the scale of mediation of the supersymmetry breaking (it could be $M_{\rm Pl}$ in the case of gravity mediation). In Composite Higgs, there are models where $a_2 = 0$ as we will discuss in the following, but in general even if it differs from zero, the size of the log is always small due to the closeness of $m_{\rm NP}$ to the scale where the theory is strongly coupled.

The above discussion is correlated to the crucial difference between SUSY and Composite Higgs: the first being a weakly-coupled, the second a strongly-coupled extension of the SM. The size of the coupling of NP has also a dramatic impact on the phenomenology and not only on the way the naturalness of the weak scale is achieved. Moreover, the discussion of the robustness of the SM against any deformation, as discussed above, naively suggests that it will not be easy to obtain natural and viable models.

1.6 Content of the thesis

In this thesis we consider natural models in the SUSY and Composite Higgs frameworks. We will show models emerge that look capable to satisfy any low-energy constraint and to provide interesting signatures for the second run of the LHC.

In the first part we will discuss Composite Higgs as a paradigm of strongly-coupled new physics. In particular:

- In chapter 2 we will give a general overview of Composite Higgs models and we discuss the tuning and the expected value of Higgs mass. Chapter 2 is mainly based on [1, 2].
- In chapter 3 we address the issue of the compatibility of Composite Higgs models with electro-weak and flavour tests. Chapter 3 is based on [3].

The second part we will be devoted to SUSY. In particular:

- In chapter 4 we discuss general aspects of the Minimal Supersymmetric Standard Model with a focus on Natural SUSY. The original part of this chapter is mainly based on [4]
- In chapter 5 we will discuss how the LHC data on the Higgs boson constrain the Higgs sector of the Next-to-Minimal Supersymmetric Standard Model. Chapter 5 relies on [4, 5].

In the end

- In chapter 6 we will make a comparison of precision measurements, also arguing what could be the impact of future measurements of Higgs couplings and electro-weak observables on explicit models. This chapter is based on [6].

Part II

Strongly coupled New Physics

Chapter 2

Composite Higgs and $m_h = 125$ GeV

In this chapter we are going to introduce the main assumptions and the general picture of composite Higgs models. After a brief introduction to the basic assumptions in section 2.1-2.2, we comment about the possibility to obtain $m_h = 125$ GeV with mild tuning in section 2.3. In the end of the chapter an explicit model is introduced to show with a concrete example the main features of natural composite models.

2.1 Composite Higgs: general picture

We assume the presence of a new strongly interacting sector near the TeV scale. It experiences a spontaneous symmetry breaking G/H at a scale f, and the Goldstone bosons (GBs) of this breaking are exactly massless excitations of the strong sector. Our aim is to have among them at least an SU(2) doublet H that can be identified as the composite Higgs boson. At this level G/H completely determines the low-energy effective theory.

Assuming that the unknown underlying theory which produces the effective strong coupling has a large-N behaviour, we can expect an infinite tower of composite resonances both of spin-1/2 and spin-1, related to conserved operators of the strong sector. Then the strong sector is characterized by a compositeness scale $m_\rho \sim g_\rho f$ set by the lightest resonances, with possibly $g_\rho \sim 4\pi/\sqrt{N}$. Solving the Hierarchy Problem calls for $m_\rho \sim$ TeV. Then in the limit where $G_{\rm SM}$ is switched off, the spectrum is made of massless GBs and massive resonances.

The Higgs mass and its interactions require that it is a pseudo-GB (pGB). Weak couplings break explicitly G/H down to $G_{\rm SM}$. At quantum level $V(h) \neq 0$ and electro-weak symmetry breaking (EWSB) can occur. As a rough estimate,

$$\delta m_h^2 \sim \frac{3y_t^2}{16\pi^2} m_\rho^2 \tag{2.1}$$

thus naturally explaining the smallness of m_h with respect to the TeV scale. This very idea goes back to the 80's [41, 42], but it has received the greatest attention only in the last decade. The entire set-up is deeply inspired by the case of the electromagnetic splitting of pions in low-energy QCD, where similarly to (2.1), and keeping the same notation for the vector boson mass

$$m_{\pi^\pm}^2 - m_{\pi_0}^2 \simeq \frac{3\alpha_{\rm QED}}{4\pi} m_\rho^2. \tag{2.2}$$

2.2 Minimal Composite Higgs

In the previous section we did not specify any particular symmetry structure G/H. As already anticipated, the low-energy lagrangian (below m_ρ) is fixed by G/H. The standard procedure [43,44] amounts to construct the lagrangian with the field $\Pi = \pi^a T^a$ belonging to the broken part of the Lie Algebra. Through an exponentiation,

$$U(\Pi) = \exp \frac{i\Pi}{f}, \tag{2.3}$$

and a projection onto broken, T^a, and unbroken, T^i, generators $U^\dagger \partial_\mu U = i d^a_\mu T^a + i E^i_\mu T^i$, we get the non-linear σ-model

$$\mathcal{L} \sim \frac{f^2}{2} d^a_\mu d^\mu_a, \tag{2.4}$$

non-linearly invariant under G.

However, we will restrict our choice to a single, specific, coset space, that delivers only one physical scalar which will be identified as the (composite) Higgs boson. The symmetry is SO(5)/SO(4) [45], which defines the Minimal Composite Higgs Model (MCHM). This coset has many virtues, the most important of which is that the strong dynamics responsible for the breaking SO(5)→ SO(4) respects the same SO(4) symmetry of the SM scalar potential, thus preserving from large contributions the $\widehat{T}$ parameter.

The breaking can be realized with a uni-modular five-plet Σ. In the basis of Ref. [45] this implies

$$\Sigma^t = \frac{s_h}{h}(h_1, h_2, h_3, h_4, h \cot_h), \quad h \equiv \sqrt{h_i h_i}, \tag{2.5}$$

where $s_h = \sin(h/f)$. The lagrangian of the low-energy σ-model is

$$\mathcal{L} = \frac{f^2}{2}(D_\mu \Sigma)^2 + \text{ (Yukawa interactions)}. \tag{2.6}$$

From the action of SM gauge fields on Σ one can establish a useful relation. When EWSB occurs, $h \to \langle h \rangle + h$ and the vector mass is $m_V^2 = g_V^2 f^2 s_h^2/4$. This gives the relation

$$\xi \;=\; \left(\frac{v}{f}\right)^2 \;=\; \sin^2 \frac{\langle h \rangle}{f}. \tag{2.7}$$

Interestingly ξ controls the deviations from the SM Higgs couplings. For example c_V of (1.32) is now $c_V = \sqrt{1-\xi}$. The suppression of the couplings of the Higgs is related to its GB nature. To satisfy the EWPT, $f \gtrsim 700$ GeV is a phenomenological viable scale (see sections 1.1). It can be shown that all the Higgs couplings to fermions (1.32) are $\delta c_f \sim O(\xi)$. However, to compute their actual values, we need to know something about the strong sector.

2.2.1 Parametrizing the strong sector

In order to discuss the implications of the above scenario we need a parametrization of the dynamics of the strong sector, which in the MCHM consists in a light scalar particle and

massive resonances. As already anticipated the strong sector can be characterized by one scale of confinement, m_ρ, corresponding to the lightest vector resonance, and one coupling g_ρ [46], related by the decay constant of the pNGB Higgs,

$$m_\rho = g_\rho f. \tag{2.8}$$

As discussed in section 1.1, spin-1 particles generally contribute at tree-level to the S parameter and for this reason their mass is constrained to the multi-TeV range, $m_\rho \gtrsim 3$ TeV. Given the symmetry of the strong sector, composite spin-1 particles in the adjont of SO(5) decompose under SO(4) and SU(2) $\times$ SU(2) as $\mathbf{10} = \mathbf{6} + \mathbf{4} = (\mathbf{3},\mathbf{1}) + (\mathbf{1},\mathbf{3}) + (\mathbf{2},\mathbf{2})$.

In general we denote the typical mass of spin-1/2 by m_ψ and the associated coupling g_ψ is defined by

$$m_\psi = g_\psi f\,. \tag{2.9}$$

This coupling can be thought of as the strength of the interaction between pGB Higgs and composite fermions in a very similar way to g_ρ.

The representations of the composite fermions add extra model-dependence. Possible SO(5) representations and their reduction under SO(4) and SU(2) $\times$ SU(2) are

$$\begin{aligned}
\mathbf{4} &= \mathbf{4} = (\mathbf{2},\mathbf{1}) + (\mathbf{1},\mathbf{2}),\\
\mathbf{5} &= \mathbf{4} + \mathbf{1} = (\mathbf{2},\mathbf{2}) + (\mathbf{1},\mathbf{1}),\\
\mathbf{10} &= \mathbf{6} + \mathbf{4} = (\mathbf{3},\mathbf{1}) + (\mathbf{1},\mathbf{3}) + (\mathbf{2},\mathbf{2}),\\
\mathbf{14} &= \mathbf{9} + \mathbf{4} + \mathbf{1} = (\mathbf{3},\mathbf{3}) + (\mathbf{2},\mathbf{2}) + (\mathbf{1},\mathbf{1}).
\end{aligned} \tag{2.10}$$

Each of them defines a different version of MCHM, denoted by $\text{MCHM}_{4,5,10,14}$ [45, 47, 48].

2.2.2 Partial compositeness

In order to complete the description we need the last ingredient: the pattern of breaking of G/H by $G_{\rm SM}$. The SM gauge bosons are introduced as elementary fields, external to the strong sector, and gauge the SM subgroup of SO(5). Notice that in order to accommodate the correct fermion hyper-charges, an extra $U(1)_X$ global symmetry is needed. The presence of this extra symmetry does not modify the general discussion. As such, the SM gauge bosons are coupled linearly to the corresponding currents and the elementary-composite gauge interactions take the form

$$\mathcal{L}_{gauge} = g\, W_\mu J^\mu\,. \tag{2.11}$$

The situation is assumed to be analogous for the SM fermions (here and in the following we are considering only the quark sector) [49]. They are introduced as elementary fields coupled linearly to the fermionic operators of the strogn sector with equal quantum numbers under the SM

$$\mathcal{L}_{fermion} = \epsilon_L m_\psi \bar\psi_L \mathcal{O}_1 + \epsilon_R m_\psi \bar\psi_R \mathcal{O}_2\,. \tag{2.12}$$

This choice is crucially different to old technicolour theories where the coupling to fermions was obtained with a 4-fermi operator.[1] Here we have a bilinear mixing which implies that

[1] In technicolour-like theories, the fermion masses are generated by operators like $\frac{c_{ij}}{\Lambda^2}\bar\psi_i\psi_j\mathcal{O}$, where ψ is a SM field, while $\mathcal{O}$ is a techni-fermion bilinear that condenses at a natural scale $\langle\mathcal{O}\rangle \sim m_{\rm TC}^3 \sim (\text{TeV})^3$. The

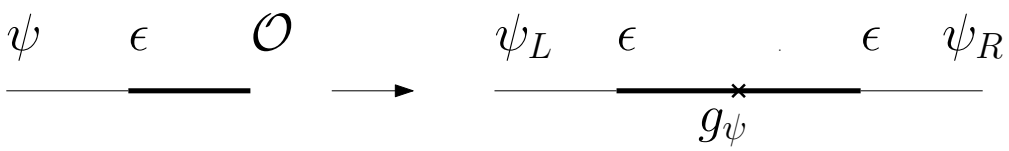

Figure 2.1. Genesis of fermion masses in the partial compositeness paradigm. The coupling of (2.12) gives rise to a Yukawa term as in (2.13).

the composite fermions must be coloured. This mechanism realizes the paradigm of partial compositeness [49, 50], according to which the SM particles (*i.e.* the mass eigenstates) are a mixture of elementary and composite states. The analogous phenomenon in QCD is the well known photon-ρ mixing.

Within the hypothesis of partial compositeness the couplings g, $\epsilon_{L,R}$ are responsible for the generation of all the interactions among the elementary states and the composite Higgs. In particular the SM Yukawas at leading order take the form

$$\hat{y}_{u,d} \simeq \epsilon_L \cdot g_\psi \cdot \epsilon_R. \tag{2.13}$$

They are matrices in flavour space but for determining the Higgs mass only the third generation will be relevant, given the largeness of y_t which is one of the coupling that breaks SO(4). There are few *caveats* with the above formula. First of all it is valid only in an expansion in the mixings, $\epsilon_{L,R} < 1$. Second, it is parametrically violated if some of the top partners, with specific quantum numbers, are accidentally lighter than the others [51].

2.3 Higgs mass and Tuning

Loops of elementary fields generate a potential for the Higgs boson, because the elementary-composite interactions of eq.s (2.11) and (2.12) break explicitly the SO(5) global symmetry. The largest contributions to the potential are typically associated to the largest couplings in the SM, the top Yukawa and the gauge couplings

$$V(h) = V(h)_{\text{top}} + V(h)_{\text{gauge}}. \tag{2.14}$$

Here and in the following we consider only the top-sector and eq. (2.13) will be used only for the top Yukawa coupling, $y_t = \epsilon_L g_\psi \epsilon_R$.

In an expansion in the elementary-composite interactions the Higgs potential is strongly constrained by the SO(5) symmetry. This is best understood by promoting g, ϵ_L and ϵ_R to spurions and noticing that the potential must formally respect the SO(5) symmetry under which both the Higgs and the spurions transform [52, 53]. With this technique it is possible to establish, order by order in the number of spurion insertions, the functional form of the

same dynamics that generates the above operator also induces 4-fermi FCNC operators suppressed by the same overall scale Λ. Hence, the bounds coming from the Kaon system, of order $\Lambda \gtrsim 10^4$TeV as discussed in chapter 1, are in contrast with the generation of the masses of the third generation quarks, which instead require $\Lambda \sim 10$ TeV.

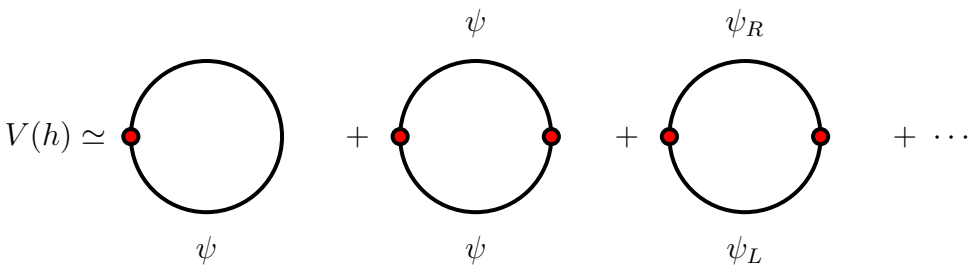

Figure 2.2. Sketch of generation of $V(h)$. A dot represents an elementary-composite insertion $\sim \epsilon^2 F_i(h/f)$, where F_i is one of the trigonometric functions in (2.16), and it can be chirality breaking and/or conserving.

Higgs potential. Making also use of naive power counting to estimate the overall size one finds, for the gauge contribution

$$V(h)_{\text{gauge}} \sim \frac{9\, g^2}{64\pi^2} \frac{m_\rho^4}{g_\rho^2} s_h^2, \tag{2.15}$$

which is rather model independent because the quantum numbers under SO(5) of the g spurion in eq. (2.11) are fixed.

The fermionic contribution, on the contrary, is not universal because it depends on the representation of the fermionic operators $\mathcal{O}_{1,2}$. Once the choice of representations is made, the classification of the invariants can be carried out in the same way as for the gauge fields. We can obtain the same result in a somewhat more explicit way by first writing down the effective action for the elementary quarks obtained by integrating out the strong sector, and afterwards computing the Coleman-Weinberg one-loop Higgs potential. Neglecting higher derivative terms, the structure of the effective Lagrangian obtained integrating out the heavy fermions is schematically

$$\begin{aligned} \mathcal{L} = &\left(1 + \epsilon_L^2 \sum_i a_i\, f_i(h/f)\right) \bar{q}_L i \not{D} q_L + \left(1 + \epsilon_R^2 \sum_i b_i\, g_i(h/f)\right) \bar{q}_R i \not{D} q_R \\ &+ \left(y_t f \sum_i c_i\, m_i(h/f) \bar{q}_L q_R + h.c.\right), \end{aligned} \tag{2.16}$$

where the functions f_i, g_i and m_i are determined by the spurionic analysis for each given choice of the fermion representation. The coefficients a_i, b_i and c_i are *a priori* $O(1)$ but their values can be reduced either by tuning or if the fermionic sector respects some (approximate) global symmetry. The sum over i takes into account possible several terms that can appear depending on the fermion representation.

The loops of SM fermions are UV divergent within the low energy theory described by eq. (2.16), but they are cut-off by the non-local form factors which account for the presence of the fermionic resonances of the full theory. The cut-off scale is provided by the scale m_ψ

	I_L, I_R	I_{LL}, I_{RR}, I_{LR}
$\mathbf{r_L = r_R = 5}$	$\sin^2(h/f)$	$\sin^{2n}(h/f)$ with $n = 1, 2$
$\mathbf{r_L = r_R = 10}$	$\sin^2(h/f)$	$\sin^{2n}(h/f)$ with $n = 1, 2$
$\mathbf{r_L = r_R = 14}$	$\sin^2(h/f)$, $\sin^4(h/f)$	$\sin^{2n}(h/f)$ with $n = 1, 2, 3, 4$
$\mathbf{r_L = r_R = 4}$	$\sin^2(h/2f)$	$\sin^{2n}(h/2f)$ with $n = 1, 2$

Table 2.1. Table with all possible invariants appearing in the Higgs potential. For the case with totally composite t_R only the I_L and I_{LL} invariants are relevant.

of the fermionic resonances, so that

$$V_{\text{leading}} \sim \frac{N_c}{16\pi^2} m_\psi^4 \sum_i \left[\epsilon_L^2\, I_L^{(i)}(h/f) + \epsilon_R^2\, I_R^{(i)}(h/f)\right] ,$$
$$V_{\text{sub-leading}} \sim \frac{N_c}{16\pi^2} m_\psi^4 \sum_i \left[\frac{y_t^2}{g_\psi^2}\, I_{LR}^{(i)}(h/f) + \epsilon_L^4 I_{LL}^{(i)}(h/f) + \epsilon_R^4 I_{RR}^{(i)}(h/f)\right] . \qquad (2.17)$$

The origin of the invariant trigonometric polynomials $I^{(i)}$ can be traced back to the f_i, g_i and m_i of eq. (2.16), and again their number is quite limited in explicit models. A sketch of the radiative generation of the Higgs potential is depicted in figure 2.2.

The invariants are listed in table 2.1 for the various cases considered. They are constructed from SO(5)-invariant objects built with fermionic representations and Σ as defined in (2.5).

One caveat to eq. (2.17) is that in the limit of full compositeness of t_R, $\epsilon_R \sim 1$, there are no contributions in ϵ_R^2 or ϵ_R^4 because the state is part of the strong sector respecting the global symmetries. In this case the y_t^2 term in the second line of eq. (2.13) becomes of the same order of the formally leading ϵ_L^2 because, as mentioned above, ϵ_L becomes of order y_t/g_ψ. Indeed in the case of total t_R compositeness there is a single source of breaking of global symmetries, the mixing of the left doublet. Therefore the expansion is truly in ϵ_L^2. Another important remark is that the very notion of leading and subleading terms becomes useless in the limit of fermionic coupling g_ψ close to 1, because the expansion in $\epsilon_{L,R}$ looses its validity. In this case, similarly to what we mentioned below eq. (2.13) concerning the estimate of the Yukawa couplings, eq. (2.17) can be violated at $O(1)$ but still it provides a valid estimate of the size of the Higgs potential.

The Higgs potential in eq. (2.17) generically has its minimum for $\langle h \rangle \sim f$. The phenomenological success of the model requires instead $\langle h \rangle < f$, *i.e.* that the parameter $\xi < 1$, as discussed in section 2.2. As a benchmark we will mainly focus on the relatively conservative choice $\xi = 0.1$, which corresponds to $f \simeq 800$ GeV. Achieving this requires unavoidably some cancellation. We refer to

$$\Delta_{\min} = 1/\xi \qquad (2.18)$$

as the "minimal tuning" because we expect that it provides the absolute lower bound for the tuning required by any model of composite Higgs. For sure this is the case for all the models we are going to discuss.

2.3.1 Double Tuning

As exhaustively discussed in ref. [51], a parametrically enhanced fine-tuning is needed in all the models where a single invariant is present in the potential at the leading order in $\epsilon_{L,R}$. The popular MCHM$_4$, MCHM$_5$ and MCHM$_{10}$ all belong to this class.

In this case the subleading terms must be taken into account in order to achieve a realistic EWSB. For instance for $\mathbf{r_L} = \mathbf{r_R} = \mathbf{5}$ or $\mathbf{10}$, table 2.1 shows that the potential has the form

$$V^{\mathbf{5+5}} = V_{\text{leading}} + V_{\text{sub-leading}} = \frac{N_c}{16\pi^2} m_\psi^4 \epsilon^2 \left[(a_L + a_R) s_h^2 + (b_L \epsilon^2 + b_R \epsilon^2) s_h^4 \right] , \tag{2.19}$$

where $a_{L,R}$ and $b_{L,R}$ are model-dependent $O(1)$ numerical coefficients.[2] In the equation above we have assumed, for simplicity, $\epsilon_L = \epsilon_R = \epsilon$.

The tuning of the Higgs VEV, provided the signs of the coefficients can be freely chosen, requires

$$\left| \frac{a_L + a_R}{b_L \epsilon^2 + b_R \epsilon^2} \right| = 2\,\xi\,. \tag{2.20}$$

The amount of cancellation implied by the equation above is

$$\Delta^{\mathbf{5+5}} = \frac{\max(|a_L|, |a_R|)}{|a_L + a_R|} \simeq \frac{1}{\xi} \frac{g_\psi}{y_t}, \tag{2.21}$$

and it is parametrically larger than $\Delta_{\min}$ for $\epsilon < 1$. This accounts for the "double" tuning which has to be performed on the potential in eq. (2.19): one must first cancel the ϵ^2 terms making them of the same order of the formally subleading ϵ^4 ones, and afterwards further tune the ϵ^2 and ϵ^4 contributions.

Once the minimization condition is imposed we can easily obtain the physical Higgs mass,

$$m_h^2 \simeq \frac{N_c}{2\pi^2} v^2 g_\psi^4 \epsilon^4\,. \tag{2.22}$$

In doubly tuned models the Higgs quartic coupling is also automatically reduced in the tuning process. In spite of the fact that the potential is generated at $O(\epsilon^2)$ indeed the Higgs mass-term scales like ϵ^4 rather than ϵ^2,

$$m_h^{\mathbf{5+5}} = 500\,\text{GeV} \left(\frac{g_\psi}{5} \right); \qquad \Delta^{\mathbf{5+5}} \simeq \frac{1}{\xi} \frac{g_\psi}{y_t}. \tag{2.23}$$

It follows that an option to get a light Higgs is to have a small overall fermionic coupling g_ψ.

Anomalously light partners

In models with a largish g_ψ, a realistic Higgs mass requires that we deviate from the estimate of eq. (2.13), and this can occur if the spectrum of the top partners is non-generic. Indeed, suppose that one of the partners, with the appropriate quantum numbers to mix strongly

[2] Very similar considerations hold in the case $\mathbf{r_L} = \mathbf{r_R} = \mathbf{4}$, the only change is in the functional form of the leading and subleading terms.

with the left- or right-handed top quark, [3] becomes anomalously light, with a mass m_p slightly smaller than m_ψ. Given that the Yukawa coupling arises from the mixing with the partners, its size will be controlled by the mass m_p of the lightest state. Therefore eq. (2.13), that assumes a common mass m_ψ for all the partners, needs to be modified and becomes [51]

$$y_t \simeq \epsilon_L \epsilon_R \frac{g_\psi^2 f}{m_p} \,. \tag{2.24}$$

This estimates reduces to eq. (2.13) if $m_p \simeq m_\psi = g_\psi f$, but it can be parametrically different in the case of a large separation $m_p < m_\psi$. Putting this estimate into (2.22), we get

$$m_h^{\mathbf{5+5}} \simeq \sqrt{\frac{N_c}{2\pi^2}} \frac{y_t m_p}{f} v = 100\,\mathrm{GeV} \left(\frac{y_t m_p}{f}\right) . \tag{2.25}$$

A realistic Higgs is thus obtained if some of the top partners are light, at least below around 1 or 2 times f, *i.e.* $\lesssim 2$ TeV for $\xi = 0.1$. No restriction is instead found on the overall scale $m_\psi = g_\psi f$ of the other fermionic resonances. The price to pay, however, is a large tuning. Eq. (2.21) indeed becomes

$$\Delta^{\mathbf{5+5}} = \frac{1}{\xi} \cdot 20 \left(\frac{125\ \mathrm{GeV}}{m_h}\right) \left(\frac{g_\psi}{5}\right)^2 , \tag{2.26}$$

and the tuning easily overcomes 100 for a realistic value of ξ.

2.3.2 Minimal Tuning

To avoid the double tuning it is enough to choose the fermionic representations in such a way that two or more invariants are allowed in the leading order potential. Sticking to irreducible representations the simplest choice is $\mathbf{r_L} = \mathbf{r_R} = \mathbf{14}$. Following table 2.1 and again assuming $\epsilon_L \simeq \epsilon_R$ the leading order potential has the form

$$V^{\mathbf{14+14}} = V_{\text{leading}} = \frac{N_c}{16\pi^2} m_\psi^4 \epsilon^2 \left[(a_L + a_R) s_h^2 + (b_L + b_R) s_h^4\right] , \tag{2.27}$$

and it can be adjusted to give a realistic EWSB without need of relying on the subleading terms. The minimization condition requires a degree of tuning

$$\frac{1}{\Delta} = \frac{|a_L + a_R|}{\max(|a_L|, |a_R|)} = 2\,\xi \frac{|b_L + b_R|}{\max(|a_L|, |a_R|)} \,. \tag{2.28}$$

Therefore, in the absence of additional cancellations among b_L and b_R, the model has minimal tuning $\Delta^{\mathbf{14+14}} \simeq \Delta_{\min} = 1/\xi$. The estimate of m_h^2 is now

$$m_h^2 \simeq \frac{N_c}{2\pi^2} v^2 g_\psi^4 \epsilon^2 \,, \tag{2.29}$$

[3] In the cases of the $\mathbf{5} + \mathbf{5}$ these states must be in the $\mathbf{4}$ and/or $\mathbf{1}$.

and it scales like ϵ^2 and not like ϵ^4 as in the case of double tuning. Adopting the naive estimate in eq. (2.13) for y_t, which implies $\epsilon \simeq \sqrt{y_t/g_\psi}$, the Higgs is extremely heavy for large g_ψ

$$m_h^{\mathbf{14+14}} \simeq \sqrt{\frac{N_c}{2\pi^2} y_t g_\psi^3 v^2} = 1\,\text{TeV}\,\left(\frac{g_\psi}{5}\right)^{3/2} . \tag{2.30}$$

As before we can achieve a 125 GeV only with smallish g_ψ.

In models where g_ψ is large, we could also rely on anomalously light top partners as we did in the case of double tuning. However this mechanism can not reduce m_h indefinitely because the partners can not be arbitrarily light. An absolute lower bound is $m_p \geq \epsilon m_\psi$, which is saturated if they are massless before elementary-composite mixing. For a minimally tuned model like the one at hand instead the bound gives

$$m_h \gtrsim \sqrt{\frac{N_c}{2\pi^2}} y_t g_\psi v = 500\,\text{GeV}\,\left(\frac{g_\psi}{5}\right) \tag{2.31}$$

which again shows that, if g_ψ is large, the Higgs is unavoidably too heavy.

2.3.3 Minimal tuning with composite t_R

Another interesting possibility, which can alleviate the issue of a too heavy Higgs in models with largish g_ψ, is that the t_R is a completely composite chiral state that emerges from the strong sector. In this case the potential is entirely generated by the left coupling ϵ_L. By looking at table 2.1 we see that a minimally tuned potential can be obtained also with a completely composite t_R if we assign the left fermionic operator to the **14**. The potential is

$$V^{\mathbf{14}} = V_{\text{leading}} = \frac{N_c}{16\pi^2} m_\psi^4 \epsilon_L^2 \left[a\, s_h^2 + b\, s_h^4\right] , \tag{2.32}$$

where a and b are, *a priori*, $O(1)$ coefficients. To tune the electro-weak VEV we have to require that the coefficient a can be artificially reduced, which corresponds to a cancellation

$$\Delta^{\mathbf{14}} = \frac{1}{|a|} \simeq \frac{1}{b\,\xi} . \tag{2.33}$$

The Higgs mass-term scales like ϵ^2 as in the previous section, *i.e.*

$$m_h^2 \simeq \frac{N_c}{2\pi^2} b v^2 g_\psi^4 \epsilon^2 . \tag{2.34}$$

The difference with the previous case is that now ϵ_L is smaller, because for a totally composite t_R the top Yukawa is simply $\epsilon_L \simeq \frac{y_t}{g_\psi}$, therefore the Higgs mass is somewhat smaller,

$$m_h^{\mathbf{14}} \simeq \sqrt{b} \sqrt{\frac{N_c}{2\pi^2} y_t^2 g_\psi^2 v^2} = \sqrt{b}\, 500\,\text{GeV}\,\left(\frac{g_\psi}{5}\right) . \tag{2.35}$$

Again, for $b \sim O(1)$ a 125 Higg can be obtained only for small g_ψ.

Notice that no help can come in the case of large g_ψ from anomalously light top partners because the absolute lower bound $\epsilon_L \geq y_t/g_\psi$ is already saturated. However, for $g_\psi \gtrsim 2$, an

alternative way to obtain a light Higgs is to reintroduce additional tuning to lower the Higgs mass. In the case at hand this could be achieved by artificially reducing the parameter b that controls the Higgs mass (see eq. (2.35)), *i.e.* by taking

$$b \simeq \frac{1}{16}\left(\frac{m_h}{125\,\mathrm{GeV}}\right)^2\left(\frac{5}{g_\psi}\right)^2 . \tag{2.36}$$

This obviously enhances the fine tuning. From eq. (2.33) we obtain

$$\Delta \simeq \frac{1}{\xi}\frac{N_c}{2\pi^2}y_t^2 g_\psi^2\frac{v^2}{m_h^2} \simeq \frac{1}{\xi}\cdot 16\left(\frac{125\,\mathrm{GeV}}{m_h}\right)^2\left(\frac{g_\psi}{5}\right)^2 . \tag{2.37}$$

The level of tuning of this scenario is comparable with the one of doubly-tuned models with anomalously light partners reported in eq. (2.26), however there is a crucial difference among the two cases. There the 125 GeV Higgs requires the existence of anomalously light partners, therefore even if the fermionic scale m_ψ is high some of the resonances will be light and easily detectable at the LHC. In the present case instead there is no need of light partners and all the fermionic and gauge resonances could be heavy, lying in the multi-TeV region. This kind of models evade the connection among light Higgs and light resonances and they could even escape the direct LHC searches. Of course they are tuned, but the level of fine-tuning is comparable with the one of the standard $\mathrm{MCHM}_{4,5,10}$ constructions.

Double tuning with composite t_R

Another logical possibility that might be considered is the one of doubly tuned models with composite t_R, for example a model where the q_L mixes with a **5** of SO(5) like the one discussed in ref. [54]. The estimates for this case are easily extracted from section 2.3.1 by remembering that now $y_L \simeq y_t$, and read

$$\Delta^{\mathbf{5}} = \frac{1}{\xi}\frac{g_\psi^2}{y_t^2} = \frac{1}{\xi}\cdot 25\left(\frac{g_\psi}{5}\right)^2 , \qquad m_h{}^{\mathbf{5}} = \sqrt{\frac{N_c}{2\pi^2}}y_t^2 v \simeq 100\,\mathrm{GeV}\,. \tag{2.38}$$

In this setup one thus expects sizable tuning, comparable with the one of the $\mathrm{MCHM}_{4,5,10}$, but no need for anomalously light top partners to obtain a light enough Higgs. We will not further discuss this option because it is difficult to realize it in an explicit calculable model. In the minimal realizations, indeed, we find that the Higgs potential is too constrained and that there is not enough freedom in the parameter space to tune ξ to a realistic value.

2.3.4 Gauge Tuning

When relevant we will also include in the tuning the gauge contribution. One interesting point is that the gauge contribution to the potential, often considered sub-leading, can be relevant in the region of small fermion mass scale, $m_\psi < m_\rho$. The amount of tuning due to the gauge can be easily estimated. In the limit $m_\psi < m_\rho$ the gauge loops can give a sizeable contribution to the Higgs mass

$$\delta m_h \sim \frac{3}{4\pi} g\, g_\rho v = 120\ \mathrm{GeV}\left(\frac{g_\rho}{3}\right) . \tag{2.39}$$

This contribution is of the size of the measured Higgs mass (125 GeV) for $g_\rho \simeq 3$. We can also quantify the tuning associated to gauge contributions as

$$\Delta_{\text{gauge}} \approx \frac{1}{\xi}\frac{9}{8\pi^2} g^2 g_\rho^2 \frac{v^2}{m_h^2}\,. \tag{2.40}$$

With obvious identifications of the couplings, one can notice that the estimate in eq. (2.40) has exactly the same structure of the fermionic tuning in the minimally tuned models with composite t_R (see eq. (2.37)). Given the bound on the S-parameter, $m_\rho \gtrsim 2.5$ TeV, eq. (2.40) implies $\Delta \gtrsim 10$ for a realistic Higgs mass. This is an irreducible source of tuning that exists in all models where the Higgs is a pNGB even beyond partial compositeness and therefore provides a lower bound.

2.4 An explicit model

When facing the construction of an explicit model for a composite Higgs, the biggest issue is usually the calculability of the Higgs potential $V(h)$ in the sense of (1.40).

A possibility for model building is usually offered by the five dimensional approach *à la* Randall-Sundrum [55], which can be thought of as equivalent to a strongly coupled four dimensional conformal field theory [56,57]. This is the context where most of the Composite Higgs models have been discussed so far [45,50] (see also [58–60]). However, five dimensional models are not the most general ones. Indeed, a common prediction of 5d models is the presence of a single mass scale for all the resonances (fermionic and bosonic) proportional to the (inverse) size $1/R$ of the extra-dimension. This very observation, together with the discussion of section 2.3, suggests that any five dimensional realization of the Composite Higgs paradigm is likely to experience significant levels of tuning because of the lower bound on $m_\rho \sim m_\psi \sim 1/R$ from EWPTs.

An alternative possibility to construct realistic composite models has been suggested by the idea of dimensional deconstruction (see for example [61]). In this case the fermionic and bosonic resonance scales can be easily disentangled from each other, allowing for scenarios with less tuning compared to the five dimensional case, provided $m_\psi/f \lesssim 2$.

Anyhow, no matter what (partial) UV completion we have in mind, a meaningful low-energy description of CHM has to have an SO(5)/SO(4) symmetry structure with a sufficient number of composite resonances below the cut-off.

A possible explicit model can be constructed with the following matter content, justified *a posteriori* by the finiteness of $V(h)$,

- Vector resonances in the adjoint of SO(5).
- Two Dirac fermions in the **5** of SO(5).

As said before, the inclusion of resonances must respect the SO(5)/SO(4) structure of the strong sector. Vector resonances can be introduced adding redundant gauge symmetries without spoiling SO(4)-invariance. Also fermions have to be introduced in a consistent way. In the following paragraphs we discuss the two sectors separately. This approach shares some similarities with [62,63] and [53].

Gauge Lagrangian

A lagrangian describing the gauge fields of the SM plus the composite resonances in the adjoint of SO(5) is

$$\mathcal{L}_{\rm gauge} = -\frac{1}{4g_0^2}W^a_{\mu\nu}W^a_{\mu\nu} + \frac{f_1^2}{4}\mathrm{Tr}\,|D_\mu\Omega|^2 + \frac{f_2^2}{2}\left(D_\mu\Phi\right)^T\left(D^\mu\Phi\right) - \frac{1}{4g_\rho^2}\rho^A_{\mu\nu}\rho^{A\mu\nu}. \tag{2.41}$$

Ω is an SO(5) matrix, while Φ a five dimensional real unit vector. The composite spin-1 resonances, ρ^a, are introduced as gauge fields. The action of SM and composite gauge fields on Ω and Φ is the following

$$D_\mu\Omega = \partial_\mu\Omega - iW_\mu\Omega + i\Omega\rho_\mu, \qquad D_\mu\Phi = \partial_\mu\Phi - i\rho_\mu\Phi. \tag{2.42}$$

Although not manifest, it can be shown that the above lagrangian has an SO(5)/SO(4) spontaneous breaking. In particular, the mass spectrum in absence of elementary-composite mixings ($g_0 \to 0$) can be classified according to SO(4)

$$m_\rho^2 = g_\rho^2 f_1^2/2, \quad \text{vectors in the } \mathbf{6}, \qquad m_{a_1}^2 = g_\rho^2(f_1^2+f_2^2)/2, \quad \text{vectors in the } \mathbf{4} \tag{2.43}$$

Moreover at global symmetry level, in the limit $g_0, g_\rho \to 0$, Ω and Φ parametrize two different coset spaces: $\mathrm{SO}(5)\times\mathrm{SO}(5)'/\mathrm{SO}(5)_d$ and $\mathrm{SO}(5)''/\mathrm{SO}(4)$ respectively. As evident from (2.42), the composite ρ_a are introduced as gauge fields of the diagonal combination of SO(5)′ and SO(5)″, thus providing a "collective" SO(5)/SO(4) coset space.

After the gauging of the SM subgroup, the elementary-composite mixing splits $\mathbf{6} \to (\mathbf{3},\mathbf{1}) + (\mathbf{1},\mathbf{3})$, with the first heavier by a factor $(1 + g_0^2/g_\rho^2)$, and the SU(2) gauge coupling is $g = g_0(g_0^2+g_\rho^2)^{-1/2}$ (here we neglect hyper-charge effects).

In order to make a comparison with section 2.3, we can show that the physical decay constant of the pGB Higgs is given by

$$f^2 = \frac{f_1^2 f_2^2}{f_1^2+f_2^2}, \tag{2.44}$$

while the pGB field of eq. (2.5) is

$$\Sigma = \Omega\Phi. \tag{2.45}$$

Fermionic sector

Each SM chiral quark is coupled to a Dirac fermion in an SO(5) representation. Here we will consider fermions in the **5**, hence the model belongs to the class of doubly tuned models. The spontaneous breaking SO(5)/SO(4) allows couplings between fermions associated to the left and right chiralities of SM fields that will eventually generate SM Yukawas. The lagrangian of the third generation is

$$\begin{aligned}\mathcal{L}^{\rm MCHM_5} &= \bar{q}_L^{el} i\not{D}^{el} q_L^{el} + \bar{t}_R^{el} i\not{D}^{el} t_R^{el} \\ &+ \Delta_{t_L}\,\bar{q}_L^{el}\Omega\Psi_T + \Delta_{t_R}\,\bar{t}_R^{el}\Omega\Psi_{\widetilde{T}} + h.c. \\ &+ \bar{\Psi}_T(i\not{D}^\rho - m_T)\Psi_T + \bar{\Psi}_{\widetilde{T}}(i\not{D}^\rho - m_{\widetilde{T}})\Psi_{\widetilde{T}} \\ &- Y_T\bar{\Psi}_{T,L}\Phi\Phi^T\Psi_{\widetilde{T},R} - m_{Y_T}\bar{\Psi}_{T,L}\Psi_{\widetilde{T},R} + h.c. \\ &+ (t\to b,\quad T\to B).\end{aligned} \tag{2.46}$$

The elementary quarks q_L^{el} and t_R^{el} couple to two different Dirac fermions Ψ_T and $\Psi_{\tilde{T}}$, in the **5** representation of SO(5), via mass mixing Δ_{t_L} and Δ_{t_R} that respect the SM gauge symmetry. The terms in the fourth line break spontaneously SO(5)/SO(4). We retain the only terms with a certain chirality as necessary to generate the SM Yukawas. We recall that the SM quark doublet must couple to two composite fermions with different charge under $U(1)_X$ to generate Yukawa of the top (X=2/3) and bottom quark (X=-1/3). Although a deviation from minimality this choice is welcomed from the point of view of EWPT (as discussed in the next chapter). Once again here we consider only the top-sector.

In general m_{Y_T} and Y_T are complex parameters, both are needed in order to reproduce the most general SO(4)-invariant mass spectrum of composites. One phase can be reabsorbed with a redefinition of the composite fields while the relative phase remains as a physical CP violating phase. This describes a strong sector that breaks CP. The same holds when the coupling to the elementary fields is included so that the action violates in general CP even with a single generation. Following the literature we will take these IR parameters to be real in what follows, i.e. we consider a CP invariant composite sector.

2.4.1 Higgs potential

The computation of $V(h)$ at loop-level follows the Coleman-Weinberg approach [43]. If we integrate out all the resonances and leave only SM quarks and W bosons in the background of h we get,

$$\mathcal{L} = \frac{P^T_{\mu\nu}}{2}\Pi_W(p^2;h)W^\mu_a W^\nu_a + \bar{q}_L \not{p}\Pi_{q_L}(p^2;h)q_L + \bar{t}_R\not{p}\Pi_{t_R}(p^2;h)t_R + (\bar{q}_L M(p^2;h)t_R + h.c.), \quad (2.47)$$

where $P^T_{\mu\nu} = \eta_{\mu\nu} - p_\mu p_\nu/p^2$. The effective potential is

$$V(h) = \int \frac{d^4p}{(2\pi)^4}\left[\log[\frac{9}{2}\Pi_W] - 2N_c \log \Pi_{b_L} - 2N_c \log(p^2\Pi_{t_L}\Pi_{t_R} - |M|^2)\right] \quad (2.48)$$

The functions Π, M, usually called form factors, can be derived by matching (2.47) with the lagrangian with resonances integrated-in (2.41),(2.46). In the case under consideration, the Higgs potential can be approximated as [47]

$$V(h) \simeq \alpha s_h^2 - \beta s_h^2 c_h^2, \quad (2.49)$$

where α, β are related to integrals of the form factors. From (2.49) we can derive

$$m_h^2 \simeq \frac{8\beta}{f^4}v^2\big(1 - \frac{v^2}{f^2}\big), \qquad \frac{v^2}{f^2} \simeq \frac{\beta - \alpha}{2\beta}. \quad (2.50)$$

In order for the coefficients α, β to be calculable and finite within the theory defined by (2.41) and (2.46), the integrand in (2.48) has to be at least a function which goes as p^{-6} at large momenta.

Gauge potential

The computation of $V(h)_{\text{gauge}}$ is particularly simple and directly shows the importance of the "axial" resonances **4** to make the potential fully calculable. Matching the two theories we can show that the gauge form factor Π_W has a simple dependence on h, as already hinted by eq. (2.39), $\Pi_W = \Pi_0(p^2) + s_h^2\Pi_1(p^2)/4$. The integral, which contributes to α in (2.49), is UV convergent because Π_1/Π_0 behaves properly

$$\frac{\Pi_1(p^2)}{\Pi_0(p^2)} = -\frac{2g_0^2 m_\rho^4\left(m_{a_1}^2 - m_\rho^2\right)}{g_\rho^2 p^2\left[p^2 - m_\rho^2\left(1+g_0^2/g_\rho^2\right)\right]\left(p^2 - m_{a_1}^2\right)} \overset{p^2\to\infty}{\longrightarrow} \frac{1}{p^6}. \tag{2.51}$$

At leading order we get [64]

$$V(h)_{\text{gauge}} \approx \int \frac{d^4p}{(2\pi)^4}\frac{9}{8}\frac{\Pi_1}{\Pi_0}\sin^2\frac{h}{f} \simeq \frac{9}{64\pi^2}\frac{g^2}{g_\rho^2}m_\rho^4 \log\left(\frac{m_{a_1}^2}{m_\rho^2}\right)\sin^2\frac{h}{f}. \tag{2.52}$$

The curvature of the potential at the origin is positive, a general feature of gauge interactions which tend to preserve the symmetry. For $m_{a_1} \to \infty$ (corresponding to $f_2 \to \infty$ in our setup) the potential becomes logarithmically divergent, showing that the coset resonances are crucial for the finiteness of the gauge potential. This explicit calculation is well in agreement with the NDA estimate in eq. (2.15). Moreover (2.52) is formally equal to the electro-magnetic mass-splitting of the pions $\Delta m_{\pi^\pm}^2$ as derived from current algebra [65] and Weinberg sum rules [66].

Fermion potential

The contribution from the top-loop in (2.48) is much more difficult to compute analytically. It can be shown that the fermionic contribution to α requires all the 2 Dirac **5** to be finite. On the contrary the fermionic contribution to β needs only one composite **5**. To show this we have to look at the form factors. Integrating out heavy fermions in the background of h from (2.46) we get the following matching conditions

$$\Pi_{t_L(p^2)} = \Pi_0^q(p^2) + \frac{s_h^2}{2}\Pi_1^q(p^2), \tag{2.53}$$

$$\Pi_{b_L}(p^2) = \Pi_0^q(p^2), \tag{2.54}$$

$$\Pi_{t_R}(p^2) = \Pi_0^u(p^2) + \frac{s_h^2}{2}\,\Pi_1^u(p^2), \tag{2.55}$$

$$M(p^2) = \frac{s_h c_h}{\sqrt{2}} M_1^u(p^2). \tag{2.56}$$

The expressions on the right-hand side encode all the relevant information on the strong sector, and they can be unambiguously computed starting from (2.46) (see [1] for details). The form factors give us information on the spectrum of the composite fermionic resonances. In the model under consideration we have four different sets of resonances once classified according to their SM quantum numbers

$$\mathbf{2}_{1/6}, \mathbf{2}_{7/6}, \mathbf{1}_{2/3}. \tag{2.57}$$

Each of the above states appears twice in the spectrum. From a computational viewpoint, the masses of the composite fermions are respectively zeros of $\Pi_0^q(p^2)$ $(m_{\mathbf{2}_{1/6}}, \tilde{m}_{\mathbf{2}_{1/6}})$, poles of $\Pi_0^q(p^2)$ $(m_{\mathbf{2}_{7/6}}, \tilde{m}_{\mathbf{2}_{7/6}})$ and zeros of $\Pi_0^u(p^2)$ $(m_{\mathbf{1}_{2/3}}, \tilde{m}_{\mathbf{1}_{2/3}})$. The top mass can be extracted from $M(p^2)$ at small momentum upon canonical normalization,

$$m_{\rm top} \simeq \frac{s_h c_h}{\sqrt{2}} \frac{M_1^u(0)}{\sqrt{\Pi_0^q(0)\Pi_0^u(0)}} = \frac{s_h c_h}{\sqrt{2}} \frac{\Delta_L \Delta_R m_T m_{\tilde{T}} Y_T}{m_{\mathbf{2}_{1/6}} \tilde{m}_{\mathbf{2}_{1/6}} m_{\mathbf{1}_{2/3}} \tilde{m}_{\mathbf{1}_{2/3}}}. \tag{2.58}$$

Following the approach of [51], we can get a simple result looking at the limit where only two top-partners are light. Expanding (2.48) in the elementary-composite mixings and matching with (2.49), the leading contribution to β is

$$\begin{aligned} \beta &\approx -2N_c \int \frac{d^4p}{(2\pi)^4} \left[\frac{(M_1^u)^2}{2p^2 \Pi_0^q \Pi_0^u} + \frac{\Pi_1^q \Pi_1^u}{4 \Pi_0^q \Pi_0^u} \right] \\ &= -2N_c \int \frac{d^4p}{(2\pi)^4} \frac{\Delta_L^2 \Delta_R^2 m_T^2 m_{\tilde{T}}^2 Y_T^2}{p^2 (p^2 - m_{\mathbf{2}_{1/6}}^2)(p^2 - \tilde{m}_{\mathbf{2}_{1/6}}^2)(p^2 - m_{\mathbf{1}_{2/3}}^2)(p^2 - \tilde{m}_{\mathbf{1}_{2/3}}^2)}. \end{aligned} \tag{2.59}$$

The form factors needed for the above computation are listed in the appendix of [1]. Using the expression for the top-mass and taking the limit $m_{\mathbf{2}_{1/6}} \ll \tilde{m}_{\mathbf{2}_{1/6}}$ and $m_{\mathbf{1}_{2/3}} \ll \tilde{m}_{\mathbf{1}_{2/3}}$, we get [48, 51, 54]

$$m_h^2 \simeq \frac{N_c}{\pi^2} \frac{m_t^2}{f^2} \frac{m_{\mathbf{2}_{1/6}}^2 m_{\mathbf{1}_{2/3}}^2}{m_{\mathbf{2}_{1/6}}^2 - m_{\mathbf{1}_{2/3}}^2} \log \frac{m_{\mathbf{2}_{1/6}}^2}{m_{\mathbf{1}_{2/3}}^2}. \tag{2.60}$$

Hence the masses of the fermions which mix with SM quarks control the Higgs mass.

2.4.2 Implications of a 125 GeV Higgs

$m_h = 125$ GeV naturally prefers small values of g_ψ ($g_\psi \lesssim 2$). Here, as an operative definition of the fermionic coupling g_ψ we adopt the geometric mean of the mass parameters of the Lagrangians divided by f. We will focus on this region of the parameter space and on a reference value $f = 800$ GeV.[4]

[4]Since in general it is impossible to get analytic expressions, we perform a scan over the 6 fermionic parameters of the model, requiring that the electro-weak VEV and top mass are correctly accounted for. We demand $m_t \in [145, 155]$ to roughly account for the running top mass in $\overline{\rm MS}$ scheme at the scale of the heavy fermions $\sim$ TeV.

In order to evaluate quantitatively the tuning in a given model we adopt the definition of fine-tuning given in ref. [67]

$$\Delta = \max_i \left| \frac{\partial \log m_Z}{\partial \log x_i} \right|, \tag{2.61}$$

where x_i are the parameters of the theory, and $m_Z = g/\cos(\theta_W) f s_h/2$, which fixes the size of $\langle h \rangle$. Keeping fixed f and the gauge couplings, eq. (2.61) is exactly equivalent to the tuning on s_h and coincides with the definition of tuning usually adopted in the composite Higgs scenarios.

For the numerical computation it is useful to notice that the tuning can be extracted directly from the Higgs potential (2.48). Using the minimum condition $V'(s_h) = 0$, the tuning measure can be cast as follows

$$\Delta = \max_i \left| \frac{2x_i}{s_h} \frac{c_h^2}{f^2 m_h^2} \frac{\partial^2 V}{\partial x_i \partial s_h} \right|. \tag{2.62}$$

Using this formula one can readily derive the tuning estimates of section 2.3.

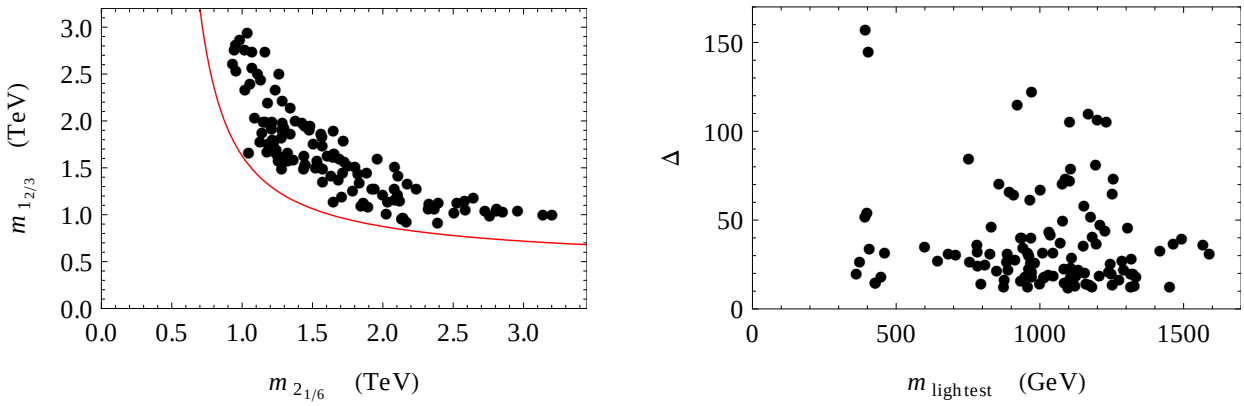

Figure 2.3. Scatter plots for 125 GeV Higgs in MCHM$_5$, $f = 800$ GeV. We varied the fermionic parameters in the range $0.5 - 5$ TeV and imposed that the mixings are smaller than 3. The gauge contribution is computed with $m_\rho = m_{a_1}/\sqrt{2} = 2.5$ TeV. Left: correlation of the doublet and singlet masses, the red solid line is eq. (2.60). Right: tuning as a function of the mass of the lightest resonance.

As originally shown in ref. [51] and here derived in eq. (2.60), m_h is sensitive to the lightest top partners. It is easy to see why a simple formula holds. In this model only one multiplet of resonances is necessary for the finiteness of β and therefore a formula depending on $m_{\mathbf{1}_{2/3}}$ and $m_{\mathbf{2}_{1/6}}$ must hold, at least at leading order in the mixings. Two multiplets are instead necessary to make α finite. This however does not affect the Higgs mass due to the fact that α must be tuned in order to obtain the correct Higgs VEV. Notice that the relation between the Higgs mass and the lightest resonance masses is a peculiarity of the models with double tuning, in which one of the invariants has a lower degree of divergence.

The correlation in a blind scan between the singlet and the doublet mass is shown on the left plot of figure 2.3. The lightest state is often an exotic doublet with hyper-charge 7/6, the custodian, that contains an exotic state of electric charge 5/3. The present experimental bound is $m_{5/3} \gtrsim 700$ GeV [68, 69] and starts carving out the natural region of the model. See also [70] for a detailed analysis of top-partners phenomenology.

In the right plot the tuning of the various points is considered. We see that no strong correlation exists between the tuning and the mass of the lightest resonance. The tuning varies between 10 and 100 with an average $\Delta_{avg} = 30$. Note that the lower bound is saturated by the gauge contribution, which amounts to an irreducible tuning $\Delta \gtrsim 10$.

2.5 Discussion

In this chapter we have provided a classification of CHM and presented an explicit model studied partly analytically and partially numerically to strengthen the estimates provided in the first part of the chapter.

The main result of this classification is that a (composite) Higgs with $m_h = 125$ GeV, typically requires fermionic partners lighter than TeV. We identified three classes of models characterized by the type of cancellation required to generate the electro-weak VEV:

1. Double tuning.

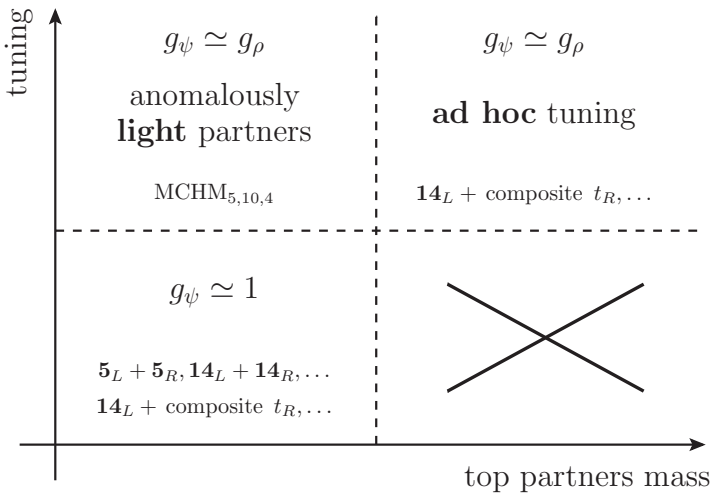

Figure 2.4. Schematic representation of the properties of the basic scenarios.

2. Minimal tuning.

3. Minimal tuning with composite t_R.

Within each class the expected size of the Higgs mass can be different and thus the recent discovery of a light Higgs can have a different impact. For the models in the second and third class it is difficult to obtain a light enough Higgs for a large strong sector coupling. However the tension with the observed Higgs mass disappears in the limit of light fermionic scale, corresponding to $g_\psi = m_\psi/f \sim 1$. In this case the double tuning issue encountered for the models in the first category tends to disappear. When g_ψ is weak the implication is that light fermionic coloured resonances, the top partners, are an expected feature of the composite Higgs models. Not observing these particles at the LHC would rapidly carry the scenario in a finely-tuned territory.

We also considered the possibility of a larger tuning (100 or larger). In this case we found two possibilities to obtain a realistic Higgs mass, as summarized in figure 2.4. One option is to stick to models with doubly-tuned potential like the standard MCHM$_{4,5,10}$. In this scenario a light Higgs requires the presence of light top partners significantly below the typical fermionic-resonance scale. The spectrum is characterized by one or two light multiplets, a four-plet or a singlet of SO(4), while all the other resonances are heavy and lie in the mass range of the vectors, $m_\rho > 2.5$ TeV. In the case of low g_ψ previously discussed, instead, all the fermionic resonances are light and they can have different quantum numbers. For instance in the model with the **14** we expect light top partners in the **4**, in the **1** and in the **9** of SO(4). Alternatively, for similar tuning, one can also have models with heavy fermionic resonances where the Higgs mass is tuned independently of the electro-weak VEV. We provided one example based on the $\mathbf{14}_L$ and totally composite t_R. This case is indicated in the upper right corner of figure 2.4. A model of this kind is rather difficult to test directly at the LHC, therefore if no top partners are found it might become the last corner where the Composite Higgs scenario could hide.

Chapter 3

Composite resonances and precision tests

In the previous chapter we have shown that one crucial parameter to obtain the correct Higgs mass in composite models is the ratio m_ψ/f,

$$m_h = O(1)\frac{\sqrt{N_c}}{\pi} m_t \frac{m_\psi}{f}, \tag{3.1}$$

The closeness of m_ψ to f suggests to study effects in precision physics.

In this chapter we will focus on Flavour and ElectroWeak precision tests. We consider a number of different options for the transformation properties of the spin-$\frac{1}{2}$ resonances under the global symmetries of the strong dynamics, motivated by the need to be consistent with the constraints from the EWPT, as well as different options for the flavour structure/symmetries, motivated by the many significant flavour bounds. We analyse in succession the different options for the flavour structures/symmetries: *Anarchy* in section 3.4, $U(3)^3$ in section 3.5, $U(2)^3$ in section 3.6. Section 3.3 describes the constraints from EWPT that apply generally to all flavour models. The summary and the conclusions are contained in section 3.7.

3.1 A "truncated" Composite Higgs

In general, Composite Higgs models predict towers of resonances. Moreover, the Higgs potential becomes calculable and finite only when a sufficient number of resonances lies below the cut-off. The aim of preserving predictivity on the Higgs potential is most of the times incompatible with low-energy phenomenological studies, where it is common and appropriate to focus on the lightest state. Then, in order to investigate the electro-weak and flavour precision tests in this class of models we make some simplifying assumptions, relying basically on [50].

The vector resonances transform in the adjoint representation of a global symmetry respected by the strong sector, which contains the SM gauge group. To protect the T parameter from tree-level contributions, we take this symmetry to be $G_c = SU(3)_c \times SU(2)_L \times SU(2)_R \times U(1)_X$. We assume all vector resonances to have mass m_ρ and coupling g_ρ. For the explicit form of their effective Lagrangian we refer to [50].

The choice of the fermion representations has important implications for the electroweak precision constraints. We will consider three cases.

1. The elementary $SU(2)_L$ quark doublets, q_L, mix with composite vector-like $SU(2)_L$ doublets, Q, one per generation. The elementary quark singlets, u_R and d_R, couple both to an $SU(2)_R$ doublet R. We will call this the **doublet model**.

2. The elementary $SU(2)_L$ quark doublets mix with a composite $L = (2,2)_{2/3}$ of $SU(2)_L \times SU(2)_R \times U(1)_X$, and the elementary quark singlets couple both to a composite triplet $R = (1,3)_{2/3}$. The model also contains a $(3,1)_{2/3}$ to preserve LR symmetry. We will call this the **triplet model**.

3. The elementary $SU(2)_L$ quark doublets mix with a $L_U = (2,2)_{2/3}$ and a $L_D = (2,2)_{-1/3}$ of $SU(2)_L \times SU(2)_R \times U(1)_X$, the former giving masses to up-type quarks, the latter to down-type quarks. The elementary up and down quark singlets couple to a $(1,1)_{2/3}$ and a $(1,1)_{-1/3}$ respectively. We will call this the **bidoublet model**.

For concreteness, the part of the Lagrangian involving fermions reads

- In the doublet model

$$\mathcal{L}_s^{\text{doublet}} = -\bar{Q}^i m_Q^i Q^i - \bar{R}^i m_R^i R^i + \left(Y^{ij}\text{tr}[\bar{Q}_L^i \mathcal{H} R_R^j] + \text{h.c}\right) , \tag{3.2}$$

$$\mathcal{L}_{\text{mix}}^{\text{doublet}} = m_Q^j \lambda_L^{ij} \bar{q}_L^i Q_R^j + m_R^i \lambda_{Ru}^{ij} \bar{U}_L^i u_R^j + m_R^i \lambda_{Rd}^{ij} \bar{D}_L^i d_R^j \, . \tag{3.3}$$

  where $\mathcal{H} = (i\sigma_2 H^*, H)$ and $R = (U \; D)^T$ is an $SU(2)_R$ doublet;

- In the triplet model

$$\begin{aligned}\mathcal{L}_s^{\text{triplet}} = & -\text{tr}[\bar{L}^i m_L^i L^i] - \text{tr}[\bar{R}^i m_R^i R^i] - \text{tr}[\bar{R}'^i m_R^i R'^i] \\ & + Y^{ij}\text{tr}[\bar{L}_L^i \mathcal{H} R_R^j] + Y^{ij}\text{tr}[\mathcal{H}\, \bar{L}_L^i R_R'^j] + \text{h.c}\,,\end{aligned} \tag{3.4}$$

$$\mathcal{L}_{\text{mix}}^{\text{triplet}} = m_L^j \lambda_L^{ij} \bar{q}_L^i Q_R^j + m_R^i \lambda_{Ru}^{ij} \bar{U}_L^i u_R^j + m_R^i \lambda_{Rd}^{ij} \bar{D}_L^i d_R^j \, . \tag{3.5}$$

  where Q is the $T_{3R} = -\frac{1}{2}$ $SU(2)_L$ doublet contained in L and U, D are the elements in the triplet R with charge 2/3 and -1/3 respectively;

- In the bidoublet model

$$\mathcal{L}_s^{\text{bidoublet}} = -\text{tr}[\bar{L}_U^i m_{Q_u}^i L_U^i] - \bar{U}^i m_U^i U^i + \left(Y_U^{ij}\text{tr}[\bar{L}_U^i \mathcal{H}]_L U_R^j + \text{h.c}\right) + (U \to D)\,, \tag{3.6}$$

$$\mathcal{L}_{\text{mix}}^{\text{bidoublet}} = m_{Q_u}^j \lambda_{Lu}^{ij} \bar{q}_L^i Q_{Ru}^j + m_U^i \lambda_{Ru}^{ij} \bar{U}_L^i u_R^j + (U, u \to D, d)\,, \tag{3.7}$$

  where again Q_u and Q_d are the doublets in L_U and L_D which have the same gauge quantum numbers of the SM left-handed quark doublet.

Everywhere i, j are flavour indices. The field content in all three cases is summarized in table 3.1.[1]

To set the correspondence between the *partial compositeness* Lagrangians that we use and models with the Higgs as a pseudo-Goldstone boson, one can take the composite Yukawa

[1]Note that we have omitted "wrong-chirality" Yukawa couplings like $\tilde{Y}^{ij}\text{tr}[\bar{Q}_R^i \mathcal{H} R_L^j]$ for simplicity. They are not relevant for the tree-level electroweak and flavour constraints and do not add qualitatively new effects to the loop contributions to the T parameter.

model		$SU(3)_c$	$SU(2)_L$	$SU(2)_R$	$U(1)_X$
doublet	Q	**3**	**2**	**1**	$\frac{1}{6}$
	R	**3**	**1**	**2**	$\frac{1}{6}$
triplet	L	**3**	**2**	**2**	$\frac{2}{3}$
	R	**3**	**1**	**3**	$\frac{2}{3}$
	R'	**3**	**3**	**1**	$\frac{2}{3}$
bidoublet	L_U	**3**	**2**	**2**	$\frac{2}{3}$
	L_D	**3**	**2**	**2**	$-\frac{1}{3}$
	U	**3**	**1**	**1**	$\frac{2}{3}$
	D	**3**	**1**	**1**	$-\frac{1}{3}$

Table 3.1. Quantum numbers of the fermionic resonances in the three models considered. All composite fields come in vector-like pairs. The X charge is related to the standard hyper-charge as $Y = T_{3R} + X$.

couplings Y^{ij} in (3.2),(3.4) and (3.6) to be proportional to m_ψ/f in (3.1), where m_ψ is a common fermion mass, up to a model dependent factor of $O(1)$. From the point of view of models with pGB Higgs, all the three models belong to the class of doubly tuned CHM, as they can be traced back to MCHM$_4$,MCHM$_5$ and MCHM$_{10}$ respectively, to which eq. (3.1) refers.

3.2 Flavour structures

Quark masses and mixings are generated after electroweak symmetry breaking from the composite-elementary mixing. To follow the conventions of chapter 1: the states with vanishing mass at $v = 0$ obtain the standard Yukawa couplings, in matrix notation,

$$\hat{y}_u \approx s_{Lu} \cdot U_{Lu} \cdot Y_U \cdot U_{Ru}^\dagger \cdot s_{Ru} \tag{3.8}$$

where

$$s_X^{ii} = \lambda_{Xi}/\sqrt{1+(\lambda_{Xi})^2},\ X = L, R\ , \tag{3.9}$$
$$\lambda_{Lu} = \mathrm{diag}(\lambda_{Lu1}, \lambda_{Lu2}, \lambda_{Lu3}) \cdot U_{Lu}\ , \tag{3.10}$$
$$\lambda_{Ru} = U_{Ru}^\dagger \cdot \mathrm{diag}(\lambda_{Ru1}, \lambda_{Ru2}, \lambda_{Ru3})\ , \tag{3.11}$$

and similarly for $\hat{y}_d$. Notice the change of notation with respect to the general formula $\hat{y}_u \simeq \epsilon_L \cdot g_\psi \cdot \epsilon_R$ given in (2.13).

Here and in the following, the left-handed mixings are different for u and d quarks, $s_{Lu} \neq s_{Ld}$, only in the bi-doublet model. At the same time, in the $v = 0$ limit, the remaining states have mass m_ψ or $m_\psi/\sqrt{1+(\lambda_X)^2}$, respectively if they mix or do not mix with the elementary fermions.

While the effective Yukawa couplings $\hat{y}_{u,d}$ must have the known hierarchical form, the Yukawa couplings in the strong sector, $Y_{U,D}$, could be structureless *anarchic* matrices (see

e.g. [60,71–77]). However, to ameliorate flavour problems, one can also impose global flavour symmetries on the strong sector. We discuss three cases in the following.

Anarchy

In the anarchic model, the $Y_{U,D}$ are anarchic matrices, with all entries of similar order, and the Yukawa hierarchies are generated by hierarchical mixings λ. From a low energy effective theory point of view, the requirement to reproduce the observed quark masses and mixings fixes the relative size of the mixing parameters up to – a priori unknown – functions of the elements in $Y_{U,D}$. We follow the common approach to replace functions of Yukawa couplings by appropriate powers of "average" Yukawas $Y_{U*,D*}$, keeping in mind that this introduces $O(1)$ uncertainties in all observables. In this convention, assuming $\lambda_{X3} \gg \lambda_{X2} \gg \lambda_{X1}$, the quark Yukawas are given by

$$y_u = Y_{U*} s_{Lu1} s_{Ru1} \ , \qquad y_c = Y_{U*} s_{Lu2} s_{Ru2} \ , \qquad y_t = Y_{U*} s_{Lu3} s_{Ru3} \ . \tag{3.12}$$

and similarly for the $Q = -1/3$ quarks. In the doublet and triplet models, the entries of the CKM matrix are approximately given by

$$V_{ij} \sim \frac{s_{Li}}{s_{Lj}} \ , \tag{3.13}$$

where $i < j$. Using eqs. (3.12) and (3.13), one can trade all but one of the $s_{L,R}$ for known quark masses and mixings. We choose the free parameter as

$$x_t \equiv s_{L3}/s_{Ru3}. \tag{3.14}$$

In the bidoublet model, instead of (3.13) one has in general two different contributions to V_{ij}

$$V_{ij} \sim \frac{s_{Ldi}}{s_{Ldj}} \pm \frac{s_{Lui}}{s_{Luj}} \ . \tag{3.15}$$

Given the values of all quark masses and mixings, the hierarchy $\lambda_{X3} \gg \lambda_{X2} \gg \lambda_{X1}$ is only compatible with s_{Lui}/s_{Luj} being at most comparable to s_{Ldi}/s_{Ldj}. In view of this, the two important parameters are

$$x_t \equiv s_{Lt}/s_{Rt} \ , \qquad z \equiv s_{Lt}/s_{Lb} \ . \tag{3.16}$$

The requirement to reproduce the large top quark Yukawa ($m_t = \frac{y_t}{\sqrt{2}} v$)

$$y_t = s_{Lt} Y_{U*} s_{Rt}, \tag{3.17}$$

restricts x_t to a limited range around one[2],

$$\frac{y_t}{Y_{U*}} < x_t < \frac{Y_{U*}}{y_t} \ , \tag{3.18}$$

while we take z throughout to be greater than or equal to 1.

From now on we identify Y_{U*} and Y_{D*} with the parameter Y of (3.1).

[2]In our numerical analysis, we will take $y_t = 0.78$, which is the running $\overline{\text{MS}}$ coupling at 3 TeV.

$\mathbf{U(3)^3}$

In the $U(3)^3$ models [78–80] one tries to ameliorate the flavour problem of the anarchic model by imposing a global flavour symmetry, at the price of giving up the potential explanation of the generation of flavour hierarchies. Concretely, one assumes the strong sector to be invariant under the diagonal group $U(3)_{Q+U+D}$ or $U(3)_{Q^u+U} \times U(3)_{Q^d+D}$. The composite-elementary mixings are the only sources of breaking of the flavour symmetry of the composite sector and of the $U(3)_q \times U(3)_u \times U(3)_d$ flavour symmetry of the elementary sector. We consider two choices.

1. In *left-compositeness*, to be called $\boldsymbol{U(3)^3_{\mathbf{LC}}}$ in short, the left mixings are proportional to the identity, thus linking q to Q (Q^u, Q^d) into $U(3)_{Q+U+D+q}$ (or $U(3)_{Q^u+Q^d+U+D+q}$), and the right mixings λ_{Ru}, λ_{Rd} are the only source of $U(3)^3$ breaking.

2. In *right-compositeness*, to be called $\boldsymbol{U(3)^3_{\mathbf{RC}}}$ in short, the right mixings link u to U and d to D into $U(3)_{Q^u+U+u} \times U(3)_{Q^d+D+d}$, while the left mixings λ_{Lu}, λ_{Ld} are the only source of $U(3)^3$ breaking.

All the composite-elementary mixings are then fixed by the known quark masses and CKM angles, up to the parameters x_t (and, in the bidoublet model, z), which are defined as in (3.14, 3.16). Compared to the anarchic case, one now expects the presence of resonances related to the global symmetry $U(3)_{Q+U+D}$ or $U(3)_{Q^u+U} \times U(3)_{Q^d+D}$, which in the following will be called flavour gauge bosons[3] and assumed to have the same masses m_ρ and g_ρ as the gauge resonances. Note that left-compositeness can be meaningfully defined for any of the three cases for the fermion representations, whereas right-compositeness allows to describe flavour violations only in the bidoublet model.

$\mathbf{U(2)^3}$

In $U(2)^3$ models one considers a $U(2)_q \times U(2)_u \times U(2)_d$ symmetry, under which the first two generations of quarks transform as doublets and the third generation as singlets, broken in specific directions dictated by minimality [27, 28]. Compared to $U(3)^3$, one has a larger number of free parameters, but can break the flavour symmetry *weakly*, since the large top Yukawa is invariant under $U(2)^3$.

Analogously to the $U(3)^3$ case, in the strong sector the flavour groups are $U(2)_{Q+U+D}$ (or $U(2)_{Q^u+U} \times U(2)_{Q^d+D}$) and:

1. In left-compositeness, to be called $\boldsymbol{U(2)^3_{\mathbf{LC}}}$, the left mixings are diagonal with the first two entries equal to each other and the only sources of $U(2)^3$ breaking reside in the right-handed mixings.

2. In right-compositenss, to be called $\boldsymbol{U(2)^3_{\mathbf{RC}}}$, the right mixings are diagonal with the first two entries equal to each other and the only sources of $U(2)^3$ breaking reside in the left-handed mixings.

[3] We will only allow flavour gauge bosons related to the $SU(3)$ subgroups of the $U(3)$ factors.

Again we expect the presence of flavour gauge bosons associated with the global symmetries of the strong sector. As before right-compositeness can be meaningfully defined only in the bidoublet model.

3.3 Electroweak precision constraints

In this section we discuss electroweak precision constraints that hold independently of the flavour structure. Among the models considered, only $U(3)^3_{\rm LC}$ is subject to additional electroweak constraints, to be discussed in section 3.5.1.

3.3.1 "UV" oblique corrections

In the models under consideration the Higgs couplings to vectors are shifted by an amount $c_V^2 = 1 - v^2/f^2$, which implies the famous IR-contributions to S, T of eq. (1.15). However, the presence of composite resonances also induces "UV" contributions to S and T.

- **S parameter**. As well known, the S parameter receives a tree-level contribution, which for degenerate composite vectors reads [50]

$$S = \frac{8\pi v^2}{m_\rho^2} \,, \tag{3.19}$$

  independently of the choice of fermion representations. Experimentally, the recent global electroweak fit [16] finds $S = 0.03 \pm 0.10$ and $T = 0.05 \pm 0.12$. Requiring 2σ consistency with these results of the tree level correction to S, which largely exceeds the IR one of eq. (1.15) and has the same sign, gives the bound

$$m_\rho > 2.6\,\text{TeV}\,. \tag{3.20}$$

- **T parameter**. It strongly depends on the choice of the fermion representations. We present here simplified formulae valid in the three models for a common fermion resonance mass m_ψ and developed to first nonvanishing order in $\lambda_{Lt}, \lambda_{Rt}$, as such only valid for small s_{Lt}, s_{Rt}.

  In the doublet model the leading contribution to $\hat{T}$, proportional to λ_{Rt}^4, reads

$$\hat{T} = \frac{71}{140}\frac{N_c}{16\pi^2}\frac{m_t^2}{m_\psi^2}\frac{Y^2}{x_t^2}\,. \tag{3.21}$$

  In the bidoublet model one obtains from a leading λ_{Lt}^4 term

$$\hat{T} = -\frac{107}{420}\frac{N_c}{16\pi^2}\frac{m_t^2}{m_\psi^2}x_t^2 Y_U^2\,. \tag{3.22}$$

  In the triplet model the leading contributions are

$$\hat{T} = \left(\log\frac{\Lambda^2}{m_\psi^2} - \frac{1}{2}\right)\frac{N_c}{16\pi^2}\frac{m_t^2}{m_\psi^2}\frac{Y^3}{y_t x_t}\,, \quad \text{and} \quad \hat{T} = \frac{197}{84}\frac{N_c}{16\pi^2}\frac{m_t^2}{m_\psi^2}x_t^2 Y^2\,, \tag{3.23}$$

Observable	Bounds on m_ψ [TeV]		
	doublet	triplet	bidoublet
T	$0.28\ Y/x_t$	$0.51\ \sqrt{Y^3/x_t}$, $0.60\ x_t Y$	$0.25\ x_t Y_U$
R_b (g^L_{Zbb})	$5.6\ \sqrt{x_t Y}$		$6.5\ Y_D\sqrt{x_t/Y_U}/z$
$B \to X_s\gamma$ (g^R_{Wtb})	$0.44\ \sqrt{Y/x_t}$	$0.44\ \sqrt{Y/x_t}$	0.61

Table 3.2. Lower bounds on the fermion resonance mass $m_\psi = Yf$ in TeV from electroweak precision observables. A blank space means no significant bound.

where the first comes from λ^2_{Rt} and the second from λ^4_{Lt}. Note the logarithmically divergent contribution to the λ^2_{Rt} term that is related to the explicit breaking of the $SU(2)_R$ symmetry in the elementary-composite fermion mixing and would have to be cured in a more complete model.

Imposing the experimental bound at 2σ, eqs. (3.21, 3.22, 3.23) give rise to the bounds on the first line in table 3.2 (where we set $\log(\Lambda/m_\psi) = 1$). Here however there are two caveats. First, as mentioned, eqs. (3.21, 3.22, 3.23) are only valid for small mixing angles. Furthermore, for moderate values of f, a cancellation could take place between the fermionic contributions and the infrared logs of the bosonic contribution to T. As we shall see, the bounds from S and T are anyhow not the strongest ones that we will encounter: they are compatible with $m_\psi \lesssim 1$ TeV for $Y = 1$ to 2 and $g_\rho = 3$ to 5. Note that here and in the following m_ψ represents the mass of the composite fermions that mix with the elementary ones, whereas, as already noticed, the "custodians" have mass $m_\psi/\sqrt{1+(\lambda_X)^2}$.

3.3.2 Modified Z couplings

In all three models for the electroweak structure, fields with different $SU(2)_L$ quantum numbers mix after electroweak symmetry breaking, leading to modifications in Z couplings which have been precisely measured at LEP. Independently of the flavour structure, an important constraint comes from the Z partial width into b quarks, which deviates by 2.5σ from its best-fit SM value [16]

$$R_b^{\rm exp} = 0.21629(66)\ , \qquad\qquad R_b^{\rm SM} = 0.21474(3)\ . \tag{3.24}$$

Writing the left- and right-handed Z couplings as

$$\frac{g}{c_w}\bar{b}\gamma^\mu\left[(-\tfrac{1}{2}+\tfrac{1}{3}s_w^2+\delta g^L_{Zbb})P_L + (\tfrac{1}{3}s_w^2+\delta g^R_{Zbb})P_R\right] bZ_\mu\,, \tag{3.25}$$

one gets

$$\delta g^L_{Zbb} = \frac{v^2Y_D^2}{2m_D^2}\frac{xy_t}{Y_U}\,a + \frac{g_\rho^2v^2}{4m_\rho^2}\frac{xy_t}{Y_U}\,b\,, \qquad \delta g^R_{Zbb} = \frac{v^2Y_D^2}{2m_D^2}\frac{y_b^2Y_U}{x_ty_tY_D^2}\,c + \frac{g_\rho^2v^2}{4m_\rho^2}\frac{y_b^2Y_U}{x_ty_tY_D^2}\,d\,, \tag{3.26}$$

with the coefficients

	doublet	triplet	bidoublet
a	$1/2$	0	$1/(2z^2)$
b	$1/2$	0	$1/z^2$

	doublet	triplet	bidoublet
c	$-1/2$	$-1/2$	0
d	$-1/2$	-1	0

The vanishing of some entries in (3.26) can be simply understood by the symmetry considerations of ref. [81]. As manifest from their explicit expressions the contributions proportional to a and c come from mixings between elementary and composite fermions with different $SU(2) \times U(1)$ properties, whereas the contributions proportional to b and d come from ρ-Z mixing. Taking $Y_U = Y_D = Y$, $m_D = Yf$ and $m_\rho = g_\rho f$, all these contributions scale however in the same way as $1/(f^2 Y)$.

It is important to note that δg^L_{Zbb} is always positive or 0, while δg^R_{Zbb} is always negative or 0, while the sign of the SM couplings is opposite. As a consequence, in all 3 models considered, the tension in eq. (3.24) is *always increased*. Allowing the discrepancy to be at most 3σ, we obtain the numerical bounds in the second row of table 3.2. The bound on m_ψ in the doublet model is highly significant since $x_t Y > 1$, whereas it is irrelevant in the triplet model and can be kept under control in the bidoublet model for large enough z (but see below). In the triplet model, there is a bound from the modification of the right-handed coupling, which is however insignificant.

3.3.3 Right-handed W couplings

Analogously to the modified Z couplings, also the W couplings are modified after EWSB. Most importantly, a right-handed coupling of the W to quarks is generated. The most relevant experimental constraint on such coupling is the branching ratio of $B \to X_s\gamma$, because a right-handed Wtb coupling lifts the helicity suppression present in this loop-induced decay in the SM [82]. Writing this coupling as

$$\frac{g}{\sqrt{2}} \delta g^R_{Wtb} (\bar{t} \gamma^\mu P_R b) W^+_\mu \,, \tag{3.27}$$

one gets

$$\delta g^R_{Wtb} = \frac{v^2 Y_U Y_D}{2 m_Q m_U} \frac{y_b}{x_t Y_U}\, a + \frac{g_\rho^2 v^2}{4 m_\rho^2} \frac{y_b}{x_t Y_U}\, b \,, \tag{3.28}$$

with the coefficients

	doublet	triplet	bidoublet
a	1	1	$-2x_t y_t/Y$
b	1	1	0

The coefficients in the bidoublet model vanish at quadratic order in the elementary-composite mixings as a consequence of a discrete symmetry [81]. The nonzero value for a in the table is due to the violation of that symmetry at quartic order [82]. The contribution to the Wilson coefficient $C_{7,8}$, defined as in [83], reads

$$C_{7,8} = \frac{m_t}{m_b} \frac{\delta g^R_{Wtb}}{V_{tb}} A_{7,8}(m_t^2/m_W^2) \tag{3.29}$$

where $A_7(m_t^2/m_W^2) \approx -0.80$ and $A_8(m_t^2/m_W^2) \approx -0.36$.

Since the $B \to X_s\gamma$ decay receives also UV contributions involving composite dynamics, we impose the conservative bound that the SM plus the IR contributions above do not exceed the experimental branching ratio by more than 3σ. In this way we find the bound in the last row of table 3.2.

3.4 Constraints on the anarchic model

We now discuss constraints that are specific to the anarchic model, as defined above, and hold in addition to the bounds described in the previous section.

3.4.1 Tree-level $\Delta F = 2$ FCNCs

In the anarchic model exchanges of gauge resonances give rise to $\Delta F = 2$ operators at tree level. Up to corrections of order v^2/f^2, the Wilson coefficients of the operators

$$Q_V^{dLL} = (\bar{d}_L^i \gamma^\mu d_L^j)(\bar{d}_L^i \gamma^\mu d_L^j)\,, \qquad Q_V^{dRR} = (\bar{d}_R^i \gamma^\mu d_R^j)(\bar{d}_R^i \gamma^\mu d_R^j)\,, \tag{3.30}$$

$$Q_V^{dLR} = (\bar{d}_L^i \gamma^\mu d_L^j)(\bar{d}_R^i \gamma^\mu d_R^j)\,, \qquad Q_S^{dLR} = (\bar{d}_R^i d_L^j)(\bar{d}_L^i d_R^j)\,, \tag{3.31}$$

can be written as

$$C_D^{dAB} = \frac{g_\rho^2}{m_\rho^2} g_{Ad}^{ij} g_{Bd}^{ij} c_D^{dAB}, \qquad A, B = L, R, \quad D = V, S, \tag{3.32}$$

and with the obvious replacements for up-type quarks, relevant for D-$\bar{D}$ mixing.

The couplings g_{qA}^{ij} with $i \neq j$ contain two powers of elementary-composite mixings. In the doublet and triplet models, one can use eqs. (3.12)–(3.14) to write them as ($\xi_{ij} = V_{tj} V_{ti}^*$)

$$g_L^{ij} \sim s_{Ldi} s_{Ldj} \sim \xi_{ij} \frac{x_t y_t}{Y}\,, \tag{3.33}$$

$$g_{Ru}^{ij} \sim s_{Rui} s_{Ruj} \sim \frac{y_{u^i} y_{u^j}}{Y y_t x_t \xi_{ij}}\,, \tag{3.34}$$

$$g_{Rd}^{ij} \sim s_{Rdi} s_{Rdj} \sim \frac{y_{d^i} y_{d^j}}{Y y_t x_t \xi_{ij}}\,. \tag{3.35}$$

In the bidoublet model, one has

$$g_{Ld}^{ij} \sim g_{Lu}^{ij} \sim \xi_{ij} \frac{x_t y_t}{Y_U}\,, \qquad g_{Rd}^{ij} \sim z^2 \frac{Y_U}{Y_D^2} \frac{y_{d^i} y_{d^j}}{y_t x_t \xi_{ij}}\,. \qquad g_{Ru}^{ij} \sim \frac{y_{u^i} y_{u^j}}{Y_U y_t x_t \xi_{ij}}\,. \tag{3.36}$$

The coefficients c_D^{AB} depend on the quantum numbers of the composite fermions and can be explicitly computed. They are of order $0.5 \div 1$ and are listed in the appendix of [3].

The experimental bounds on the real and imaginary parts of the Wilson coefficients have been given in [84, 85]. Since the phases of the coefficients can be of order one and are uncorrelated, we derive the bounds assuming the phase to be maximal. We obtain the bounds in the first eight rows of table 3.3. As is well known, by far the strongest bound,

Observable	Bounds on m_ψ [TeV]		
	doublet	triplet	bidoublet
ϵ_K (Q_S^{LR})	14	14	14 z
ϵ_K (Q_V^{LL})	2.7 x_t	3.9 x_t	3.9 x_t
B_d-$\bar{B}_d$ (Q_S^{LR})	0.7	0.7	0.7
B_d-$\bar{B}_d$ (Q_V^{LL})	2.3 x_t	3.4 x_t	3.4 x_t
B_s-$\bar{B}_s$ (Q_S^{LR})	0.6	0.6	0.6
B_s-$\bar{B}_s$ (Q_V^{LL})	2.3 x_t	3.4 x_t	3.4 x_t
D-$\bar{D}$ (Q_S^{LR})	0.5	0.5	0.5
D-$\bar{D}$ (Q_V^{LL})	0.4 x_t	0.6 x_t	0.6 x_t
$K_L \to \mu\mu$ $(f$–$\psi)$	0.56 $\sqrt{Y/x_t}$	0.56 $\sqrt{Y/x_t}$	
$K_L \to \mu\mu$ $(Z$–$\rho)$	0.39 $\sqrt{Y/x_t}$	0.56 $\sqrt{Y/x_t}$	

Table 3.3. Flavour bounds on the fermion resonance mass m_ψ in TeV in the anarchic model.

shown in the first row, comes from the scalar left-right operator in the kaon system which is enhanced by RG evolution and a chiral factor. Note in particular the growth with z of the bound in the bidoublet case, which counteracts the $1/z$ behaviour of the bound from R_b. But also the left-left vector operators in the kaon, B_d and B_s systems lead to bounds which are relevant in some regions of parameter space. The bounds from the D system are subleading.

3.4.2 Flavour-changing Z couplings

Similarly to the modified flavour-conserving Z couplings discussed in section 3.3.2, also *flavour-changing* Z couplings are generated in the anarchic model. In the triplet and doublet models, as well as in the bidoublet model, since the down-type contributions to the CKM matrix are not smaller than the up-type contributions in (3.15), one has

$$\delta g^L_{Zd^id^j} \sim \frac{s_{Ldi}s_{Ldj}}{s^2_{Lb}}\,\delta g^L_{Zbb} \sim \xi_{ij}\,\delta g^L_{Zbb}\,, \tag{3.37}$$

$$\delta g^R_{Zd^id^j} \sim \frac{s_{Rdi}s_{Rdj}}{s^2_{Rb}}\,\delta g^R_{Zbb} \sim \frac{y_{d^i}y_{d^j}}{y_b^2\xi_{ij}}\,\delta g^R_{Zbb}\,. \tag{3.38}$$

In the $b \to s$ case, a global analysis of inclusive and exclusive $b \to s\ell^+\ell^-$ decays [83] finds $|\delta g^{L,R}_{Zbs}| \lesssim 8\times10^{-5}$, while in the $s \to d$ case, one finds $|\delta g^{L,R}_{Zsd}| \lesssim 6\times10^{-7}$ from the $K_L \to \mu^+\mu^-$ decay [86][4]. Using (3.37) one finds that the resulting constraints on the left-handed coupling are comparable for $b \to s$ and $s \to d$. Since they are about a factor of 3 weaker than the corresponding bound from $Z \to b\bar{b}$, we refrain from listing them in table 3.3, but their presence shows that the strong bound from R_b cannot simply be circumvented by a fortuitous

[4]The decay $K^+ \to \pi^+\nu\bar{\nu}$ leads to a bound $|\delta g^{L,R}_{Zsd}| \lesssim 3\times10^{-6}$ at 95% C.L. and is thus currently weaker than $K_L \to \mu^+\mu^-$, even though it is theoretically much cleaner.

cancellation. In the case of the right-handed coupling, one finds that the constraint from $K_L \to \mu^+\mu^-$ is an order of magnitude stronger than the one from $b \to s\ell^+\ell^-$, and also much stronger than the bound on the right-handed coupling coming from $Z \to b\bar{b}$. The numerical bounds we obtain are shown in the last two rows of table 3.3 from the contributions with fermion or gauge boson mixing separately since, in constrast to $Z \to b\bar{b}$, the two terms are multiplied by different $O(1)$ parameters in the flavour-violating case.

3.4.3 Loop-induced chirality-breaking effects

Every flavour changing effect discussed so far originates from tree-level chirality-conserving interactions of the vector bosons, either the elementary W_μ and Z_μ or the composite ρ_μ. At loop level, chirality-breaking interactions occur as well, most notably with the photon and the gluon, which give rise in general to significant $\Delta F = 1$ flavour-changing effects ($b \to s\gamma$, ϵ'_K, $\Delta A_{CP}(D \to PP)$), as well as to electric dipole moments of the light quarks. In the weak mixing limit between the elementary and the composite fermions, explicit calculations of some of the $\Delta F = 1$ effects have been made in [82, 87, 88], obtaining bounds in the range $m_\psi > (0.5\text{–}1.5)Y$ TeV. For large CP-violating phases the generated EDMs for the light quarks can be estimated consistent with the current limit on the neutron EDM only if $m_\psi > (3\text{–}5)Y$ TeV, where the limit is obtained from the analysis of [89].

3.4.4 Direct bounds on vector resonances

Direct production of vector resonances and subsequent decay to light quarks can lead to a peak in the invariant mass distribution of $pp \to jj$ events at the LHC. In the anarchic model, due to the small degree of compositeness of first generation quarks, the coupling of vector resonances to a first generation quark-antiquark pair is dominated by mixing with the SM gauge bosons and thus suppressed by $g_{\rm el}^2/g_\rho$. For a 3 TeV gluon resonance at the LHC with $\sqrt{s} = 8$ TeV, we expect

$$\sigma(pp \to G^*) = \frac{2\pi}{9s}\frac{g_3^4}{g_\rho^2}\left[\mathcal{L}_{u\bar{u}}(s, m_\rho^2) + \mathcal{L}_{d\bar{d}}(s, m_\rho^2)\right] \approx \frac{5\text{ fb}}{g_\rho^2}, \tag{3.39}$$

where $\mathcal{L}_{q\bar{q}}(s, \hat{s})$, with $q = u, d$, is the parton-parton luminosity function at hadronic (partonic) center of mass energy $\sqrt{s}$ ($\sqrt{\hat{s}}$). The ATLAS collaboration has set an upper bound of 7 fb on the cross section times branching ratio to two jets times the acceptance [90], and a similar bound has been obtained by CMS [91]. Given that the gluon resonance will decay dominantly to top quarks, we conclude that the bound is currently not relevant, even for small g_ρ.

A similar argument holds in the case of the dijet angular distribution, which can be used to constrain local four-quark operators mediated by vector resonances. Following the discussion in the appendix of [3], we obtain the bound

$$m_\rho > \frac{4.5\text{ TeV}}{g_\rho} \tag{3.40}$$

which, in combination with the bound on m_ρ from the S parameter, is irrelevant for $g_\rho \gtrsim 1.5$.

Partial summary and prospects on anarchy

If the bound coming from the Q_S^{LR} contribution to ϵ_K is taken at face value, the fermion resonances should be far too heavy to be consistent with a naturally light Higgs boson and certainly unobservable, either directly or indirectly. Note in particular the growth of this bound with z in the bidoublet model.

In view of the fact that this bound carries an $O(1)$ uncertainty, one might however speculate on what happens if this constraint is ignored. As visible from table 3.3, with the exception of the first line, all the strongest bounds on m_ψ in the bidoublet or in the triplet models can be reduced down to about 1 TeV by taking $x_t = \frac{1}{3}$ to $\frac{1}{4}$. This however correspondingly requires $Y = 3$ to 4 (and maximal right-handed mixing) which pushes up the bounds from $K_L \to \mu^+\mu^-$ and is not consistent with $m_\psi = Yf$ and $f \gtrsim 0.5$ TeV. The loop-induced chirality-breaking effects on ϵ' and ΔA_{CP} in $D \to PP$ decays would also come into play. Altogether, even neglecting the bound from $\epsilon_K(Q_S^{LR})$, fermion resonances below about 1.5 TeV seem hard to conceive.

3.5 Constraints on $U(3)^3$

We now discuss the constraints specific to $U(3)^3$. In $U(3)^3_{\rm LC}$ the sizable degree of compositeness of light left-handed quarks leads to additional contributions to electroweak precision observables; in $U(3)^3_{\rm RC}$ FCNCs arise at the tree level. In both cases collider bounds on the compositeness of light quarks place important constraints. Our analysis follows and extends the analysis in [80].

3.5.1 Electroweak precision constraints specific to $U(3)^3$

The bounds from R_b as well as the S and T parameters discussed in section 3.3 are also valid in $U(3)^3$, with one modification: in $U(3)^3_{\rm LC}$ the contributions to the $\hat{T}$ parameter proportional to s_{Lt}^4 have to be multiplied by 3 since all three generations of left-handed up-type quarks contribute. The corresponding bounds remain nevertheless relatively mild.

In addition, an important constraint arises from the partial width of the Z into hadrons normalized to the partial width into leptons, which was measured precisely at LEP

$$R_h^{\rm exp} = 20.767(25)\ , \qquad\qquad R_h^{\rm SM} = 20.740(17)\ , \tag{3.41}$$

showing a 1.1σ tension with the best-fit SM prediction [16].

In $U(3)^3_{\rm LC}$ the modified left-handed Z couplings of up and down quarks are equal to the ones of the t and b respectively, while the same is true in $U(3)^3_{\rm RC}$ for the right-handed modified couplings. Analogously to the discussion in section 3.3.2, one can write the modified Z coupling of the top as

$$\frac{g}{c_w}\bar{t}\gamma^\mu\left[(\tfrac{1}{2} - \tfrac{2}{3}s_w^2 + \delta g^L_{Ztt})P_L + (-\tfrac{2}{3}s_w^2 + \delta g^R_{Ztt})P_R\right] tZ_\mu\,, \tag{3.42}$$

and one has

$$\delta g^L_{Ztt} = \frac{v^2Y_U^2}{2m_U^2}\frac{x_t y_t}{Y_U}\,a + \frac{g_\rho^2 v^2}{4m_\rho^2}\frac{x_t y_t}{Y_U}\,b\,, \qquad \delta g^R_{Ztt} = \frac{v^2Y_U^2}{2m_U^2}\frac{y_t}{x_t Y_U}\,c + \frac{g_\rho^2 v^2}{4m_\rho^2}\frac{y_t}{x_t Y_U}\,d\,, \tag{3.43}$$

with

	doublet	triplet	bidoublet
a	$-1/2$	-1	$-1/2$
b	$-1/2$	-1	-1

	doublet	triplet	bidoublet
c	$1/2$	0	0
d	$1/2$	0	0

Since the right-handed Z coupling to b and t receives no contribution in the bidoublet model, there is no additional bound from R_h in $U(3)^3_{\rm RC}$. In $U(3)^3_{\rm LC}$we find the numerical bounds shown in table 3.4.

In $U(3)^3_{\rm LC}$ an additional bound arises from violations of quark-lepton universality. Writing the W couplings as

$$\frac{g}{\sqrt{2}}(1+\delta g^L_W)\bar{u}\,V_{ui}\gamma^\mu P_L d_i W^+_\mu\,, \tag{3.44}$$

we find

$$\delta g^L_W = \frac{Y_U^2 v^2}{2m_U^2}\frac{x_t y_t}{Y_U}\,a_u + \frac{Y_D^2 v^2}{2m_D^2}\frac{x_t y_t}{Y_U}\,a_d + \frac{g_\rho^2 v^2}{4m_\rho^2}\frac{x_t y_t}{Y_U}\,b\,, \tag{3.45}$$

with

	doublet	triplet	bidoublet
a_u	$-1/2$	$-1/2$	$-1/2$
a_d	$-1/2$	$-1/2$	$-1/(2z^2)$
b	-1	-1	-1

The usual experimental constraint on the strength of the $W\bar{u}d_i$ couplings, normalized to the leptonic ones, is expressed by $(1+\delta g^L_W)^2\sum_i|V_{ui}|^2-1=(-1\pm 6)\times 10^{-4}$, which, from the unitarity of the V_{ij} matrix, becomes $2\delta g^L_W=(-1\pm 6)\times 10^{-4}$. By requiring it to be fulfilled within 2σ, we find the numerical bounds in table 3.4.

Finally we note that, in contrast to the anarchic case, there are no *flavour-changing* Z couplings neither in $U(3)^3_{\rm LC}$ nor in $U(3)^3_{\rm RC}$. In the former case this is a general property of chirality-conserving bilinears, while in the latter it is a consequence of the fact that only the down-type mixings λ_{Ld} affect the Z vertex, which thus becomes flavour-diagonal in the mass basis.

3.5.2 Tree-level $\Delta F = 2$ FCNCs

While in $U(3)^3_{\rm LC}$ there are no tree-level FCNCs at all [80], minimally flavour violating tree-level FCNCs are generated in $U(3)^3_{\rm RC}$ [28, 92]. The Wilson coefficients of $\Delta F=2$ operators are given by (3.32), and the couplings

$$g^{ij}_{Ld} = \xi_{ij}\frac{x_t y_t}{Y_U}\,, \qquad\qquad g^{ij}_{Rd}\approx 0\,. \tag{3.46}$$

g^{ij}_{Ld} has the same form of the K^{ij}_{LL} structure in the effective $U(3)^3$ approach, see eq. (1.24) in chapter 1. However, there is also a suppression proportional to s^2_{Lt} coming from the elementary-composite mixing. We obtain the bounds shown in table 3.5. The bound from D-$\bar{D}$ mixing turns out to be numerically irrelevant.

Observable	Bounds on m_ψ [TeV]		
	doublet	triplet	bidoublet
R_h	$7.2\ \sqrt{x_t Y}$	$6.0\ \sqrt{x_t Y}$	$4.9\ \sqrt{x_t Y_U}$
$V_{\rm CKM}$	$7.4\ \sqrt{x_t Y}$	$7.4\ \sqrt{x_t Y}$	$6.0\ \sqrt{x_t Y_U}$
$pp \to jj$ ang. dist.	$3.4\ x_t$	$4.2\ x_t$	$4.2\ x_t$

Table 3.4. Lower bounds on the fermion resonance mass m_ψ in TeV in $U(3)^3_{\rm LC}$.

Observable	Bounds on m_ψ [TeV]
$\epsilon_K(Q_V^{LL})$	$3.7\ x_t$
B_d-$\bar{B}_d$	$3.2\ x_t$
B_s-$\bar{B}_s$	$3.6\ x_t$
$pp \to jj$ ang. dist.	$3.0/x_t$

Table 3.5. Lower bounds on the fermion resonance mass m_ψ in TeV in $U(3)^3_{\rm RC}$ (bidoublet model).

We stress that, in contrast to the anarchic case, there is no $O(1)$ uncertainty in these bounds since the composite Yukawas are proportional to the identity. Furthermore, since the model is minimally flavour violating, there is no contribution to the meson mixing phases and the new physics effects in the K, B_d and B_s systems are prefectly correlated.

3.5.3 Loop-induced chirality-breaking effects

Flavour-changing chirality-breaking effects in $U(3)^3$ occur when elementary-composite mixings are included inside the loops. At least for moderate mixings, the bounds are of the form $m_\psi > (0.5\text{–}1.5)\sqrt{Y/x_t}$ TeV in the $U(3)^3_{\rm LC}$ case, or $m_\psi > (0.5\text{–}1.5)\sqrt{Y x_t}$ TeV in the $U(3)^3_{\rm RC}$ case. The stronger bounds from quark EDMs, similar to the ones of the anarchic case, disappear if the strong sector conserves CP. This is automatically realized, in our effective Lagrangian description, if the "wrong chirality" Yukawas vanish or are aligned in phase with the Y's. On the contrary, in the anarchic case this condition is in general not sufficient to avoid large EDMs.

3.5.4 Compositeness constraints

Since one chirality of first-generation quarks has a sizable degree of compositeness in the $U(3)^3$ models, a significant constraint arises from the angular distribution of dijet events at LHC, which is modified by local four-quark operators obtained after integrating out the heavy vector resonances related to the global $SU(3)_c \times SU(2)_L \times SU(2)_R \times U(1)_X$ as well as the flavour symmetry in the strong sector, $U(3)$ in the case of $U(3)^3_{\rm LC}$ and $U(3) \times U(3)$ in the case of $U(3)^3_{\rm RC}$.

In general, there are ten four-quark operators in the dijet angular distribution [93]. The relevant ones in $U(3)^3_{\rm LC}$ are $\mathcal{O}^{(1)}_{qq} = (\bar{q}_L \gamma^\mu q_L)^2$ and $\mathcal{O}^{(8)}_{qq} = (\bar{q}_L \gamma^\mu T^a q_L)^2$. Their Wilson coeffi-

cients can be explicitly computed and read

$$C_{qq}^{(1)} = -\frac{a}{36}\frac{g_\rho^2}{m_\rho^2}\left(\frac{x_t y_t}{Y_U}\right)^2 , \qquad C_{qq}^{(8)} = -\frac{g_\rho^2}{m_\rho^2}\left(\frac{x_t y_t}{Y_U}\right)^2 , \tag{3.47}$$

where $a = 5$ in the doublet model and $a = 17$ in the triplet and bidoublet models. Using the updated version of [93], we obtain the bound in the last row of table 3.4. In $U(3)^3_{\rm RC}$ the operators with right-handed quarks are relevant. Numerically, we find the bound on $\mathcal{O}_{uu}^{(1)} = (\bar{u}_R\gamma^\mu u_R)^2$ to give the most significant constraint on the model parameters. Its Wilson coefficient reads

$$C_{uu}^{(1)} = -\frac{5}{9}\frac{g_\rho^2}{m_\rho^2}\left(\frac{y_t}{x_t Y_U}\right)^2 \tag{3.48}$$

and the resulting numerical constraint is shown in the last row of table 3.5.

3.5.5 Direct bounds on vector resonances

As discussed in section 3.4.4, direct bounds on m_ρ are obtained from searches for peaks in the invariant mass of dijets at LHC. In $U(3)^3$ the production cross sections can be larger than in the anarchic case due to the sizable degree of compositeness of first-generation quarks. Neglecting the contribution due to mixing of the vector resonances with the gauge bosons, the production cross section of a gluon resonance reads

$$\sigma(pp \to G^*) = \frac{2\pi}{9s} g_\rho^2 \left[s_{L,Ru}^4 \mathcal{L}_{u\bar{u}}(s, m_\rho^2) + s_{L,Rd}^4 \mathcal{L}_{d\bar{d}}(s, m_\rho^2) \right] , \tag{3.49}$$

where the L is valid in $U(3)^3_{\rm LC}$ and the R in $U(3)^3_{\rm RC}$. In $U(3)^3_{\rm LC}$ the branching ratio to two jets reads approximately

$$\mathrm{BR}(G^* \to jj) = \frac{2s_{Lu}^4 + 3s_{Ld}^4 + s_{Rb}^4}{3s_{Lu}^4 + s_{Rt}^4 + 3s_{Ld}^4 + s_{Rb}^4} , \tag{3.50}$$

and is typically larger than in the anarchic case. Similarly, in $U(3)^3_{\rm RC}$ one has

$$\mathrm{BR}(G^* \to jj) = \frac{2s_{Ru}^4 + s_{Lb}^4 + 3s_{Rd}^4}{s_{Lt}^4 + 3s_{Ru}^4 + s_{Lb}^4 + 3s_{Rd}^4} . \tag{3.51}$$

To judge if the most recent experimental bounds by ATLAS [90] and CMS [91] have already started to probe the $U(3)^3$ parameter space, we evaluate the cross section for maximal mixing, i.e. $x_t = Y/y_t$ in $U(3)^3_{\rm LC}$ and $x_t = y_t/Y$ in $U(3)^3_{\rm RC}$, for a 3 TeV gluon resonance, i.e. only marginally heavier than allowed by the S parameter (cf. table 3.2). For $U(3)^3_{\rm LC}$ we obtain

$$\sigma(pp \to G^*) \approx 13 g_\rho^2 \text{ fb} , \qquad \mathrm{BR}(G^* \to jj) \approx 58\%\ (83\%) \text{ for } Y = 1\ (4\pi) , \tag{3.52}$$

and for $U(3)^3_{\rm RC}$

$$\sigma(pp \to G^*) \approx 30 g_\rho^2 \text{ fb} , \qquad \mathrm{BR}(G^* \to jj) \approx 69\%\ (67\%) \text{ for } Y = 1\ (4\pi) . \tag{3.53}$$

This is to be compared to the ATLAS bound $\sigma \times \mathrm{BR} \times A < 7$ fb, where A is the acceptance. We conclude that, assuming an acceptance of the order of 60% [90], maximal mixing is on the border of exclusion in $U(3)^3_{\rm LC}$ and already excluded in $U(3)^3_{\rm RC}$ for a 3 TeV gluon resonance. We note however that maximal mixing is already disfavoured by the indirect bounds discussed above.

Partial summary on $U(3)^3$

As apparent from tables 3.4 and 3.5, a fermion resonance at about 1 TeV is disfavoured. In $U(3)^3_{\rm LC}$ the crucial constrains come from the EWPT due to the large mixing of the first generations quarks in their left component. Note that $x_t Y$ cannot go below $y_t \sim 1$. In $U(3)^3_{\rm RC}$ there is a clash between the tree-level $\Delta F = 2$ FCNC effects, which decrease with x_t, and the bound from the $pp \to jj$ angular distributions due to the composite nature of the light quarks in their right component, which goes like $1/x_t$. We stress again that these conclusions are more robust than in the anarchic case, since there is no uncertainty related to the composite Yukawas, which are flavour universal in the $U(3)^3$ case.

3.6 Constraints on $U(2)^3$

In $U(2)^3_{\rm LC}$ and $U(2)^3_{\rm RC}$ the first and second generation elementary-composite mixings are expected to be significantly smaller than the third generation ones, so that the electroweak precision constraints and the collider phenomenology are virtually identical to the anarchic case and the most serious problems plaguing the $U(3)^3$ models are absent. The most important difference concerns the flavour constraints.

3.6.1 Reference formulae for $U(2)^3$

For ease of the reader we recall the setup of $U(2)^3$. The strong sector can be taken invariant under a $U(2)_{Q+U+D}$ flavour symmetry acting on the first two generations of composite quarks. In right-compositeness – meaningful only in the bidoublet model – in order to generate the CKM matrix one has to consider a larger $U(2)_{Q^u+U} \times U(2)_{Q^d+D}$ symmetry. Let us define

$$Q^u = \begin{pmatrix} \boldsymbol{Q^u} \\ Q^u_3 \end{pmatrix}, \qquad U = \begin{pmatrix} \boldsymbol{U} \\ T \end{pmatrix}, \qquad q_L = \begin{pmatrix} \boldsymbol{q_L} \\ q_{3L} \end{pmatrix}, \qquad u_R = \begin{pmatrix} \boldsymbol{u_R} \\ t_R \end{pmatrix}, \tag{3.54}$$

where the first two generation doublets are written in boldface, and the same for down-type quarks. The mixing Lagrangians in the cases of *left-compositeness* and *right-compositeness* are respectively[5]

$$\begin{aligned} \mathcal{L}^{U(2)^3_{\rm LC}}_{\rm mix} &= m_{U3}\lambda_{Lu3}\,\bar{q}_{3L}Q^u_{3R} + m_{U2}\lambda_{Lu2}\,\bar{\boldsymbol{q}}_{\boldsymbol{L}}\boldsymbol{Q^u_R} + m_{U3}\lambda_{Ru3}\,\bar{T}_L t_R \\ &\quad + m_{U2}\,d_u\,(\bar{\boldsymbol{U}}_{\boldsymbol{L}}\boldsymbol{V})t_R + m_{U2}\,\bar{\boldsymbol{U}}_{\boldsymbol{L}}\Delta_u\boldsymbol{u_R} + \text{h.c.} + (u,U,t,T \to d,D,b,B) \end{aligned} \tag{3.55}$$

[5] We write the Lagrangians for the bidoublet model. The doublet and triplet cases are analogous, with Q^u and Q^d replaced by a single Q.

and

$$\mathcal{L}_{\rm mix}^{U(2)^3_{\rm RC}} = m_{U3}\lambda_{Ru3}\,\bar{T}_L t_R + m_{U2}\lambda_{Ru2}\,\bar{\boldsymbol{U}}_{\boldsymbol{L}}\boldsymbol{u}_{\boldsymbol{R}} + m_{U3}\lambda_{L(u)3}\,\bar{q}_{3L}Q^u_{3R} + m_{U3}\,d_u\,(\bar{\boldsymbol{q}}_{\boldsymbol{L}}\boldsymbol{V})Q^u_{3R} + m_{U2}\,\bar{\boldsymbol{q}}_{\boldsymbol{L}}\Delta_u\boldsymbol{Q}^{\boldsymbol{u}}_{\boldsymbol{R}} + \text{h.c.} + (u,U,t,T\to d,D,b,B). \tag{3.56}$$

The mixings in the first line of (3.55) and (3.56) break the symmetry of the strong sector down to $U(2)_q\times U(2)_u\times U(2)_d$. This symmetry is in turn broken minimally by the spurions

$$\boldsymbol{V}\sim(\mathbf{2},\mathbf{1},\mathbf{1}),\qquad \Delta_u\sim(\mathbf{2},\mathbf{2},\mathbf{1}),\qquad \Delta_d\sim(\mathbf{2},\mathbf{1},\mathbf{2}). \tag{3.57}$$

Using $U(2)^3$ transformations of the quarks they can be put in the simple form

$$\boldsymbol{V}=\begin{pmatrix}0\\ \epsilon_L\end{pmatrix},\qquad \Delta_u=\begin{pmatrix}c_u & s_u e^{i\alpha_u}\\ -s_u e^{-i\alpha_u} & c_u\end{pmatrix}\begin{pmatrix}\lambda_{Xu1} & 0\\ 0 & \lambda_{Xu2}\end{pmatrix},\qquad (u\leftrightarrow d), \tag{3.58}$$

where $X=R,L$ in left- and right-compositeness, respectively. Here we do not discuss the case of generic $U(2)^3$ breaking introduced in [89].

The SM Yukawa couplings (3.8) can be written as in eq. (1.27)

$$\hat{y}_u=\begin{pmatrix}a_u\,\Delta_u & b_t e^{i\phi_t}\boldsymbol{V}\\ 0 & y_t\end{pmatrix},\qquad \hat{y}_d=\begin{pmatrix}a_d\,\Delta_d & b_b e^{i\phi_b}\boldsymbol{V}\\ 0 & y_b\end{pmatrix}, \tag{3.59}$$

where the top-yukawa is $y_t=Y_{U3}s_{Lu3}s_{Ru3}$ and the other parameters read $a_u=Y_{U2}s_{Lu2}$, $b_t=Y_{U2}s_{Lu2}\,d_u$ in $U(3)^3_{\rm LC}$ and $a_u=Y_{U2}s_{Ru2}$, $b_t=Y_{U3}s_{Ru3}\,d_u$ in $U(3)^3_{\rm RC}$. Similar expressions hold for a_d, b_b and y_b. Here and in the following we consider all the parameters real, factoring out the phases everywhere as in (3.59).

The $\hat{y}_{u,d}$ of (3.59) are diagonalized to a sufficient level of approximation by pure unitary transformations of the left-handed quarks [28]

$$U_u\simeq\begin{pmatrix}c_u & s_u e^{i\alpha_u} & -s_u s_t e^{i(\alpha_u+\phi_t)}\\ -s_u e^{-i\alpha_u} & c_u & -c_u s_t e^{i\phi_t}\\ 0 & s_t e^{-i\phi_t} & 1\end{pmatrix},\quad U_d\simeq\begin{pmatrix}c_d & s_d e^{i\alpha_d} & -s_d s_b e^{i(\alpha_d+\phi_b)}\\ -s_d e^{-i\alpha_d} & c_d & -c_d s_b e^{i\phi_b}\\ 0 & s_b e^{-i\phi_b} & 1\end{pmatrix}, \tag{3.60}$$

where

$$s_t=Y_{U2}s_{Lu2}\frac{d_u\epsilon_L}{y_t},\qquad s_b=Y_{D2}s_{Ld2}\frac{d_d\epsilon_L}{y_b},\qquad \text{in left-compositeness,} \tag{3.61}$$

$$s_t=Y_{U3}s_{Ru3}\frac{d_u\epsilon_L}{y_t},\qquad s_b=Y_{D3}s_{Rd3}\frac{d_d\epsilon_L}{y_b},\qquad \text{in right-compositeness.} \tag{3.62}$$

The CKM matrix is $V=U_uU_d^\dagger$ and, after a suitable redefinition of quark phases, takes the form

$$V\simeq\begin{pmatrix}1-\lambda^2/2 & \lambda & s_u s e^{-i\delta}\\ -\lambda & 1-\lambda^2/2 & c_u s\\ -s_d s\,e^{i(\phi+\delta)} & -s c_d & 1\end{pmatrix}, \tag{3.63}$$

where

$$s_u c_d - c_u s_d e^{-i\phi}\equiv\lambda e^{i\delta},\qquad s_b e^{i\phi_b}-s_t e^{i\phi_t}\equiv s e^{i\chi}. \tag{3.64}$$

Given the above formulae and the observation that, differently from $U(3)^3$, the Y_U, s_{Ru} and s_{Lu} are no longer proportional to the identity but are still diagonal with only the first two entries equal to each other, we can derive a few basic consequences:

- In $U(2)^3_{\rm RC}$ the transformations in (3.60) lead to exactly the same suppression as in $U(3)^3_{\rm RC}$ (see eq. (3.46)).

- In the $U(2)^3_{\rm LC}$ we have a non trivial coupling g_L^{ij} absent in $U(3)^3_{\rm LC}$. In fact, contrary to the $U(3)^3_{\rm LC}$ case, s_{Lu}, although still diagonal, is not proportional to the unit matrix. Hence a flavour violation survives (see next section) controlled by a new free complex parameter

$$r_b = \frac{s_b}{s} e^{i(\chi-\phi_b)}. \tag{3.65}$$

3.6.2 Tree-level $\Delta F = 2$ FCNCs

The Wilson coefficients of $\Delta F = 2$ operators generated in $U(2)^3_{\rm LC}$ and $U(2)^3_{\rm RC}$ are again given by (3.32). The flavour-changing couplings in $U(2)^3_{\rm LC}$ read

$$g_{Ld}^{i3} = \xi_{i3}\, r_b \frac{x_t y_t}{Y_U}\,, \qquad g_{Ld}^{12} = \xi_{12}\, |r_b|^2 \frac{x_t y_t}{Y_U}\,, \qquad g_{Rd}^{ij} \approx 0\,, \tag{3.66}$$

with r_b defined in (3.65). As a consequence there is a new, universal phase in B_d and B_s mixing, while the K-$\bar{K}$ amplitude is aligned in phase with the SM. This is the expected scenario in the minimally broken effective $U(2)^3$ approach, see eq. (1.28) in chapter 1. We find the bounds in table 3.6. If the parameter $|r_b|$ is somewhat less than 1, these bounds can be in agreement with experiment even for light fermion resonances. We note that the contribution to the $\Delta C = 2$ operator is proportional to $|1 - r_b|^2$, so it cannot be reduced simultaneously. However, it turns out that it is numerically insignificant. Since furthermore the contribution is real – a general prediction of the $U(2)^3$ symmetry for $1 \leftrightarrow 2$ transitions – the expected improvement of the bound on CP violation in D-$\bar{D}$ mixing will have no impact.

As discussed in section 3.6.1, in $U(2)^3_{\rm RC}$ the flavour-changing couplings are the same as in $U(3)^3_{\rm RC}$,

$$g_{Ld}^{i3} = \xi_{i3}\, \frac{x_t y_t}{Y_U}\,, \qquad g_{Ld}^{12} = \xi_{12}\, \frac{x_t y_t}{Y_U}\,, \qquad g_{Rd}^{ij} \approx 0\,. \tag{3.67}$$

Thus, as in $U(3)^3_{\rm RC}$, there is no new phase in meson-antimeson mixing and the NP effects in the K, B_d and B_s systems are perfectly correlated. The resulting bounds are shown in table 3.7.

3.6.3 Loop-induced chirality-breaking effects

One expects in general flavour-changing chirality-breaking effects in $U(2)^3$ with bounds on the fermion resonances similar to the one of the anarchic case, $m_\psi > (0.5\text{–}1.5)Y$ TeV. With CP conservation in the strong sector, however, the contributions to the quarks EDMs would arise only at higher orders in the $U(2)^3$ breaking terms, so that they would not be significant for the current limit on the neutron EDM.

Observable	Bounds on m_ψ [TeV]		
	doublet	triplet	bidoublet
$\epsilon_K(Q_V^{LL})$	$2.3\ x_t\lvert r_b\rvert^2$	$3.3\ x_t\lvert r_b\rvert^2$	$3.3\ x_t\lvert r_b\rvert^2$
B_d-$\bar{B}_d$	$2.3\ x_t\lvert r_b\rvert$	$3.4\ x_t\lvert r_b\rvert$	$3.4\ x_t\lvert r_b\rvert$
B_s-$\bar{B}_s$	$2.3\ x_t\lvert r_b\rvert$	$3.4\ x_t\lvert r_b\rvert$	$3.4\ x_t\lvert r_b\rvert$
$K_L \to \mu\mu$	$3.8\ \sqrt{x_t Y\lvert r_b\rvert}$		$3.8\ Y_D\lvert r_b\rvert\sqrt{x_t/Y_U}/z$
$b \to s\ell\ell$	$3.5\ \sqrt{x_t Y\lvert r_b\rvert}$		$3.5\ Y_D\sqrt{x_t\lvert r_b\rvert/Y_U}/z$

Table 3.6. Lower bounds on the fermion resonance mass m_ψ in TeV in $U(2)^3_{\rm LC}$.

Observable	Bounds on m_ψ [TeV]
$\epsilon_K(Q_V^{LL})$	$3.3\ x_t$
B_d-$\bar{B}_d$	$2.8\ x_t$
B_s-$\bar{B}_s$	$3.1\ x_t$

Table 3.7. Lower bounds on the fermion resonance mass m_ψ in TeV in $U(2)^3_{\rm RC}$ (bidoublet model).

3.6.4 Flavour-changing Z couplings

In $U(2)^3_{\rm RC}$ flavour-changing Z couplings are absent at tree level. In $U(2)^3_{\rm LC}$ the left-handed couplings do arise, while the right-handed couplings are strongly suppressed. Similarly to the anarchic case, one can write them as

$$\delta g^L_{Zbd^i} \sim \xi_{i3}\ r_b\ \delta g^L_{Zbb}\ , \qquad \delta g^L_{Zsd} \sim \xi_{12}\ |r_b|^2\ \delta g^L_{Zbb}\ . \tag{3.68}$$

One obtains the bounds in the last two lines of table 3.6, which are weaker than the analogous bounds from R_b unless $|r_b| > 1$. An important difference with respect to the anarchic case is the absence of sizable flavour-changing *right-handed* Z couplings, which can be probed e.g. in certain angular observables in $B \to K^*\mu^+\mu^-$ decays [94].

Partial summary on $U(2)^3$

Two important differences distinguish the $U(2)^3$ case from the $U(3)^3$ one: i) both for the bidoublet (at large enough z) and for the triplet models, the bounds from the EWPT or from compositeness become irrelevant; ii) a single complex parameter correlates the various observables, r_b in the $U(2)^3_{\rm LC}$ case. As apparent from table 3.6, values of x_t and r_b somewhat smaller than one can reduce the bounds on the fermion resonance mass at or even below the 1 TeV level. This is also formally possible in $U(2)^3_{\rm RC}$, where $r_b = 1$, but requires $x_t \lesssim 0.3$, i.e. $Y \gtrsim 3$, not consistent with $m_\psi = Yf$ and $f \gtrsim 0.5$ TeV.

	doublet	triplet	bidoublet
Ⓐ	4.9	1.7	1.2∗
$U(3)^3_{\rm LC}$	6.5	6.5	5.3
$U(3)^3_{\rm RC}$	-	-	3.3
$U(2)^3_{\rm LC}$	4.9	0.6	0.6
$U(2)^3_{\rm RC}$	-	-	1.1∗

Table 3.8. Minimal fermion resonance mass m_ψ in TeV compatible with all the bounds (except for the Q_S^{LR} contribution to ϵ_K in the anarchic model), fixing $O(1)$ parameters in anarchy to 1 and assuming the parameter $|r_b|$ in $U(2)^3_{\rm LC}$ to be ~ 0.2. The bounds with a $*$ are obtained for a value of $Y \approx 2.5$, that minimizes the flavour and EWPT constraints consistently with $m_\psi = Yf$ and $f \gtrsim 0.5$ TeV.

3.7 Discussion

We have adopted some simple *partial-compositeness* Lagrangians and assumed that they catch the basic phenomenological properties of the theories under consideration. This allows us to consider a grid of various possibilities, represented, although at the risk of being too simplistic, in table 3.8, which tries to summarize all the more detailed tables 3.2 to 3.7 discussed throughout the chapter. For any given case, this table estimates a lowest possible value for the mass of the composite fermions that mix with the elementary ones and which are heavier than the "custodians" by a factor of $\sqrt{1+(\lambda_X)^2}$. In the case of *anarchy* we are neglecting the constraint coming from ϵ_K (first line of table 3.3, particularly problematic for the bidoublet model, maybe accidentally suppressed) and the various $O(1)$ factors that plague most of the other flavour observables in table 3.3. In every case we also neglect the constraint coming from one-loop chirality-breaking operators, relevant to direct CP violation both in the K and in the D systems, as well as to the quark electric dipole moments. This is a subject that deserves further detailed study.

The general message that emerges from table 3.8, taken at face value, is pretty clear. To accommodate top partners at or below 1 TeV is often not possible and requires a judicious choice of the underlying model: an approximate $U(2)^3$ flavour symmetry appears favorite, if not necessary. Note that the bounds with a $*$ (bidoublet model with anarchic or $U(2)^3_{\rm RC}$ flavour structure) are obtained for a value of $Y \approx 2.5$, that minimizes the flavour and EWPT constraints consistently with $m_\psi = Yf$ and $f \gtrsim 0.5$ TeV. There are two simple reasons for the emergence of $U(2)^3$: i) in common with $U(3)^3$, the suppression of flavour changing effects in four-fermion operators with both left- and right-handed currents, present in the anarchic case; ii) contrary to $U(3)^3$ but as in anarchy, the disentanglement of the properties (their degree of compositeness) of the first and second from the third generation of quarks.

Part III

Weakly coupled New Physics

Chapter 4

Minimal SUSY and the impact of Higgs couplings

In this chapter we are going to briefly review a few aspects of low-scale supersymmetry (see [95] and reference therein), with a focus on the Minimal Supersymmetric Standard Model. After a definition of the model in section 4.1 we analyse in section 4.2 the conclusions that can be drawn on its parameter space after the discovery of the Higgs boson and the measurements of its couplings. We conclude in section 4.3.

4.1 Minimal Supersymmetric Standard Model

The minimal gauge lagrangian of the SM, if equipped with supersymmetry, will automatically imply the presence of s-particle. *Gauginos*, $\tilde{A}^a$ are spin-1/2 partners of gauge fields A^a_μ which (together with a real scalar auxiliary field D^a) form the *vector multiplet*. *S-quarks* and *s-leptons*, ϕ_i, are complex scalars partners of chiral fermions ψ_i which (together with an auxiliary complex scalar F_i) form *chiral multiplets*. All the new s-particles have gauge interactions according to their quantum numbers, given that SUSY commutes with gauge symmetries. Moreover, SUSY enforces other kind of interactions summarized by

$$\mathcal{L}_{\text{SUSY,int}} = \sum_i \left|\frac{\delta \mathcal{W}}{\delta \phi_i}\right|^2 + \frac{1}{2}\sum_a (\phi^* T^a \phi)^2 - (\sqrt{2} g (\phi^* T^a \psi)\tilde{A}^a + c.c.) + \frac{1}{2}\left(\frac{\delta^2 \mathcal{W}}{\delta\phi_i \delta\phi_j}\psi_i\psi_j + c.c.\right), \quad (4.1)$$

where $\mathcal{W}$ is an holomorphic polynomial in chiral super-fields, with each monomial of mass dimension less or equal to three. These two properties are necessary and sufficient to have a *renormalizable* supersymmetric theory.

In the case of the MSSM, the holomorphicity of the superpotential implies the presence of two Higgs doublets in order to give mass to both up and down type (s)fermions. Concretely the MSSM is defined by

$$\mathcal{W}_{\text{MSSM}} = \lambda_u Q U^c H_u + \lambda_d Q D^c H_d + \lambda_e L E^c H_d + \mu H_u H_d. \quad (4.2)$$

SUSY is powerful enough that $\mathcal{W}$ is not renormalized at perturbative level. Only wave-function renormalization is possible. This is why SUSY is an efficient protection mechanism for the Higgs mass.

4.1.1 Soft supersymmetry breaking

Supersymmetry must be broken, hopefully in a dynamical way. However, no matter what the SUSY breaking mechanism is, a consistent EFT description below the scale of SUSY breaking is provided by

$$\begin{aligned} -\mathcal{L}_{\text{soft}} = & \frac{1}{2}(M_3\tilde{g}\tilde{g} + M_2\tilde{W}\tilde{W} + M_1\tilde{B}\tilde{B} + c.c.) \\ & + (\tilde{u}A_u\tilde{Q}H_u + \tilde{d}A_d\tilde{Q}H_d + \tilde{e}A_e\tilde{L}H_d + c.c.) \\ & + \sum_{q=Q,L,u,d,e} m_{\tilde{q}}^2\tilde{q}^*\tilde{q} + m_{H_u}^2|H_u|^2 + m_{H_d}^2|H_d|^2 + (bH_uH_d + c.c.), \end{aligned} \tag{4.3}$$

where the name 'soft' means that only terms of dimension less or equal to three are introduced that preserve the absence of quadratic divergences of the original supersymmetric lagrangian. Gauginos have Majorana masses, A-terms and mass terms are 3x3 complex matrices, with $m_{\tilde{q}}^2$ hermitian.

It can be shown that the parameters of the superpotential (4.2) do not renormalize if SUSY is softly broken as defined in eq.(4.3).

In this framework, the Higgs mass receives additive quantum corrections $\delta m_h^2 \sim m_{\text{soft}}^2$, where m_{soft} is the overall scale of (4.3). In fact δm_h^2 is now sensitive to imperfect loop-cancellations between particles and s-particles. Given that y_t is the largest coupling, the leading contribution is related to the top-stop 1-loop effect. Solving the Hierarchy Problem roughly suggests $m_{\text{soft}} \lesssim$ TeV.

4.1.2 SUSY problems

The abundance of s-particles, the richness of flavour and CP violations from the soft terms, together with the non-observation of a single new particle so far, suggest that SUSY, if present at all at the TeV scale, should be augmented with some additional structure.

- R**-parity**. A drawback of the MSSM is that the superpotential can accommodate supersymmetric renormalizable operators which break lepton and baryon number. These can be avoided imposing a discrete symmetry $(-1)^{3(L-B)+2s}$, as done in writing (4.2). This means that s-particles are pair-produced and the lightest of them (LSP) is stable.

- **SUSY flavor problem**. As discussed in the Introduction, NP should be highly non-generic if close to the electro-weak scale. The MSSM is no exception, especially with the plethora of soft terms which mix flavours, m_{ij}, A_{ij}. To keep consistency with an approximate CKM picture requires that some mechanisms be operative. As we will see below heavy third generation squarks are in constrast with Naturalness argument. This can be paired with a solution of the SUSY flavor problem by taking the first two generations of squarks heavy enough and a light third generation poorly mixed with the first two.

- **SUSY CP problem**. Differently from the SM, the MSSM has flavour-blind phases, *i.e.* sources of CPV not vanishing when the full $U(3)^5$ flavour symmetry is restored.

$\Delta F = 0$ CP-odd observables, such as the electron or the neutron dipole moments constrain these phases. If these phases are sizeable, they also require heavy sfermions of the first generation.

On top of these issues there is the question if the MSSM can really be thought as a natural theory, given the absence of any new s-particle so far and in view of the observed Higgs mass.

4.1.3 Quantifying the naturalness of the MSSM

The naive request for a natural MSSM is $m_{\rm soft} \sim$ TeV. We make this statement more precise as follows [96]. The scalar potential (restricted to $H_{u,d}$) can always be put in the following form,

$$V = (|\mu|^2 + m_{H_u}^2)|H_u^0|^2 + (|\mu|^2 + m_{H_d}^2)|H_d^0|^2 - (bH_u^0 H_d^0 + c.c.) + \frac{m_Z^2}{2v^2}(|H_u^0|^2 - |H_d^0|^2)^2 \quad (4.4)$$

In the limit $\tan\beta \equiv \langle H_u^0\rangle/\langle H_d^0\rangle \gg 1$, the minimization conditions give

$$-\frac{m_Z^2}{2} \simeq |\mu|^2 + m_{H_u}^2. \quad (4.5)$$

Eq. (4.5) requires a negative soft mass $m_{H_u}^2$, which is naturally obtained by the IR flow from the input scale, and a cancellation between the two terms in the right-hand side. Requiring a fine-tuning of such cancellation less than Δ, we can set an upper bound on μ,

$$\mu \lesssim 250\ {\rm GeV}\left(\frac{m_h}{125\ {\rm GeV}}\right)\left(\frac{\Delta}{5}\right)^{1/2}. \quad (4.6)$$

We can also constrain the value of m_{H_u}. In this case, while μ does not get corrected by soft terms, m_{H_u} is 1-loop sensitive to the stop sector. In addition, the stops get large corrections from gluinos to which they are strongly coupled. These two effects are summarized as

$$\delta m_{H_u}^2|_{\rm stops} \simeq -\frac{2y_t^2}{16\pi^2}(m_{Q_3}^2 + m_{u_3}^2 + |A_t|^2)\log\left(\frac{\Lambda}{\rm TeV}\right), \quad (4.7)$$

$$\delta m_{H_u}^2|_{\rm gluinos} \simeq -\frac{2y_t^2}{\pi^2}\frac{\alpha_s}{\pi}|M_3|^2\log^2\left(\frac{\Lambda}{\rm TeV}\right). \quad (4.8)$$

Applying the naturalness criterion as before we get upper bounds on the stop average mass and the gluino mass [96]

$$\sqrt{m_{\tilde t_1}^2 + m_{\tilde t_1}^2} \lesssim 600\ {\rm GeV}\frac{\sin\beta}{(1+x_t^2)^2}\left(\frac{\log(\Lambda/{\rm TeV})}{3}\right)^{-1/2}(\frac{m_h}{125\ {\rm GeV}})\left(\frac{\Delta}{5}\right)^{1/2}, \quad (4.9)$$

$$M_3 \lesssim 900\ {\rm GeV}\left(\frac{\log(\Lambda/{\rm TeV})}{3}\right)^{-1}(\frac{m_h}{125\ {\rm GeV}})\left(\frac{\Delta}{5}\right)^{1/2}, \quad (4.10)$$

where $x_t = A_t/\sqrt{m_{\tilde t_1}^2 + m_{\tilde t_1}^2}$. This shows that the naturalness bound on the stops depends on their mixing.

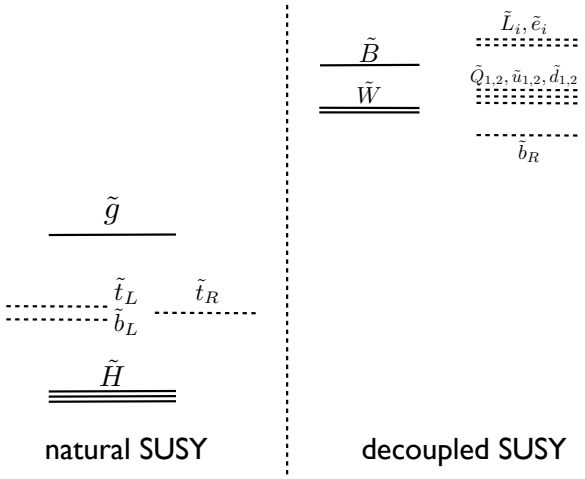

Figure 4.1. Natural SUSY spectrum. Only Higgs-inos, stops (and left-handed sbottom) and gluinos are required to be light as discussed in (4.6,4.9,4.10). Figure taken from [96].

Given the upper bounds on μ, stop and gluino masses, a natural spectrum of SUSY s-particles require only light Higgsinos, third generation stops and gluinos. The other s-particles are poorly constrained from naturalness arguments: the bound on the first two generations of squarks is at 5-10 TeV scale, while on the B-ino, W-inos is in the 2-3 TeV region [96–99].

The MSSM spectrum is constrained from below by direct searches. Most relevant are lower bounds on the lightest stop and gluinos. Conservative lower bounds, derived by re-considering some existing direct searches, are $m_{\tilde{t}_1} \geq 200 \div 300$ GeV (if $\mu \gtrsim 150 \div 250$ GeV) and $m_{\tilde{g}} \geq 1000$ GeV. Neglecting points with peculiar correlations in the parameter space, we can infer stronger bounds, $m_{\tilde{t}_1} \geq 700$ GeV and $m_{\tilde{g}} \geq 1300$ GeV [100]. This shows that direct searches are directly probing the natural territory of the MSSM.

The Higgs mass in the MSSM

Besides direct searches, also the observed Higgs mass pushes the MSSM towards large fine-tuning. At tree-level $m_h < m_Z$ because the quartic coupling is set by the gauge contribution to the Higgs potential (4.4). Taking into account the dominant stop-top correction, it is

$$m_h^2 \simeq m_Z^2 \cos^2\beta + \Delta_t^2 \tag{4.11}$$

where

$$\Delta_t^2 \simeq \frac{G_F^2 m_t^4}{\sqrt{2}\pi^2}\left[\log\left(\frac{\bar{m}_{\tilde{t}}^2}{m_t^2}\right) + \frac{X_t^2}{\bar{m}_{\tilde{t}}^2}\left(1 - \frac{X_t^2}{12\bar{m}_{\tilde{t}}^2}\right)\right], \tag{4.12}$$

with $X_t = A_t - \mu\cot\beta$, and $\bar{m}_{\tilde{t}}^2$ is an average stop mass (see [101, 102] for more details on this formula).

To accommodate 125 GeV, $\Delta_t \gtrsim 85$ GeV is unavoidable. Such 1-loop correction can be achieved with heavy stops and/or large mixing and it pushes the MSSM towards a %-ish fine tuning. This calls for deviations from minimal SUSY, *i.e.* models where the Higgs mass can evade the upper bound m_Z already at tree-level, as we will discuss in the next chapter.

4.2 Higgs sector of the MSSM

The measurements of the Higgs mass and branching ratios have a significant impact on the parameter space of the MSSM Higgs sector (see for example [103, 104]).

The CP-even scalar sector is an admixture of two doublet states: h_v, that gets the vacuum expectation value v and its orthogonal combination $h_v^\perp$ with vanishing VEV. For the combination of standard MSSM parameters $(\mu A_t)/\langle m_{\tilde{t}}^2\rangle$ below unity, the mass matrix in the $(h_v, h_v^\perp)$ basis is well approximated by

$$\mathcal{M} = \begin{pmatrix} m_{hh}^2 = m_Z^2(\frac{1-\tan^2\beta}{1+\tan^2\beta})^2 + \Delta_t^2 & 2m_Z^2 \frac{\tan\beta\left(1-\tan^2\beta\right)}{\left(1+\tan^2\beta\right)^2} - \frac{\Delta_t^2}{\tan\beta} \\ 2m_Z^2 \frac{\tan\beta\left(1-\tan^2\beta\right)}{\left(1+\tan^2\beta\right)^2} - \frac{\Delta_t^2}{\tan\beta} & m_A^2 + 4m_Z^2 \frac{\tan^2\beta}{\left(1+\tan^2\beta\right)^2} + \frac{\Delta_t^2}{\tan^2\beta} \end{pmatrix}, \tag{4.13}$$

where we call m_{hh}^2 the 1,1 entry for later convenience. One can trade m_A and Δ_t for the masses of the two eigenstates, h and H, and express in terms of these masses and $\tan\beta$ the mixing angle δ, defined by

$$h = \cos\delta\ h_v - \sin\delta\ h_v^\perp, \qquad H = \cos\delta\ h_v^\perp + \sin\delta\ h_v. \tag{4.14}$$

An expression, accurate for $m_H \gtrsim 400$ GeV and any value of $\tan\beta$, is

$$\sin\delta = -\frac{m_h^2}{\tan\beta m_H^2} + \frac{1-\tan^2\beta}{1+\tan^2\beta}\frac{m_Z^2}{\tan\beta m_H^2} + O(\frac{1}{m_H^4}). \tag{4.15}$$

From eq. (4.14) and the fixed form of the supersymmetric Yukawa couplings, all the Higgs couplings are given by

$$\frac{g_{hu\bar{u}}}{g_{hu\bar{u}}^{\rm SM}} = \cos\delta + \frac{\sin\delta}{\tan\beta}, \quad \frac{g_{hd\bar{d}}}{g_{hd\bar{d}}^{\rm SM}} = \cos\delta - \tan\beta\sin\delta, \quad \frac{g_{hVV}}{g_{hVV}^{\rm SM}} = \cos\delta. \tag{4.16}$$

$$\frac{g_{Hu\bar{u}}}{g_{hu\bar{u}}^{\rm SM}} = \sin\delta - \frac{\cos\delta}{\tan\beta}, \quad \frac{g_{Hd\bar{d}}}{g_{hd\bar{d}}^{\rm SM}} = \sin\delta + \tan\beta\cos\delta, \quad \frac{g_{HVV}}{g_{hVV}^{\rm SM}} = \sin\delta. \tag{4.17}$$

The simplification of this approach is that only two parameters are free and they can be taken to be the mass of the heavy Higgs m_H and $\tan\beta$. In terms of these two quantities we can quantify the impact of a fit to the Higgs couplings (using the data collected so far) and analytically compute as a function of them all the relevant cross sections and branching ratios of the extra Higgs H. This allows to make a clear connection between the measured properties of h, identified with the state at 125 GeV and called hereafter $h_{\rm LHC}$, and the direct searches for H (or the pseudo-scalar state A). The assumption is that no other radiative correction affects the mass matrix (4.13) than the non decoupling top-stop 1-loop correction

(4.12). This simplification is extremely accurate in the limit $(\mu A_t)/\langle m_{\tilde{t}}^2\rangle \ll 1$ (see [102]) and especially when the other Higgs is heavier than the state at 125 GeV. However, in the following we will comment also on the possibility that $h_{\rm LHC}$ be not the lightest scalar state.

From the simple formulae above, the MSSM requires a minimum value of $\Delta_t \gtrsim 85$ GeV that is needed to accommodate the 125 GeV Higgs boson as the lightest CP-even neutral scalar, while this is not necessary if it is not the lightest scalar. Also for this reason we let Δ_t vary and we show in figure 4.2-left the allowed regions by the fit to current experimental data on the signal strengths of $h_{\rm LHC}$. The Higgs coupling fit is based on the code of the authors of ref. [29]. We used all ATLAS [105], CMS [106] and TeVatron [107] data collected so far. The isoline $m_{hh} = m_h$ separates the regions where $h_{\rm LHC}$ or H are the lightest states. Both configurations are still allowed by the Higgs coupling fit under the assumptions described here.

The literature has several examples of such a kind of studies: a recent paper [108] analyses the Higgs system of the MSSM in a way similar to ours and gives comments about the heavy Higgs searches in different channels (see also [109]).

4.2.1 MSSM: $h_{\rm LHC}$ as the lightest scalar

To quantify the impact of Higgs coupling measurements in the standard scenario where $m_H > m_h$ we can choose m_H as a free parameter. Figure 4.2 right is a zoom of the corresponding allowed region of figure 4.2 left. Note that in the plane $(\tan\beta, m_H)$ the isolines of Δ_t are increasingly large at lower $\tan\beta$: a sign of increasing fine tuning.

Given the allowed range for the mass of H (and A) it is interesting to know what are its main production and decay channels. To this end we compute in terms of the same two parameters of the fit the relevant observables: gluon fusion cross section and branching ratios of H. The couplings (4.16) allow to write the gluon-fusion production cross section of H by means of [110]

$$\sigma(gg \to H) = \sigma^{\rm SM}(gg \to H(m_H))\left|\mathcal{A}_t \frac{g_{Htt}}{g_{htt}^{\rm SM}} + \mathcal{A}_b \frac{g_{Hbb}}{g_{hbb}^{\rm SM}}\right|^2, \tag{4.18}$$

where

$$\mathcal{A}_{t,b} = \frac{F_{\frac{1}{2}}(\tau_{t,b})}{F_{\frac{1}{2}}(\tau_t) + F_{\frac{1}{2}}(\tau_b)}, \qquad \tau_{t,b} = 4\frac{m_{t,b}^2}{m_H^2}, \tag{4.19}$$

and $F_{\frac{1}{2}}(\tau)$ is a one-loop function that can be found e.g. in [111, 112]. We use the values of $\sigma^{\rm SM}$ at NNLL precision provided in [113], and the running masses $m_{t,b}$ at NLO precision. We checked the validity of this choice by performing the same computation both with the use of masses at LO precision and K-factors [114], and with the program `HIGLU` [115, 116], finding in both cases an excellent agreement. We also performed a further check of our results with the ones recently presented in [117] and [108], finding an equally good agreement.

We show in figures 4.3-4.5 the gluon-fusion production cross sections and the widths of H. In the same $(\tan\beta, m_H)$ plane $\sigma(gg \to A)$ is therefore also determined, which allows to delimit the currently excluded region by the direct searches for $A, H \to \tau^+\tau^-$. Such a region is known to be significant, especially for growing $\tan\beta$. In figures 4.2-4.5 we draw the region excluded by such search, as inferred from [118].

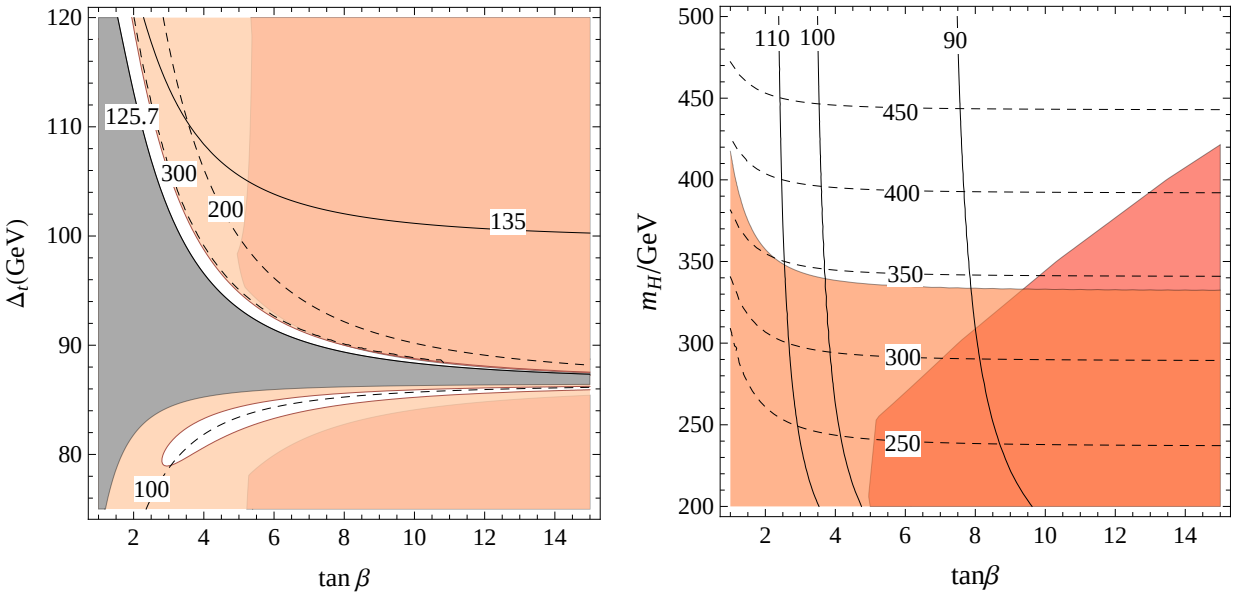

Figure 4.2. MSSM. Left: isolines of m_{hh} (solid) and $m_{H^\pm}$ (dashed), the gray region is unphysical because of $m_A^2 < 0$. Right: isolines of Δ_t(GeV) (solid) and $m_{H^\pm}$ (dashed). Light colored regions are excluded at 95%C.L. by the Higgs fit, the red region is excluded by CMS direct searches for $A, H \to \tau^+\tau^-$.

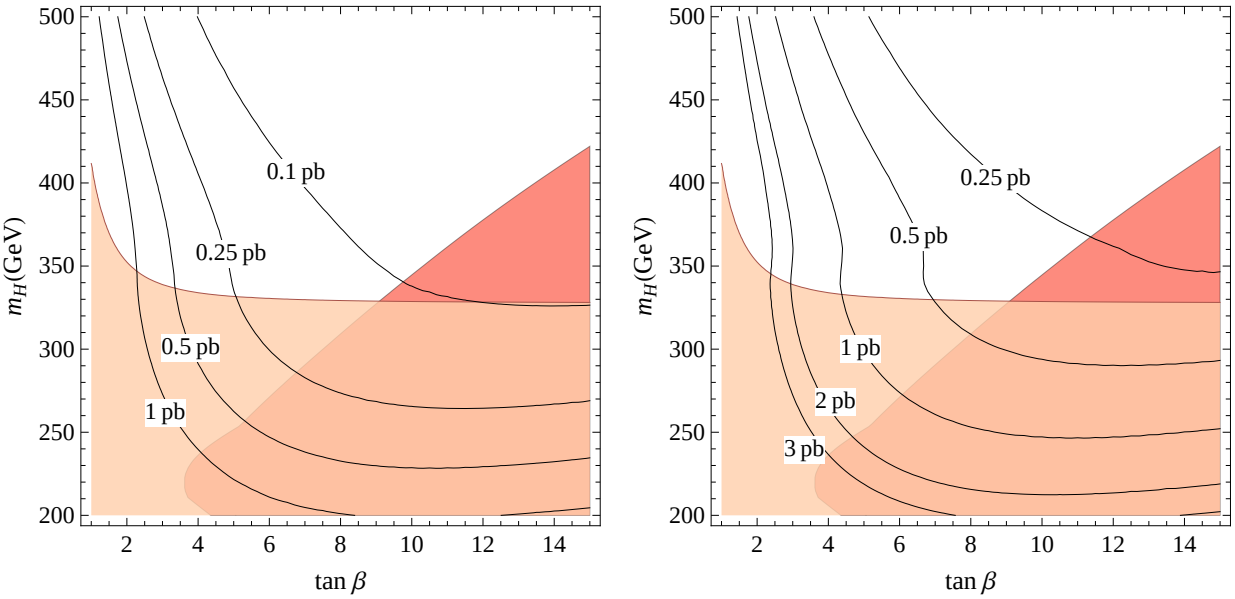

Figure 4.3. MSSM. Isolines of gluon fusion production cross section $\sigma(gg \to H)$. Light colored region is excluded at 95%C.L., the red region is excluded by CMS direct searches for $A, H \to \tau^+\tau^-$. Left: LHC8. Right: LHC14.

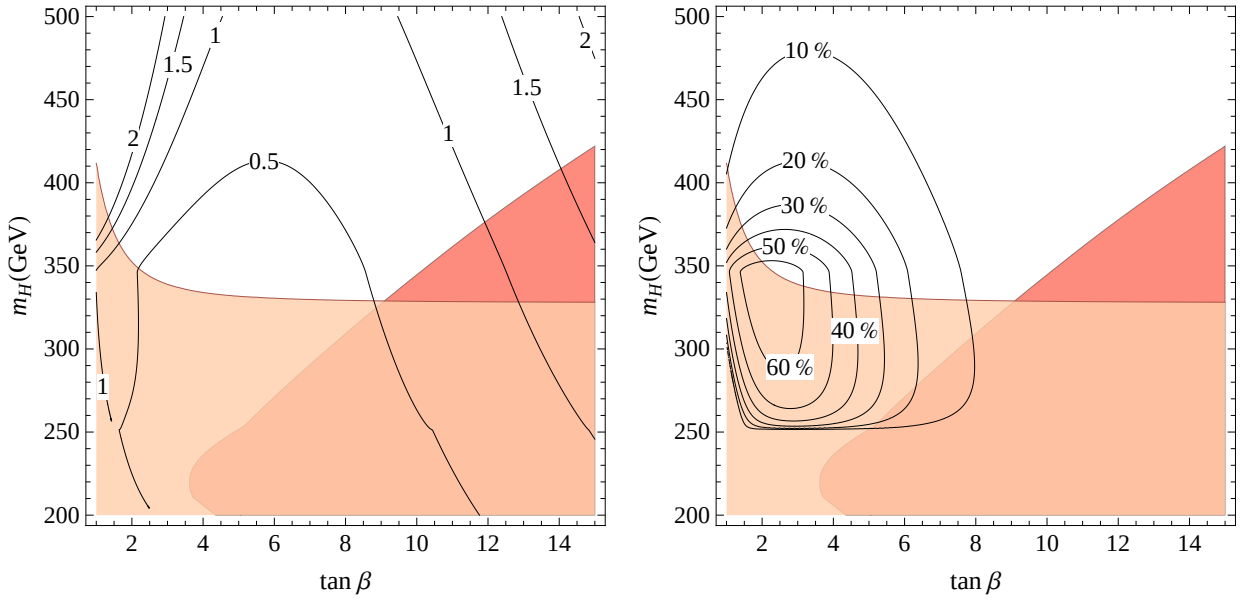

Figure 4.4. MSSM. Left: Isolines of the total width Γ_H (GeV). Right: isolines of BR($H \to hh$). The light colored region is excluded at 95%C.L., the red region is excluded by CMS direct searches.

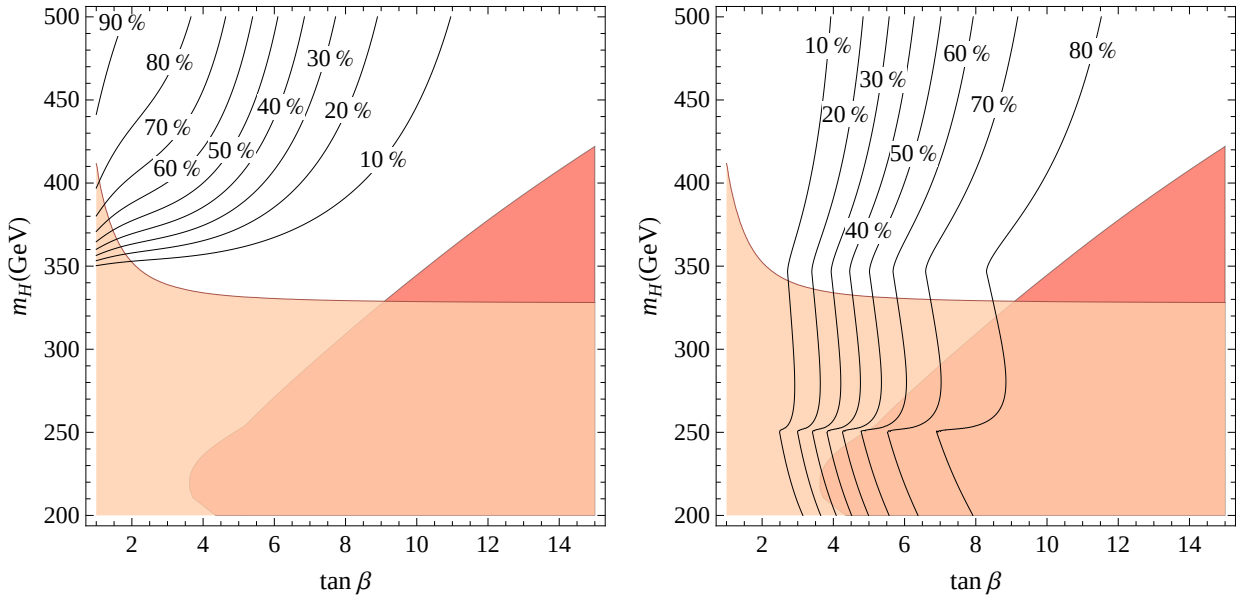

Figure 4.5. MSSM. Left: isolines of BR($H \to t\bar{t}$). Right: isolines of BR($H \to b\bar{b}$). The light colored region is excluded at 95%C.L., the red region is excluded by CMS direct searches.

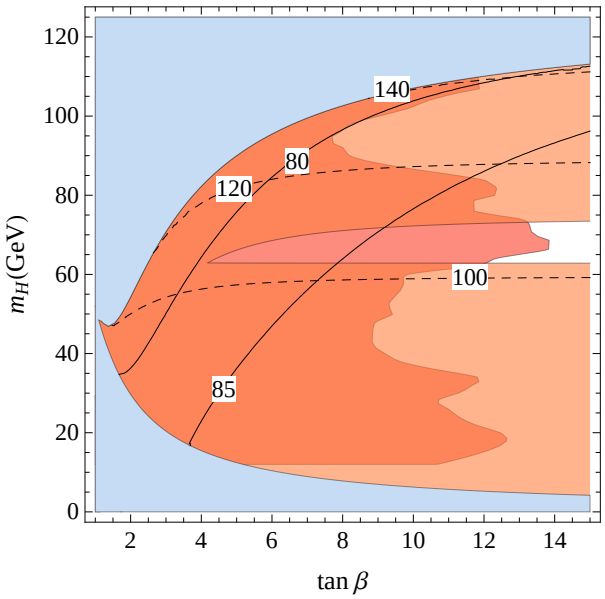

Figure 4.6. MSSM, $h_{\rm LHC} > H$. Isolines of Δ_t (solid) and $m_{H^\pm}$ (dashed) at $(\mu A_t)/\langle m_{\tilde{t}}^2\rangle \ll 1$. The red region is excluded by LEP direct searches for $H \to b\bar{b}$. The light colored region is excluded at 95%C.L.

4.2.2 MSSM: $h_{\rm LHC}$ as the heaviest scalar

As anticipated, the case where there is a CP-even H below 125 GeV is still a possibility. Again, the allowed area in the plane $(\tan\beta, m_H)$ depicted in figure 4.6 is the zoomed version of the corresponding region in figure 4.2-left. As expected, figure 4.6 makes clear that a large value of Δ_t is needed to make the MSSM consistent with a 125 GeV Higgs boson. Notice that this low-mass region is difficult to explore at the LHC. However LEP data provided limits on a scalar resonance decaying to bottom quarks [119] that exclude the residual region for low enough $\tan\beta$. Figure 4.6 is affected by growing values of $\mu A_t/\langle m_{\tilde{t}}^2\rangle$, which modifies the radiative corrections to (4.13).

4.3 Discussion

In spite of an embarassing %-ish fine tuning, the MSSM may still be realized in nature with some particles at the TeV scale. With this attitude in mind, we have analysed the phenomenological consequences of the MSSM Higgs sector when confronted with data coming from the LHC, both from direct searches of its extra scalar bosons and Higgs coupling measurements.

Several comments can be drawn, which we summarize schematically:

- If $h_{\rm LHC}$ is the lightest CP-even scalar, H is bounded to be heavier than 350 GeV by the Higgs coupling fit over the full range of values of $\tan\beta$ not excluded by the search of $H, A \to \tau^+\tau^-$.

- The bounds from the Higgs couplings are stronger than the direct ones for moderate $\tan\beta$.
- On the direct searche side, H decaying to $t\bar{t}$ and $b\bar{b}$ is worth to be investigated in the small and large-$\tan\beta$ limit respectively, as shown in figure 4.5.
- If h_{LHC} is the next-to-lightest scalar, H in the range of 80 GeV is still allowed by current data (figure 4.6).

Chapter 5

Extended Higgs sector of a general NMSSM

After an introduction to the NMSSM, where we discuss how it alleviates the tuning in (v, m_h), we show how the measurements of the couplings of the 125 GeV Higgs boson constrain the region of the physical parameters of a generic NMSSM most relevant to this context. In the same region of parameter space we determine the cross section for the production of a heavier CP-even scalar together with its total width and its most relevant branching ratios.

5.1 The Next-to-MSSM

Chapter 4 was devoted to the phenomenology of the MSSM Higgs sector. A motivated alternative is the so called Next-to-Minimal Supersymmetric Standard Model (NMSSM). In the NMSSM, a singlet superfield S couples to the Higgs superfields, H_u and H_d, via the Yukawa-like coupling $\lambda S H_u H_d$ [120] (see [121] for a review). The superpotential is of the form,[1]

$$\mathcal{W} = \mathcal{W}_{\text{MSSM}} + \lambda S H_u H_d + f(S). \tag{5.1}$$

Consequently, also $\mathcal{L}_{\text{soft}}$ of (4.3) is supplemented with additional terms involving the singlet. The inclusion of such Yukawa coupling affects directly the Higgs mass. We have a tree-level contribution

$$m_h^2 \simeq m_Z^2 s_{2\beta}^2 + \lambda^2 v^2 c_{2\beta}^2 + \Delta_t^2. \tag{5.2}$$

This equation shows that we can get 125 GeV with a largish λ coupling instead of invoking large top-stop corrections. This is certainly a welcome situation from the point of view of naturalness: the large contribution from Δ_t which is needed in the MSSM, here is softened by the presence of λ.

Moreover, values of $\lambda \gtrsim 1$ suppress the sensitivity of the Higgs VEV with respect to changes in the soft supersymmetry breaking masses, thus still keeping the fine tuning at a moderate level even for stop masses up to 1 TeV [122–124]. A recent analysis [125] finds that the fine tuning in the NMSSM can be above 5% for stop masses up to 1.2 TeV and gluino masses up to 3 TeV for $\lambda \approx 1$ and moderate $\tan\beta$,

$$m_{\tilde{t}} \lesssim 1 \text{ TeV}, \quad m_{\tilde{g}} \lesssim 3 \text{ TeV}. \tag{5.3}$$

[1] In some NMSSM versions $\mathcal{W}_{\text{MSSM}}$ does not include the μ term, like in the scale-invariant version.

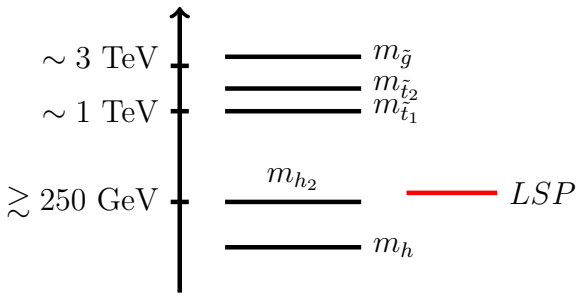

Figure 5.1. Simplified spectrum of the NMSSM scenario under consideration.

These bounds depend on the model under consideration: ref. [125] considered the scale-invariant superpotential and a low mediation scale $M = 20$ TeV, which is welcome to relax the tuning, as eq. (1.45) shows in chapter 1. There is a simple way to understand the appearance of such milder natural upper bounds on s-particles coupled to the top-stop sector. Let us consider the dependence of v on the parameter of the model. In the NMSSM the minimization condition gives,

$$v^2 \sim \frac{\tilde{m}^2}{\lambda} \tag{5.4}$$

to be confronted with $v^2 \sim 4\tilde{m}^2/g^2$ in the MSSM, here $\tilde{m}$ is a soft mass parameter. The different dependence allows the s-particles of the NMSSM to be parametrically higher than those of the MSSM,

$$\tilde{m}_{\rm NMSSM} \simeq \frac{2\lambda}{g}\tilde{m}_{\rm MSSM}. \tag{5.5}$$

With this natural NMSSM, it is conceivable, if not likely, that the lightest new particles around can be the extra scalar partners of the Higgs, except perhaps for the LSP. In general terms, to see whether the newly found resonance at 125 GeV is part of an extended Higgs system is a primary task of the current and future experimental studies. Given the above motivations, this appears to be especially true for the extra Higgs states of the NMSSM, which can be thought as having the spectrum sketched in figure 5.1.

A well known objection to this scenario is its compatibility with gauge coupling unification. Requiring λ to stay semi-perturbative up to the GUT scale bounds λ at the weak scale at about 0.7 [126]. This value is in fact influenced by the presence of vector-like matter in full $SU(5)$ multiplets that slows down the running of λ by increasing the gauge couplings at high energies. However, even adding three vector-like five-plets at 1 TeV, in which case α_G still remains perturbative, does not allow λ at the weak scale to go above 0.8 [127, 128].

As we are going to see current data on the Higgs couplings prefer values of λ below $1 \div 1.5$. There are several ways [129–136] in which λ could go to $1 \div 1.5$ without spoiling unification nor affecting the consequences at the weak scale of the NMSSM Lagrangian, as treated above (see also section VI of [4]). In any event even a value of $\lambda \simeq 0.7 \div 0.8$ is of relevance to our discussion.

5.2 A general description of the NMSSM Higgs sector

The many parameters that can enter the general NMSSM do not prevent for studying in relatively simple terms the CP-even scalar sector under a few assumptions justified *a posteriori*.

In particular we have in mind the spectrum of figure 5.1, where the lightest new particles are the extra Higgses and the coloured s-particles are heavy enough that many of their radiative effects can be neglected. Assuming also a negligibly small violation of CP in the Higgs sector, we take as a starting point the form of the squared mass matrix of the neutral CP-even Higgs system in the general NMSSM (5.1):

$$\mathcal{M}^2 = \begin{pmatrix} m_Z^2\cos^2\beta + m_A^2\sin^2\beta & (2v^2\lambda^2 - m_A^2 - m_Z^2)\cos\beta\sin\beta & vM_1 \\ (2v^2\lambda^2 - m_A^2 - m_Z^2)\cos\beta\sin\beta & m_A^2\cos^2\beta + m_Z^2\sin^2\beta + \delta_t^2 & vM_2 \\ vM_1 & vM_2 & M_3^2 \end{pmatrix} \tag{5.6}$$

in the basis $\mathcal{H} = (H_d^0, H_u^0, S)^T$. In this equation

$$m_A^2 = m_{H^\pm}^2 - m_W^2 + \lambda^2 v^2, \tag{5.7}$$

where $m_{H^\pm}$ is the physical mass of the single charged Higgs boson, $v \simeq 174$ GeV, and $\delta_t^2 = \Delta_t^2(m_{\tilde{t}_1}, m_{\tilde{t}_2}, \theta_{\tilde{t}})/\sin^2\beta$ is the well known effect of the top-stop loop corrections to the quartic coupling of H_u, with $m_{\tilde{t}_{1,2}}$ and $\theta_{\tilde{t}}$ physical stop masses and mixing. We neglect the analogous correction to (5.7) [102], which lowers $m_{H^\pm}$ by less than 3 GeV for stop masses below 1 TeV. We leave unspecified the other parameters in (5.6), M_1, M_2, M_3, which are not directly related to physical masses and depend on the particular NMSSM under consideration.

The vector of the three physical mass eigenstates $\mathcal{H}_{\rm ph}$ is related to the original scalar fields by

$$\mathcal{H} = R_\alpha^{12} R_\gamma^{23} R_\sigma^{13} \mathcal{H}_{\rm ph} \equiv R\mathcal{H}_{\rm ph}, \tag{5.8}$$

where R_θ^{ij} is the rotation matrix in the ij sector by the angle $\theta = \alpha, \gamma, \sigma$. Defining $\mathcal{H}_{\rm ph} = (h_3, h_1, h_2)^T$, we have $R^T\mathcal{M}^2 R = \mathrm{diag}(m_{h_3}^2, m_{h_1}^2, m_{h_2}^2)$.

We identify $h_1 = h_{\rm LHC}$ with the state found at LHC, so that $m_{h_1} = 125.7$ GeV. From (5.8) $h_{\rm LHC}$ is related to the original fields by $h_1 = c_\gamma(-s_\alpha H_d + c_\alpha H_u) + s_\gamma S$, where $s_\theta = \sin\theta, c_\theta = \cos\theta$. Similar relations, also involving the angle σ, hold for h_2 and h_3.

5.3 Higgs coupling fit in the NMSSM

We can compute the couplings of $h_{\rm LHC}$ to the fermions or to vector boson pairs, $VV = WW, ZZ$, normalized to the corresponding couplings of the SM Higgs boson. Defining $\delta = \alpha - \beta + \pi/2$, they are given by (see also [110, 137])

$$\frac{g_{h_{\rm LHC}tt}}{g_{htt}^{\rm SM}} = c_\gamma(c_\delta + \frac{s_\delta}{\tan\beta}), \quad \frac{g_{h_{\rm LHC}bb}}{g_{hbb}^{\rm SM}} = c_\gamma(c_\delta - s_\delta\tan\beta), \quad \frac{g_{h_{\rm LHC}VV}}{g_{hVV}^{\rm SM}} = c_\gamma c_\delta. \tag{5.9}$$

One can notice that the formal difference with respect to the MSSM case (4.16) is the

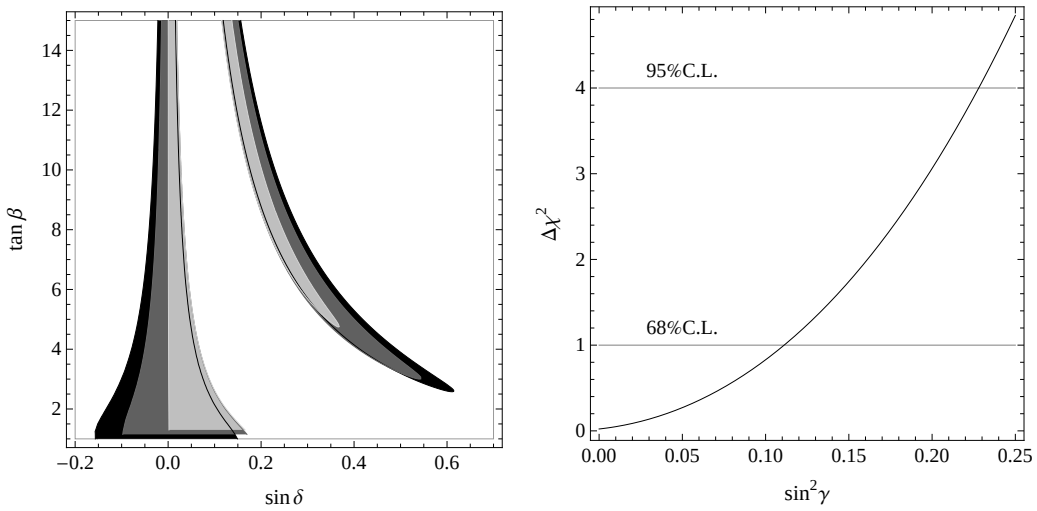

Figure 5.2. Fit of the measured signal strengths of $h_{\rm LHC}$. Left: 3-parameter fit of $\tan\beta$, s_δ and s_γ^2. The allowed regions at 95%C.L. are given for $s_\gamma^2 = 0$ (black), 0.15 (dark grey), 0.3 (light grey). The regions overlap in part, but their borders are also shown. Right: fit of s_γ^2 in the case of $\delta = 0$.

presence of the extra mixing angle γ. Similarly to what as been done in the chapter 4 for the MSSM, also here we fit all ATLAS [105], CMS [106] and TeVatron [107] data collected so far on the Higgs signal strengths. As a result we obtain the bounds on δ for different fixed values of γ shown in figure 5.2 left and the bound on γ for $\delta = 0$ shown in figure 5.2 right. To make this fit, we adapt the code provided by the authors of [29]. As stated below, we do not include in this fit any supersymmetric loop effects. Note that in the region of s_δ close to zero, a larger s_γ^2 forces δ to take a larger central value.

5.3.1 Reference equations

In full generality the mixing angles $\delta \equiv \alpha - \beta + \pi/2, \gamma, \sigma$ can be expressed in terms of the physical masses $m_{h_{\rm LHC},h_2,h_3}$ and $m_{H^\pm}$, the charged Higgs boson mass, as [4]

$$s_\gamma^2 = \frac{\det M^2 + m_{h_{\rm LHC}}^2 (m_{h_{\rm LHC}}^2 - \operatorname{tr} M^2)}{(m_{h_{\rm LHC}}^2 - m_{h_2}^2)(m_{h_{\rm LHC}}^2 - m_{h_3}^2)}, \tag{5.10}$$

$$s_\sigma^2 = \frac{m_{h_2}^2 - m_{h_{\rm LHC}}^2}{m_{h_2}^2 - m_{h_3}^2} \frac{\det M^2 + m_{h_3}^2 (m_{h_3}^2 - \operatorname{tr} M^2)}{\det M^2 - m_{h_2}^2 m_{h_3}^2 + m_{h_{\rm LHC}}^2 (m_{h_2}^2 + m_{h_3}^2 - \operatorname{tr} M^2)}, \tag{5.11}$$

$$\begin{aligned} s_{2\delta} = & \Big[2 s_\sigma c_\sigma s_\gamma \left(m_{h_3}^2 - m_{h_2}^2\right) \left(2\tilde{M}_{11}^2 - m_{h_{\rm LHC}}^2 c_\gamma^2 - m_{h_2}^2 (s_\gamma^2 + s_\sigma^2 c_\gamma^2) - m_{h_3}^2 (c_\sigma^2 + s_\gamma^2 s_\sigma^2)\right) \\ & + 2\tilde{M}_{12}^2 \left(m_{h_3}^2 \left(c_\sigma^2 - s_\gamma^2 s_\sigma^2\right) + m_{h_2}^2 \left(s_\sigma^2 - s_\gamma^2 c_\sigma^2\right) - m_{h_{\rm LHC}}^2 c_\gamma^2\right) \Big] \\ & \times \Big[\left(m_{h_3}^2 - m_{h_2}^2 s_\gamma^2 - m_{h_{\rm LHC}}^2 c_\gamma^2\right)^2 + \left(m_{h_2}^2 - m_{h_3}^2\right)^2 c_\gamma^4 s_\sigma^4 \\ & + 2 \left(m_{h_2}^2 - m_{h_3}^2\right) \left(m_{h_3}^2 + m_{h_2}^2 s_\gamma^2 - m_{h_{\rm LHC}}^2 \left(1 + s_\gamma^2\right)\right) c_\gamma^2 s_\sigma^2 \Big]^{-1}, \end{aligned} \tag{5.12}$$

where $s_\theta = \sin\theta, c_\theta = \cos\theta$, M^2 is the 2×2 submatrix in the 12 sector of the full 3×3 squared mass matrix $\mathcal{M}^2$ of the neutral CP-even scalars in the $\mathcal{H}$ basis

$$M^2 = \begin{pmatrix} m_Z^2 c_\beta^2 + m_A^2 s_\beta^2 & (2v^2\lambda^2 - m_A^2 - m_Z^2)\, c_\beta s_\beta \\ (2v^2\lambda^2 - m_A^2 - m_Z^2)\, c_\beta s_\beta & m_A^2 c_\beta^2 + m_Z^2 s_\beta^2 + \delta_t^2 \end{pmatrix} \tag{5.13}$$

and $\tilde{M}^2 = R_{\beta-\pi/2} M^2 R^t_{\beta-\pi/2}$ in eq. (5.12).

More importantly we have also not included in eq. (5.13) the one loop corrections to the 12 and 11 entries, respectively proportional to the first and second power of $(\mu A_t)/\langle m_{\tilde{t}}^2\rangle$, to which we shall return.

5.3.2 Optimizing the strategy

We shall in particular be interested in two limiting cases:

- H decoupled: $m_{h_3} \gg m_{h_{\rm LHC},h_2}$ and $\sigma, \delta \equiv \alpha - \beta + \pi/2 \to 0$,
- S decoupled: $m_{h_2} \gg m_{h_{\rm LHC},h_3}$ and $\sigma, \gamma \to 0$,

but we use eq.s (5.10, 5.11, 5.12) to control the size of the deviations from the limiting cases when the heavier mass is lowered. In the two respective cases the reference equations are

- H decoupled:

$$s_\gamma^2 = \frac{m_{hh}^2 - m_{h_{\rm LHC}}^2}{m_{h_2}^2 - m_{h_{\rm LHC}}^2}, \tag{5.14}$$

  where

$$m_{hh}^2 = m_Z^2 c_{2\beta}^2 + \lambda^2 v^2 s_{2\beta}^2 + \Delta_t^2; \tag{5.15}$$

- S decoupled:

$$s_{2\alpha} = s_{2\beta}\, \frac{2\lambda^2 v^2 - m_Z^2 - m_A^2|_{m_{h_{\rm LHC}}}}{m_A^2|_{m_{h_{\rm LHC}}} + m_Z^2 + \delta_t^2 - 2m_{h_{\rm LHC}}^2}, \tag{5.16}$$

$$m_{h_3}^2 = m_A^2|_{m_{h_{\rm LHC}}} + m_Z^2 + \delta_t^2 - m_{h_{\rm LHC}}^2, \tag{5.17}$$

  where

$$m_A^2\big|_{m_{h_{\rm LHC}}} = \frac{\lambda^2 v^2(\lambda^2 v^2 - m_Z^2)s_{2\beta}^2 - m_{h_{\rm LHC}}^2(m_{h_{\rm LHC}}^2 - m_Z^2 - \delta_t^2) - m_Z^2\delta_t^2 c_\beta^2}{m_{hh}^2 - m_{h_{\rm LHC}}^2}. \tag{5.18}$$

All the equations in this section are valid in a generic NMSSM. Specific versions of it may limit the range of the physical parameters $m_{h_{\rm LHC},2,3}, m_{H^\pm}$ and α, γ, σ but cannot affect any of these equations. Notice that in the limit $\lambda = 0$, eq. (5.16) coincides with the MSSM case.

When considering the couplings of the CP-even scalars to SM particles, relevant to their production and decays, we shall not include any supersymmetric loop effect other than the top-stop loop effect. This is motivated by the kind of spectrum outlined in section 5.1, with all s-particles at their "naturalness limit", and provides in any event a useful well defined reference case. We also do not include any invisible decay of the CP-even scalars, e.g. into a

pair of neutralinos. To correct for this is straightforward with all branching ratios and signal rates that will have to be multiplied by a factor $\Gamma/(\Gamma + \Gamma_{\chi\chi})$. Finally we do not consider the two neutral CP-odd scalars, since in the general NMSSM both their masses and their composition in terms of the original fields depend upon extra parameters not related to the masses and the mixings of the CP-even states nor to the mass of the charged Higgs.

In all the cases we always discriminate between two configurations:

- $h_{\rm LHC}$ is the lightest state, *i.e.* we identify the observed particle with the lightest CP-even scalar in the NMSSM.

- $h_{\rm LHC}$ is the next-to-lightest state, *i.e.* we investigate the configuration where there is a particle lighter than 125 GeV. In this case we consider also the "invisible" decay of $h_{\rm LHC}$ into a pair of the lightest CP-even scalars.

5.4 H decoupled

In this limiting case, only $h_{\rm LHC}$ and h_2 are relevant, and all phenomenological consequences can be drawn just by studying γ and m_{h_2}. By comparing eq. (5.14) with eq. (5.16), notice that in this case there is only a single relation between the mixing angle γ and the mass of the extra CP-even state m_{h_2}, involving $\tan\beta, \lambda$ and Δ_t. Due to the singlet nature of S it is straightforward to see that the couplings of $h_{\rm LHC} = h_{\rm LHC}$ and h_2 to fermions or to vector boson pairs, $VV = WW, ZZ$, normalized to the same couplings of the SM Higgs boson, are given by

$$\frac{g_{h_{\rm LHC}ff}}{g^{\rm SM}_{hff}} = \frac{g_{h_{\rm LHC}VV}}{g^{\rm SM}_{hVV}} = c_\gamma, \qquad \frac{g_{h_2ff}}{g^{\rm SM}_{hff}} = \frac{g_{h_2VV}}{g^{\rm SM}_{hVV}} = -s_\gamma. \tag{5.19}$$

The fit of all experimental data collected so far gives the bound on s^2_γ shown in figure 5.2 right,

$$\sin^2\gamma < 0.22. \tag{5.20}$$

Here an invisible branching ratio of $h_{\rm LHC}$, $\mathrm{BR}_{\rm inv}$, would strengthen the bound on the mixing angle to $s^2_\gamma < (0.22 - 0.78\mathrm{BR}_{\rm inv})$.

5.4.1 H decoupled, $h_{\rm LHC}$ lightest

Upon use of (5.14) the impact of the bound (5.20) on the parameter space is shown in figure 5.3 for $\lambda = 0.8$ and 1.4, together with the isolines of different values of s^2_γ that might be probed by future improvements in the measurements of the $h_{\rm LHC}$ signal strengths. Larger values of λ already exclude a significant portion of the parameter space at least for moderate $\tan\beta$, as preferred by naturalness. In this section we are taking a fixed value of $\Delta_t = 73$ GeV, which is obtained, e.g., for $m_{\tilde{t}_1} = 600$ GeV, $m_{\tilde{t}_2} = 750$ GeV and mixing angle $\theta_t = 45^0$ [101]. As long as one stays at $\Delta_t \lesssim 85$ GeV, in a range of moderate fine tuning, and $\lambda \gtrsim 0.8$, our results do not depend significantly on Δ_t.

In the same $(\tan\beta, m_{h_2})$ plane of figure 5.3 and for the same values of λ, figure 5.4 shows the gluon-fusion production cross sections of h_2 at LHC for 8 or 14 TeV c.o.m. energies,

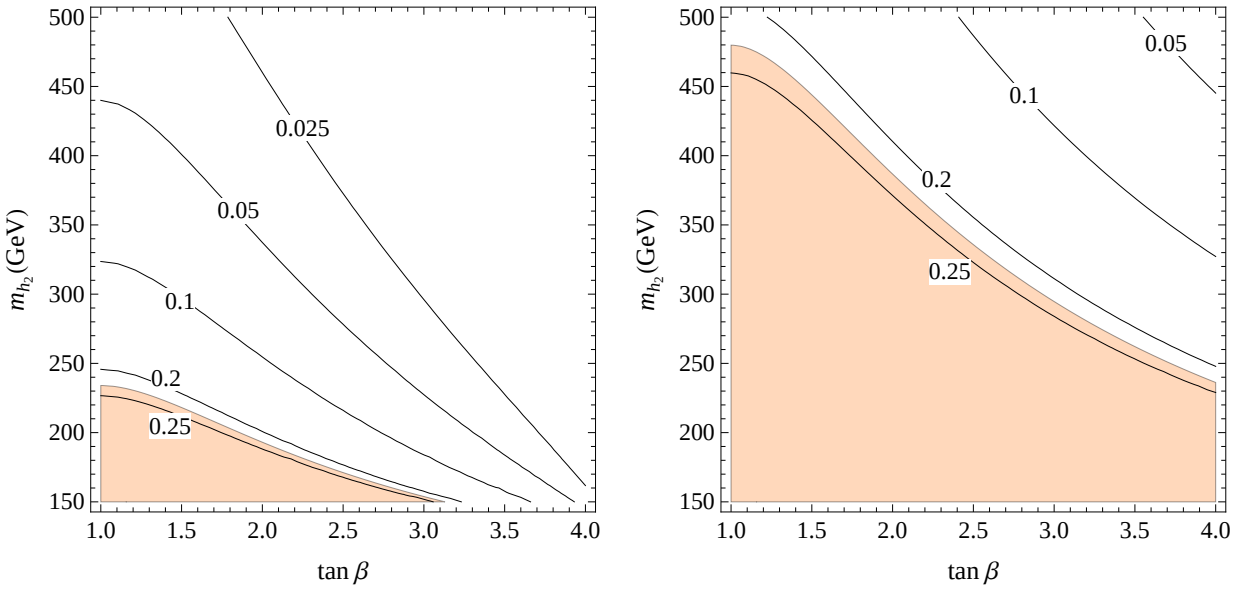

Figure 5.3. H decoupled, $h_{\rm LHC}$ lightest. Isolines of $\sin^2\gamma$. Left: $\lambda = 0.8$. Right: $\lambda = 1.4$. The colored region is excluded at 95%C.L. by the experimental data for the signal strengths of $h_{\rm LHC}$.

where we rescaled by c_γ^2 the NNLL ones provided in [113]. All other h_2 production cross sections, relative to the gluon-fusion one, scale as in the SM with $m_{h_{\rm SM}} = m_{h_2}$.

To determine the decay properties of h_2 it is crucial to know its coupling $(g_{h_2 h^2_{\rm LHC}}/2) h_2 h^2_{\rm LHC}$ to the lighter state. In the general NMSSM and in the large m_H limit considered in this section, the leading λ^2-term contribution to this coupling, as well as the one to the cubic $h_{\rm LHC}$-coupling $(g_{h^3_{\rm LHC}}/6) h^3_{\rm LHC}$, are given by

$$\begin{aligned} g_{h_2 h^2_{\rm LHC}} &= \frac{\lambda^2 v}{8\sqrt{2}} \left(4\frac{v_S}{v}\cos\gamma + 12\frac{v_S}{v}\cos 3\gamma - 7\sin\gamma + 12\cos 4\beta\cos^2\gamma\sin\gamma + 9\sin 3\gamma \right) \\ &\quad - \frac{3}{\sqrt{2}v}\Delta_t^2\cos^2\gamma\sin\gamma, \end{aligned} \tag{5.21}$$

$$\frac{g_{h^3_{\rm LHC}}}{g^{\rm SM}_{h^3_{\rm LHC}}} = \frac{\lambda^2 v^2}{8 m^2_{h_{\rm LHC}}}\cos\gamma \left(10 - 4\cos 4\beta\cos^2\gamma - 6\cos 2\gamma + 8\frac{v_S}{v}\sin 2\gamma \right) + \frac{\Delta_t^2}{m^2_{h_{\rm LHC}}}\cos^3\gamma, \tag{5.22}$$

where v_S is the VEV of the singlet. Figure 5.5 shows the h_2 branching ratio into a pair of light states for some choices of v_S. The other most significant decay mode of h_2 is into a W-pair, with a branching ratio given in figure 5.6. Figure 5.7 shows the triple $h_{\rm LHC}$-coupling normalized to the SM one. It can be shown that h_2 is always a narrow resoances with total width $\Gamma_{h_2} \sim 1 \div 3 (2 \div 10)$ GeV for $\lambda = 0.8(1.4)$.

These results depend on the value taken by v_S, in particular we note that the Higgs fit still allows the triple Higgs coupling to get a relative enhancement of a factor of a few (with a negative or positive sign) with respect to the Standard Model one, thus yielding potentially large effects in Higgs pair production cross sections [138].

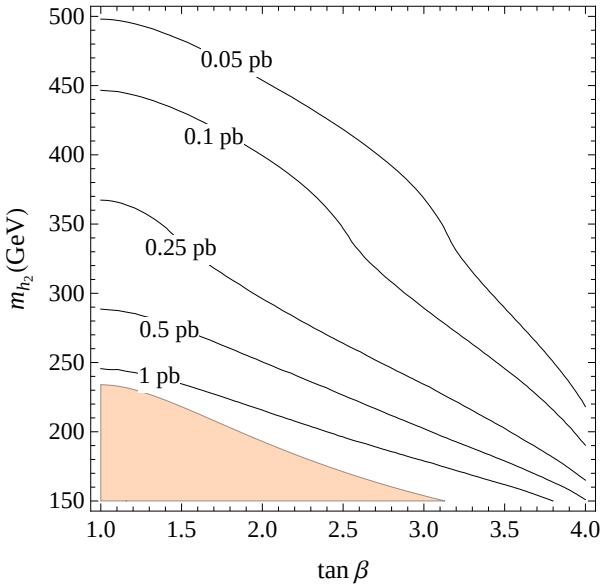

(a) 8 TeV, $\lambda = 0.8$

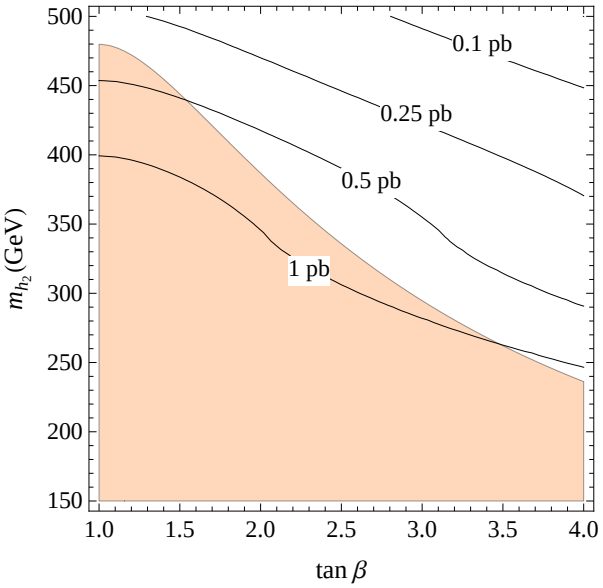

(b) 8 TeV, $\lambda = 1.4$

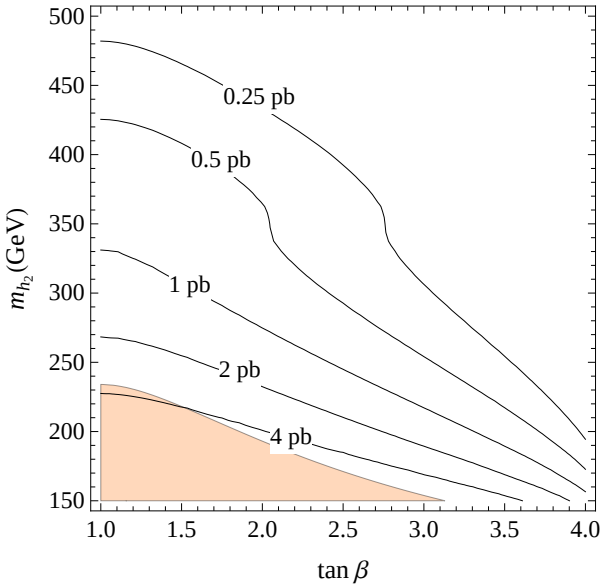

(c) 14 TeV, $\lambda = 0.8$

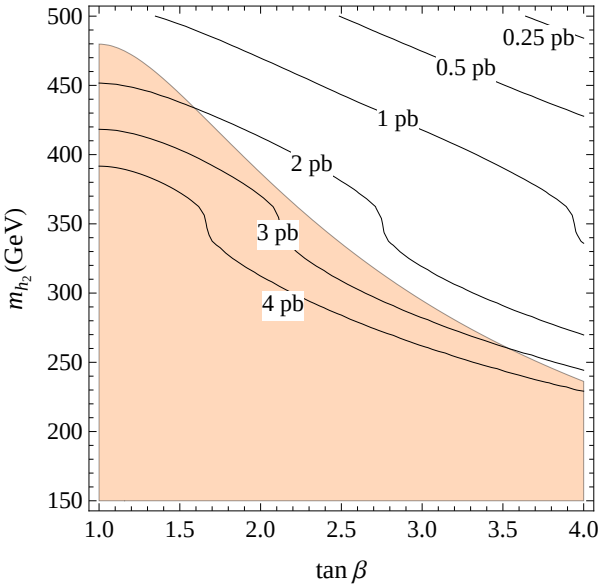

(d) 14 TeV, $\lambda = 1.4$

Figure 5.4. H decoupled, $h_{\rm LHC}$ lightest. Isolines of gluon fusion cross section $\sigma(gg \to h_2)$ at LHC8 and LHC14, for the values $\lambda = 0.8$ and $\lambda = 1.4$. The colored region is excluded at 95%C.L.

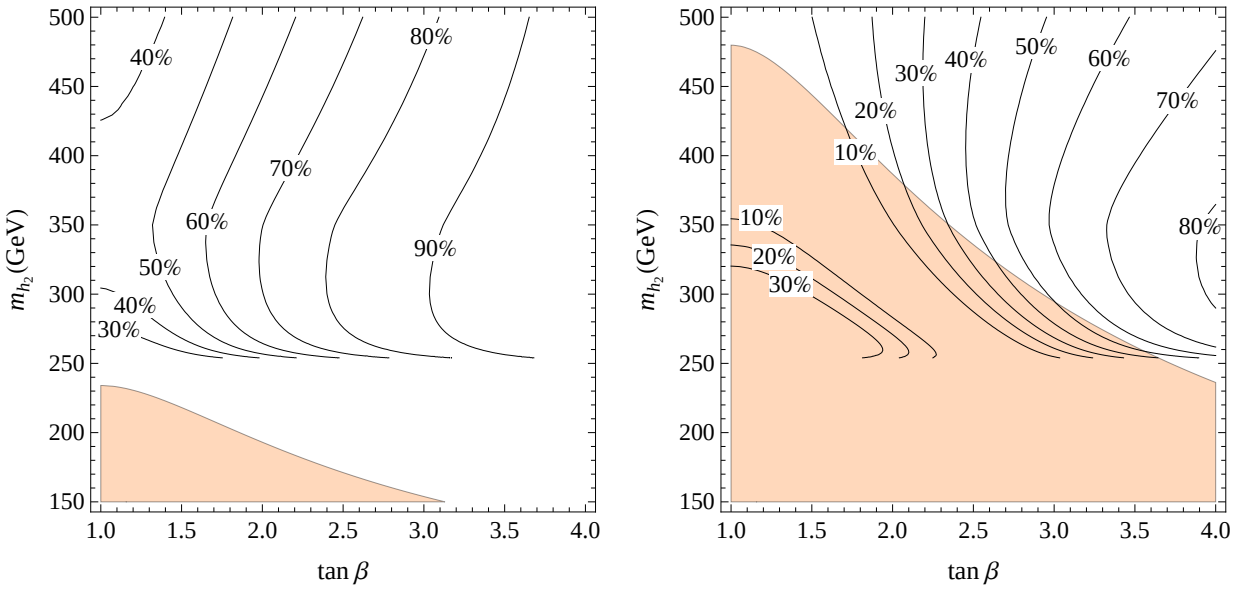

Figure 5.5. H decoupled, $h_{\rm LHC}$ lightest. Isolines of BR($h_2 \to hh$). Left: $\lambda = 0.8$ and $v_S = 2v$. Right: $\lambda = 1.4$ and $v_S = v$. The colored region is excluded at 95%C.L.

As a small comment, it is clear that the parameter space in the case $h_{\rm LHC} < h_2 (< h_3 (= H))$ is still largely unexplored at $\lambda = 0.7 \div 1$. Most promising in this case are the direct searches of h_2 with gluon-fusion production cross-sections at LHC14 in the picobarn range and a large branching ratio, when allowed by phase space, into a pair of $h_{\rm LHC}$ or vector bosons as shown in figures 5.5 and 5.6. Furthermore large deviations from the SM value can occur in the cubic $h_{\rm LHC}$-coupling.

5.4.2 H decoupled, $h_{\rm LHC}$ next-to-lightest

Here we consider the configuration when $h_2 < h_{\rm LHC}$. We are going to discuss two possible ranges of λ.

- The low λ case ($\lambda = 0.1$) is shown in figure 5.8 for two values of Δ_t together with the isolines of s^2_γ. The current fit of the signal strengths measured at LHC constrain $s^2_\gamma < 0.22$ at 95% C.L., which explains the lighter excluded regions in figure 5.8. The red regions are due to the negative searches of $h_2 \to \bar{b}b$ at LEP [139].

- For λ close to unity we take as in the S-decoupled case $\Delta_t = 75$ GeV, but any choice lower than this would not change the conclusions. The currently allowed region is shown in figure 5.9 for two values of λ. Note that, for large λ, no solution is possible at low enough $\tan\beta$, since, before mixing, m^2_{hh} in eq. (5.15) has to be below the mass squared of $h_{\rm LHC}$.

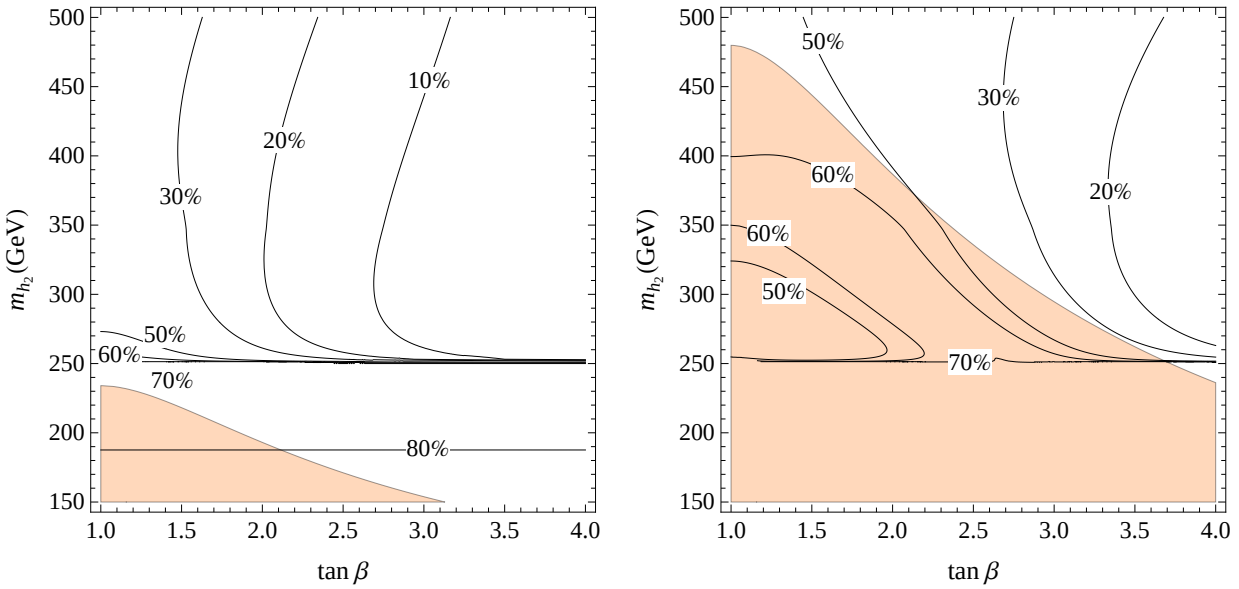

Figure 5.6. H decoupled, $h_{\rm LHC}$ lightest. Isolines of BR($h_2 \to W^+W^-$). Left: $\lambda = 0.8$ and $v_S = 2v$. Right: $\lambda = 1.4$ and $v_S = v$. The colored region is excluded at 95%C.L.

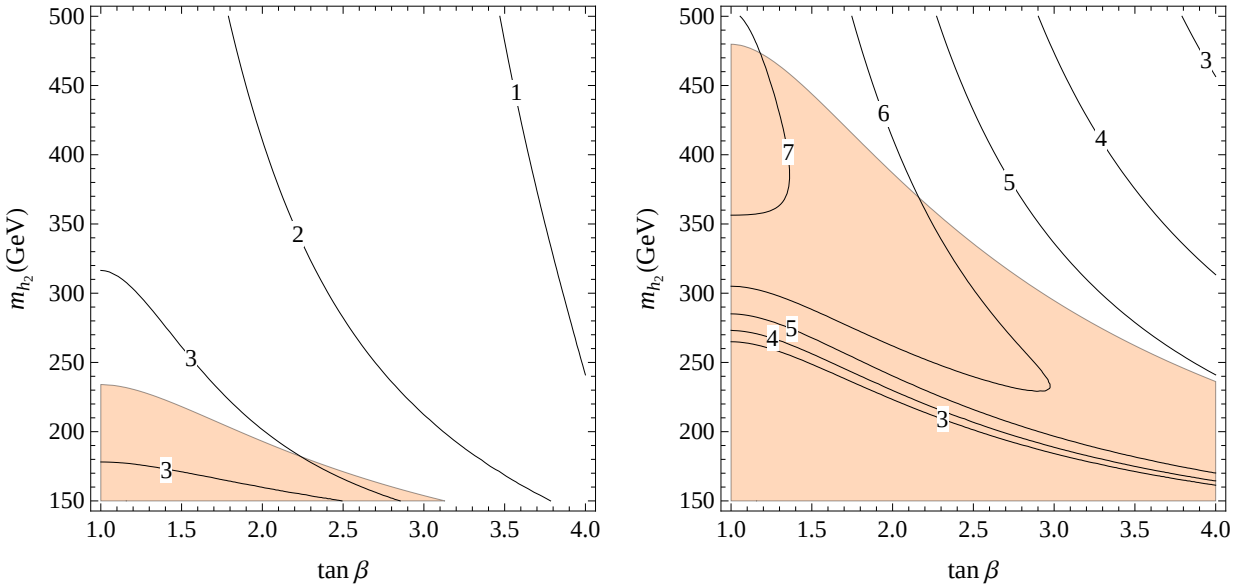

Figure 5.7. H decoupled, $h_{\rm LHC}$ next-to-lightest. Isolines of $g_{hhh}/g_{hhh}^{\rm SM}$. Left: $\lambda = 0.8$ and $v_S = 2v$. Right: $\lambda = 1.4$ and $v_S = v$. The colored region is excluded at 95%C.L.

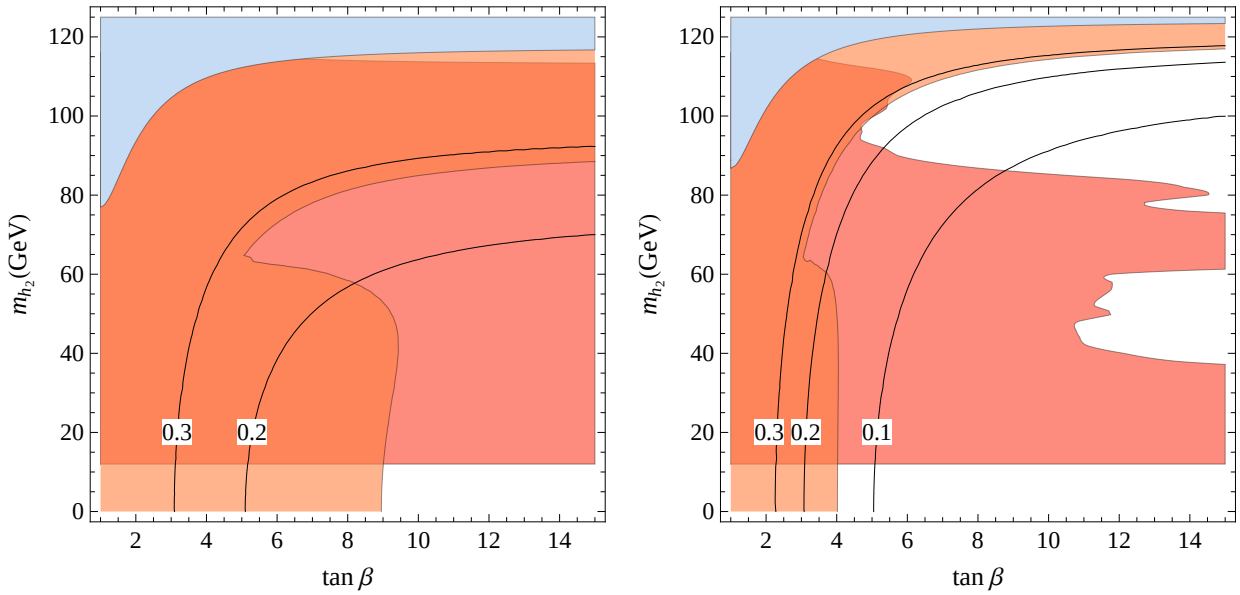

Figure 5.8. H decoupled, $h_{\rm LHC}$ next-to-lightest. Isolines of s^2_γ. $\lambda = 0.1$ and $v_S = v$. Left: $\Delta_t = 75$ GeV. Right: $\Delta_t = 85$ GeV. The orange region is excluded at 95%C.L. by the experimental data for the signal strengths of $h_{\rm LHC}$, while the blue one is unphysical. The red region is excluded by LEP direct searches for $h_2 \to b\bar{b}$.

In both cases we include in the fit the "invisible" decay $h_{\rm LHC} \to h_2 h_2$ when kinematically allowed. [2]

How will it be possible to explore the regions of parameter space currently still allowed in this $h_2 < h_{\rm LHC} (< h_3 (= H))$ case in view of the reduced couplings of the lighter state? Together with an expected improvements in the Higgs coupling measurement, a significant deviation from the case of the SM can occur in the cubic $h_{\rm LHC}$-coupling, $g_{h_1^3}$, as shown in figure 5.10. The LHC14 in the high-luminosity regime is expected to get enough sensitivity to be able to see such deviations [140–142]. At that point, on the other hand, the searches for directly produced s-partners should have already given some clear indications on the relevance of the entire picture.

5.5 S decoupled

When S is decoupled, notice the difference with respect to the single relation (5.14) of the H-decoupled case. Identifying as before $h_{\rm LHC}$ with the resonance found at the LHC, this determines the mass of h_3 (and of $H^\pm$) for any given value of λ and $\tan\beta$.

From our point of view the main motivation for considering the NMSSM is in the possibility to account for the mass of $h_{\rm LHC}$ with not too big values of the stop masses. For this

[2] To include $h_{\rm LHC} \to h_2 h_2$ we rely on the triple Higgs couplings as computed by retaining only the λ^2-contributions. This is a defendable approximation for λ close to unity, where $h_{\rm LHC} \to h_2 h_2$ is important. In the low λ case the λ^2-approximation can only be taken as indicative, but there $h_{\rm LHC} \to h_2 h_2$ is less important.

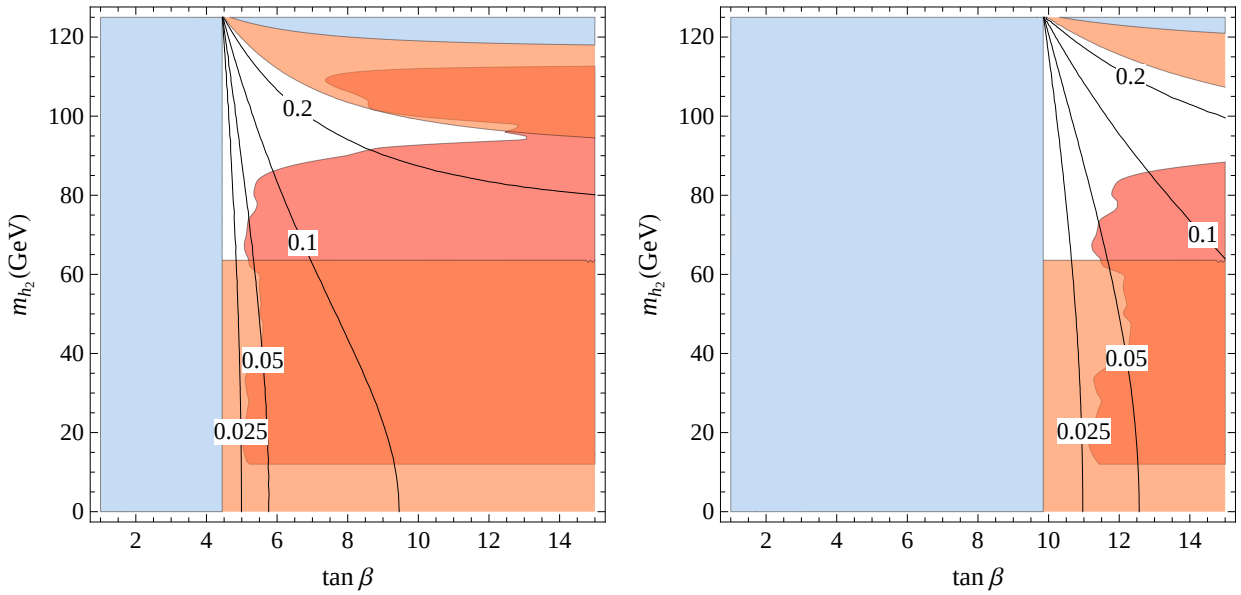

Figure 5.9. H decoupled, $h_{\rm LHC}$ next-to-lightest. Isolines of s_γ^2. $\Delta_t = 75$ GeV and $v_S = v$. Left: $\lambda = 0.8$. Right: $\lambda = 1.4$. Orange and blue regions as in figure 5.8. The red region is excluded by LEP direct searches for $h_2 \to b\bar{b}$.

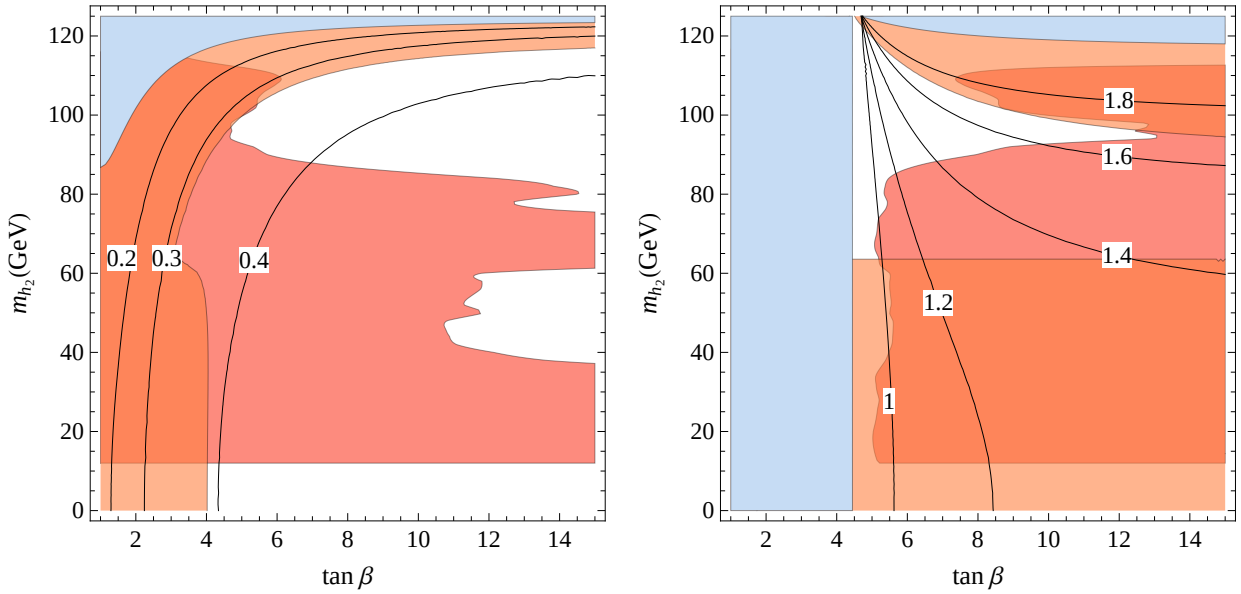

Figure 5.10. H decoupled, $h_{\rm LHC}$ next-to-lightest. Isolines of $g_{h^3}/g_{h^3}\big|_{\rm SM}$. Left: $\lambda = 0.1$, $\Delta_t = 85$ GeV and $v_S = v$. Right: $\lambda = 0.8$, $\Delta_t = 75$ GeV and $v_S = v$. Orange and blue regions as in figure 5.8. The red region is excluded by LEP direct searches for $h_2 \to b\bar{b}$.

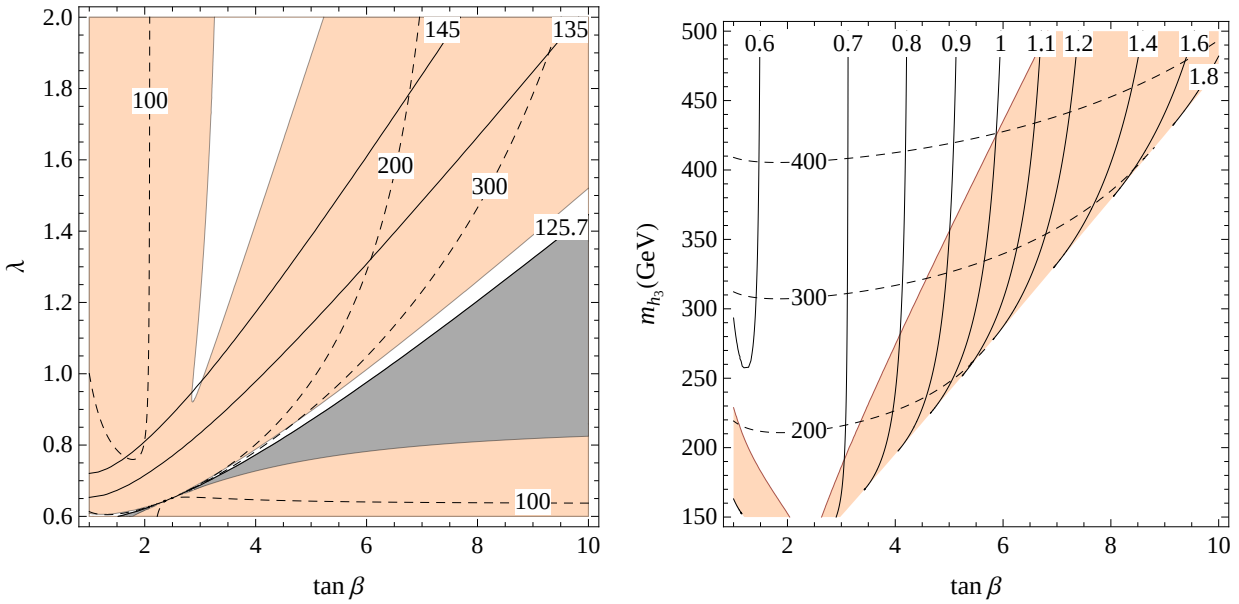

Figure 5.11. S decoupled. Left: isolines of m_{hh} (5.15) (solid), the grey region is unphysical due to $m^2_{H^\pm} < 0$. Right: isolines of λ in the region with $m_{hh} \simeq 125$ GeV. The dashed isolines are for $m_{H^\pm}$. The colored regions are excluded at 95%C.L.

reason we take $\Delta_t = 75$ GeV, which can be obtained, e.g., for an average stop mass of about 700 GeV. In turn, as it will be seen momentarily, the consistency of eq.s (5.16)-(5.18) requires not too small values of the coupling λ. It turns out in fact that for any value of $\Delta_t \lesssim 85$ GeV, the dependence on Δ_t itself can be neglected, so that $m_{h_3}, m_{H^\pm}$ and δ are determined by $\tan\beta$ and λ only. For the same reason it is legitimate to neglect the one loop corrections to the 11 and 12 entries of the mass matrix, eq. (5.13), as long as $(\mu A_t)/\langle m_t^2\rangle \lesssim 1$, which is again motivated by naturalness.

Defining as before $\delta = \alpha - \beta + \pi/2$, the couplings of h_3 become formally the same of the MSSM case (4.16)

$$\frac{g_{h_3tt}}{g^{\rm SM}_{htt}} = \sin\delta - \frac{\cos\delta}{\tan\beta}, \quad \frac{g_{h_3bb}}{g^{\rm SM}_{hbb}} = \sin\delta + \tan\beta\cos\delta, \quad \frac{g_{h_3VV}}{g^{\rm SM}_{hVV}} = \sin\delta. \tag{5.23}$$

We are not considering the possible decays of $h_{\rm LHC}$ and/or of h_3 into invisible particles, such as dark matter, or into any undetected final state, because of background, like, e.g., a pair of light pseudo-scalars. The existence of such decays, however, would not alter in any significant way the excluded regions from the measurements of the signal strengths of $h_{\rm LHC}$, which would all be modified by a common factor $(1 + \Gamma_{\rm inv}/\Gamma_{\rm vis})^{-1}$. This is because the inclusion in the fit of the LHC data of an invisible branching ratio of $h_{\rm LHC}$, $\mathrm{BR}_{\rm inv}$, leaves essentially unchanged the allowed range for δ at different $\tan\beta$ values, provided $\mathrm{BR}_{\rm inv} \lesssim 0.2$.

5.5.1 S decoupled, $h_{\rm LHC}$ lightest

The allowed regions in the plane $(\tan\beta, \lambda)$ shown in figure 5.11 left are determined by a 2-parameter fit of $\tan\beta$, $\sin\delta$. This fit results in an allowed region which is virtually the

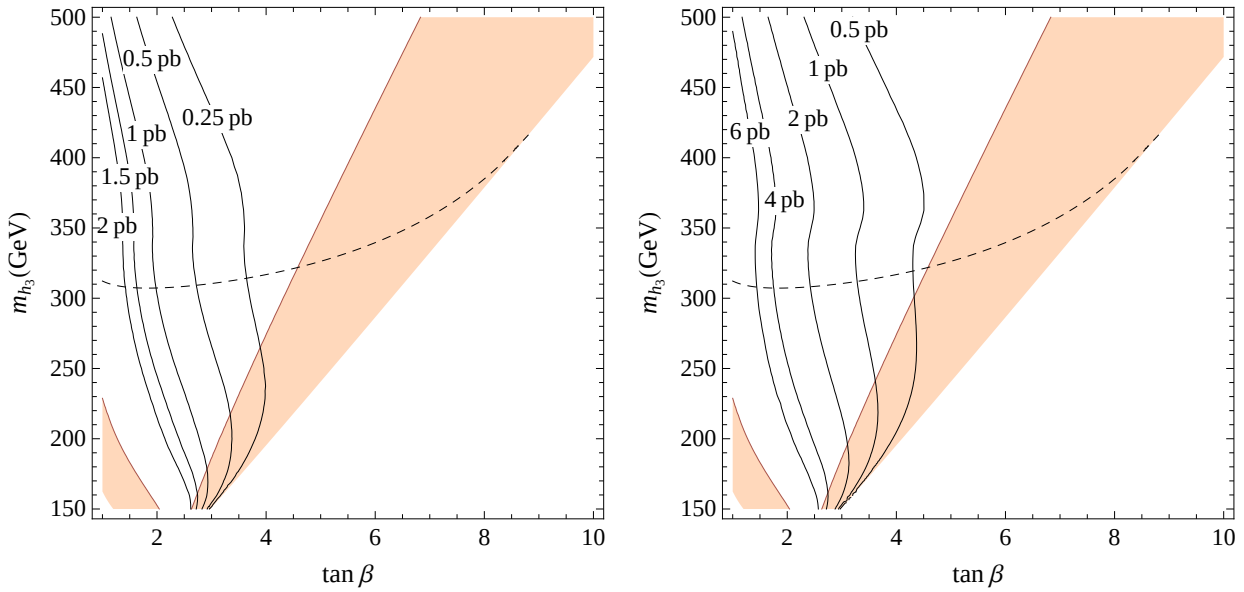

Figure 5.12. S decoupled, $h_{\rm LHC}$ lightest. Isolines of gluon fusion production cross section $\sigma(gg \to h_3)$. The colored regions are excluded at 95%C.L., and the dashed line shows $m_{H^\pm} = 300$ GeV. Left: LHC8. Right: LHC14.

same as the one with $\gamma = 0$ in figure 5.2 left. When inverting λ as a function of $\tan\beta, m_{h_3}$, there are two solutions. In figure 5.11 right, we show only the one which corresponds to the narrow allowed region with m_{hh} close to 125 GeV. Note that λ is restricted to relatively small values. As a consequence the analysis becomes more sensitive to values of Δ_t at or above 80 GeV.

The other two allowed regions in figure 5.11 left, when translated to the $(\tan\beta, m_{h_3})$ plane, correspond to the other solution for λ, and are not displayed in figure 5.11 right. The first one with $\tan\beta \simeq 3$ and $\lambda \gtrsim 1$ always implies a charged Higgs mass $m_{H^\pm}$ below 150 GeV, which is disfavored by indirect constraints [143]. Note that this region, corresponding to the allowed region with large δ in figure 5.2, is mainly allowed because of the large error in the measurement of the $b\bar{b}$ coupling of $h_{\rm LHC}$. Reducing this error down to about 30% around $g_{h_{\rm LHC}bb}/g^{\rm SM}_{hbb} \simeq 1$ would exclude the region. The second one with $\tan\beta \sim 1$, allowed by the Higgs fit, is also excluded by the bounds on $m_{H^\pm}$.

The couplings (5.23) allow to compute the gluon-fusion production cross section of h_3 by means of the techniques described in section 4.2. This cross section is shown in figure 5.12.

The coupling of h_3 to the lighter state $\dfrac{g_{h_3 h^2_{\rm LHC}}}{2} h_3 h^2_{\rm LHC}$ and the triple Higgs coupling

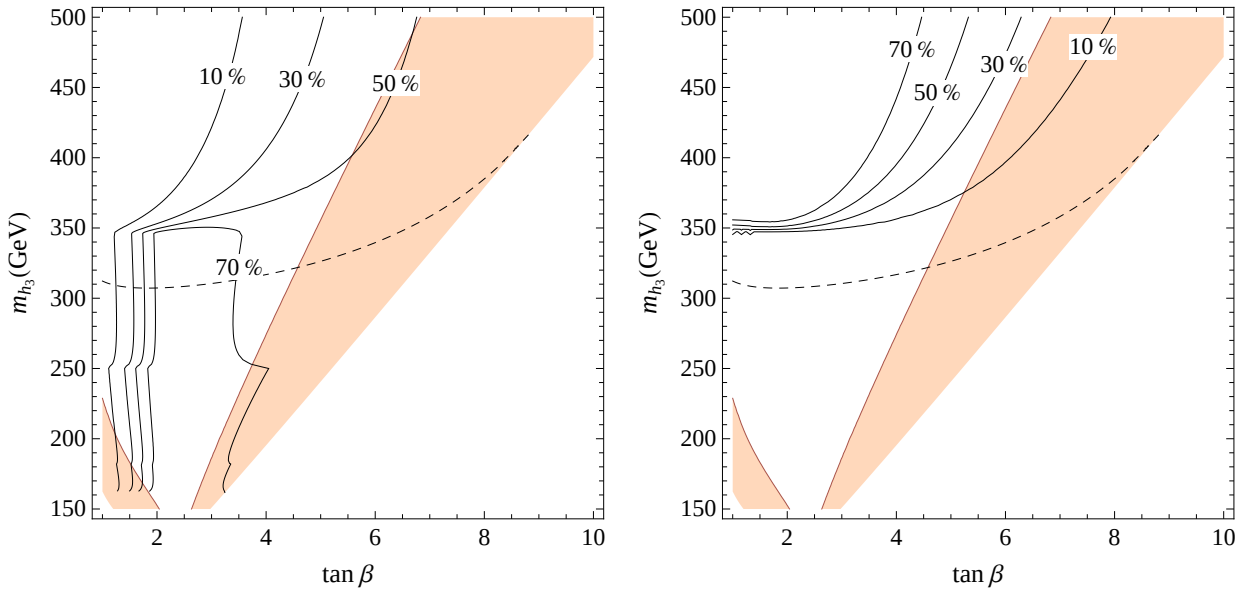

Figure 5.13. S decoupled, $h_{\rm LHC}$ lightest. Left: isolines of BR($h_3 \to b\bar{b}$). Right: isolines of BR($h_3 \to t\bar{t}$). The colored regions are excluded at 95%C.L., and the dashed line shows $m_{H^\pm} = 300$ GeV.

$\frac{g_{h^3_{\rm LHC}}}{6} h^3_{\rm LHC}$ are given by

$$g_{h_3 h^2_{\rm LHC}} = \frac{[(m_Z^2 + v^2\lambda^2)\sin\delta + 3(m_Z^2 - \lambda^2 v^2)\sin(4\beta + 3\delta)]}{2\sqrt{2}v} - \frac{3\Delta_t^2}{\sqrt{2}v}\frac{\cos(\beta+\delta)\sin^2(\beta+\delta)}{\sin^3\beta}, \tag{5.24}$$

$$\frac{g_{h^3_{\rm LHC}}}{g^{\rm SM}_{h^3_{\rm LHC}}} = \frac{(m_Z^2 + v^2\lambda^2)\cos\delta + (m_Z^2 - v^2\lambda^2)\cos(4\beta+3\delta)}{2m^2_{h_{\rm LHC}}} + \frac{\Delta_t^2}{m^2_{h_{\rm LHC}}}\frac{\sin^3(\beta+\delta)}{\sin^3\beta}. \tag{5.25}$$

Figure 5.13 shows the most relevant widths of h_3. Here differently from H-decoupled case BR($h_3 \to h\bar{h}$) is not particularly relevant, see [5] for more details.

5.5.2 S decoupled, $h_{\rm LHC}$ next-to-lightest

We can represent in figure 5.14 the allowed regions in the plane $(\tan\beta, m_{h_3})$ and the isolines of λ and $m_{H^\pm}$ for $h_3 < h_{\rm LHC} (< h_3 (= S))$. At the same time the knowledge of δ in every point of the same $(\tan\beta, m_{h_3})$ plane fixes the couplings of h_3 and $h_{\rm LHC}$, which allows to draw the currently excluded regions from the measurements of the signal strengths of $h_{\rm LHC}$. As declared, we do not include any supersymmetric loop effect other than the ones that give rise to eq. (5.13).

Note, as anticipated, that in every case λ is bound to be above about 0.6. To go to lower values of λ would require considering $\Delta_t \gtrsim 85$ GeV, i.e. heavier stops. On the other hand in this S-decoupled case lowering λ and raising Δ_t makes the NMSSM close to the MSSM.

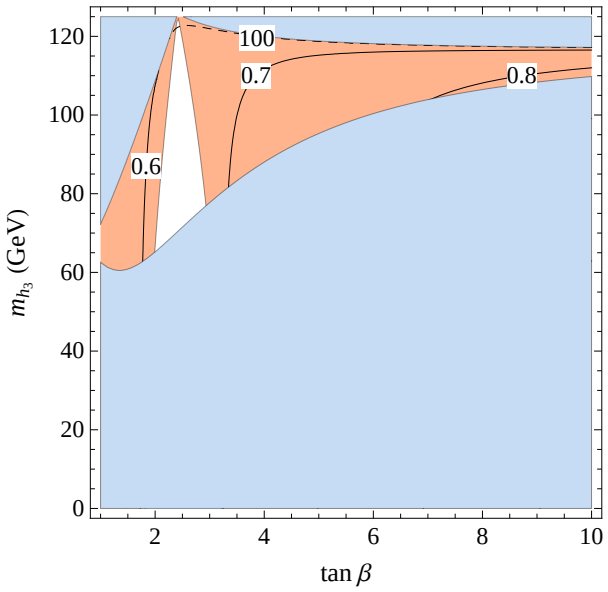

Figure 5.14. S decoupled, $h_{\rm LHC}$ next-to-lightest. Isolines of λ (solid) and $m_{H^\pm}$ (dashed). The orange region is excluded at 95%C.L. by the experimental data for the signal strengths of $h_{\rm LHC}$. The blue region is unphysical.

5.6 Fully mixed scenario

In the general case, when H or S are not completely decoupled, the three angles δ, γ and σ can all be different from zero, and the three masses m_{h_2}, m_{h_3} and $m_{H^\pm}$ are all virtually independent. In this section we present a spectrum where h_3 is parametrically heavier than $h_{\rm LHC}, h_2$. Such configuration can be seen as a deformation of the H-decoupled case. Again, we are considering both the cases where $h_{\rm LHC}$ is and is not the lightest CP-even scalar.

5.6.1 Fully mixed scenario, $h_{\rm LHC}$ lightest

In figure 5.15 we show the excluded regions in the plane $(\tan\beta, m_{h_2})$ for $m_{h_3} = 750$ GeV and $\lambda = 1.4$, setting s_σ^2 to two different values in order to fix $m_{H^\pm}$. When $s_\sigma^2 = 0$ one recovers the previous H decoupled case in the limit $m_{h_3} \to \infty$. With respect to this case, both γ and δ are free parameters in the fit to the couplings of $h_{\rm LHC}$, and as a consequence the bounds are milder than what is expected from using only γ. If $s_\sigma^2 \neq 0$, h_2 and h_3 are not decoupled, and their masses can not be split too much consistently with all the other constraints. This is reflected in a broader excluded region for low m_{h_2} in figure 5.15 right, where we take $s_\sigma^2 = 0.25$.

5.6.2 Fully mixed scenario, $h_{\rm LHC}$ next-to-lightest

In this configuration, we consider the case of a state h_2 lighter than $h_{\rm LHC}$, lowering m_{h_3} to 500 GeV, to see if it could have an enhanced signal strength into $\gamma\gamma$, as discussed also in [144]. Using eq.s (5.10)-(5.12), for fixed values of σ, λ and Δ_t, the two remaining angles α

(or $\delta = \alpha - \beta + \pi/2$) and γ are determined in any point of the $(\tan\beta, m_{h_2})$ plane and so are all the branching ratios of h_2 and of $h_{\rm LHC}$. More precisely δ is fixed up to the sign of $s_\sigma c_\sigma s_\gamma$ (see first line of eq. (5.12)), which is the only physical sign that enters the observables we are considering.

The corresponding situation is represented in figure 5.16, for two choices of λ and Δ_t. The sign of $s_\sigma c_\sigma s_\gamma$ has been taken negative in order to suppress BR($h_2 \to b\bar{b}$). This constrains s_σ^2 to be very small in order to leave a region still not excluded by the signal strengths of $h_{\rm LHC}$, with δ small and negative. To get a signal strength for $h_2 \to \gamma\gamma$ close to the SM one for the corresponding mass is possible for a small enough value of s_γ^2, while the dependence on m_{h_3} is weak for values of m_{h_3} greater than 500 GeV. Note that the suppression of the coupling of h_2 to b-quarks makes it necessary to consider the negative LEP searches for $h_2 \to$ hadrons [119], which have been performed down to $m_{h_2} = 60$ GeV.

Looking at the similar problem when $h_2 > h_{\rm LHC}$, we find it harder to get a signal strength close to the SM one, although this might be possible for a rather special choice of the parameters.[3] Our purpose here is more to show that in the fully mixed situation the role of the measured signal strengths of $h_{\rm LHC}$, either current or foreseen, plays a crucial role.

5.7 Discussion

We have outlined a possible overall strategy to search for signs of the CP-even states of the general NMSSM by suggesting a relatively simple analytic description of different situations. To make this possible at all we have made some simplifying assumptions on the parameter space, which are motivated by naturalness requirements and have been in any case specified whenever needed. In our view the advantages of having an overall coherent analytic picture justify the introduction of these assumptions.

A clear difference emerges between the two cases we have considered, the S-decoupled and the H-decoupled cases: the influence on the signal strengths of $h_{\rm LHC}$ of the mixing with a doublet or with a singlet makes the relative effects visible at different levels. With present data, although the signal strengths of $h_{\rm LHC}$ are close to those expected in the SM, they still allow for a new further state nearby in the NMSSM if $h_{\rm LHC}$ is the lightest state. This is unlike the case of the MSSM, where a CP-even scalar heavier than $h_{\rm LHC}$ and below about 350 GeV is unlikely, as shown in chapter 4. If $h_{\rm LHC}$ is the next-to-lightest state only the H-decoupled case shows a sizeable parameter space still allowed.

Needless to say, in any case the direct searches will be essential. The new states behave differently in the two limiting cases.

The state h_2 of the H-decoupled case has a large BR into a pair of $h_{\rm LHC}$, whenever allowed by phase space, with VV as subdominant decay (figures 5.5-5.6). With the production cross sections shown in figure 5.4 its direct search at LHC8 or LHC14 may be challenging, although perhaps not impossible [146, 147]. A recent analysis of a scalar resonance decaying into $\gamma\gamma b\bar{b}$ shows that the LHC experiments start becoming sensitive to interesting regions of the parameter space [148]. For the case of h_2 decaying into vectors an interesting possibility is offered by searches for an heavy Higgs in the ZZ channel, see [149] and the next chapter.

[3] An increasing significance of the excess found by the CMS [145] at 136 GeV would motivate such special choice.

On the other hand the reduced value of λ allowed in the S decoupled case makes the $b\bar{b}$ channel, and so the $\tau\bar{\tau}$, most important, below the $t\bar{t}$ threshold (figure 5.13). This makes the state h_3 relatively more similar to the CP-even H state of the MSSM (figures 4.4 and 4.5), which is being actively searched.

It is also interesting that, in the H-decoupled case, large deviations from the SM value are possible in the triple Higgs coupling $g^3_{h_{\rm LHC}}$, contrary to the S-decoupled and MSSM cases.

Finally, in case of a positive signal, direct or indirect, it may be important to try to interpret it in a fully mixed scheme, involving all the three CP-even states. To this end the analytic relations of the mixing angles to the physical masses given in eq.s (5.10)-(5.12) offer a useful tool, as illustrated in the examples of a $\gamma\gamma$ signal of figure 5.16.

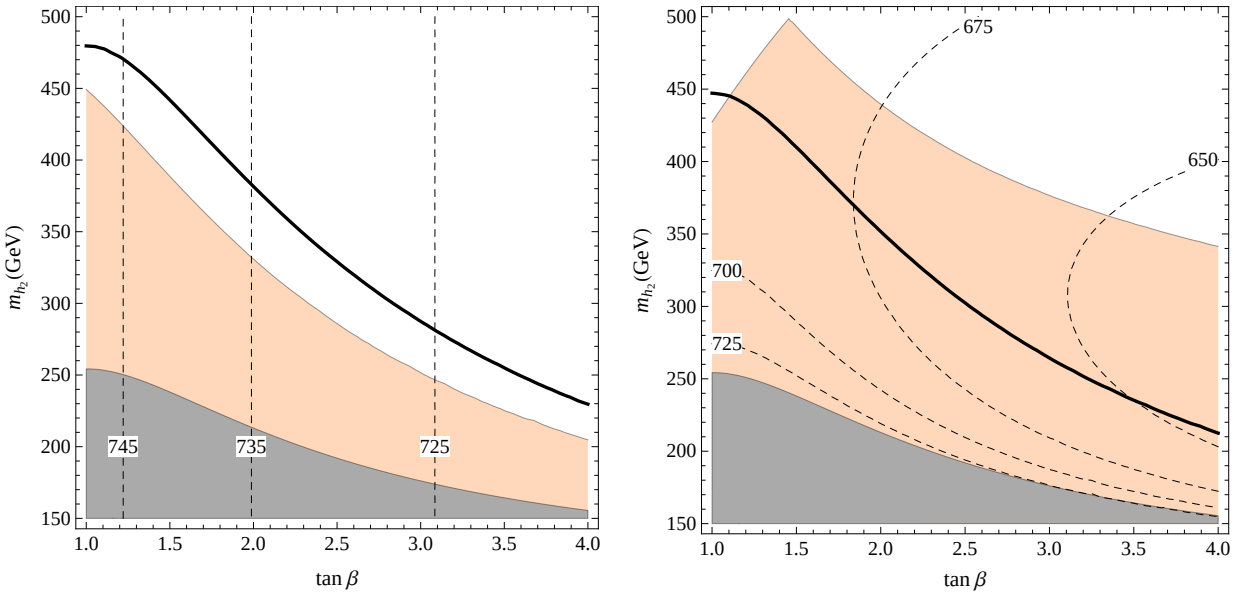

Figure 5.15. "Fully mixed scenario", $h_{\rm LHC}$ lightest, with $\lambda = 1.4$ and $m_{h_3} = 750$ GeV. The dashed isolines are for $m_{H^\pm}$. Left: $\sin^2\sigma = 0$. Right: $\sin^2\sigma = 0.25$. The colored region is excluded at 95%C.L. In the grey area there is no solution for δ. The thick line shows the naïve exclusion limit from s^2_γ only.

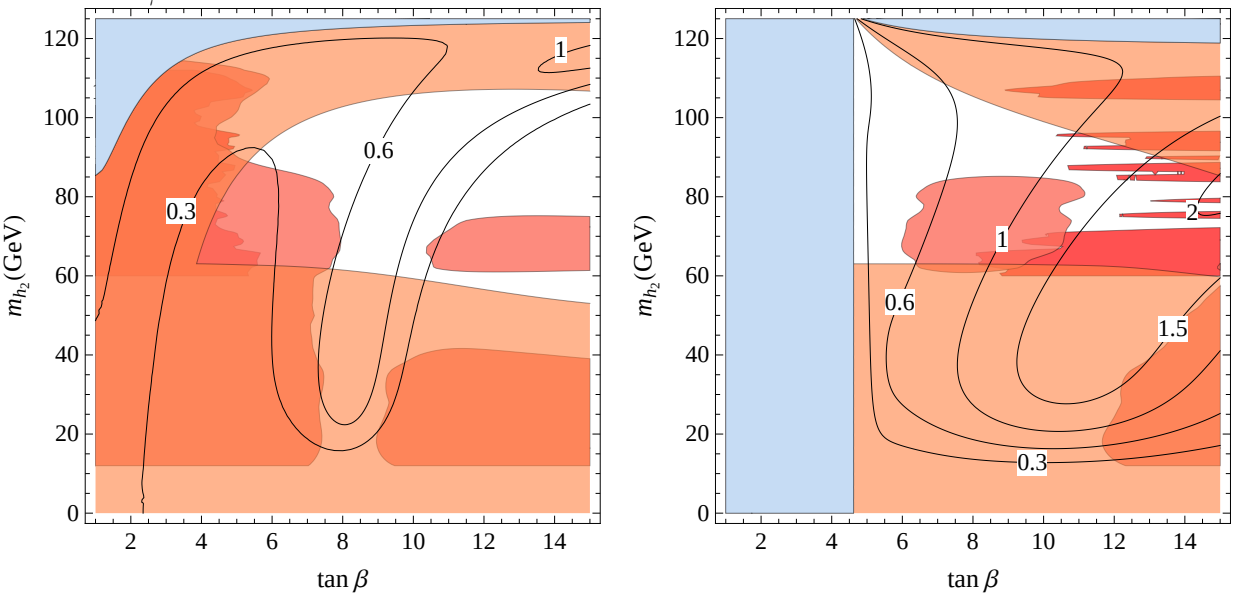

Figure 5.16. "Fully mixed scenario", $h_{\rm LHC}$ next-to-lightest,. Isolines of the signal strength of $h_2 \to \gamma\gamma$ normalized to the SM. We take $m_{h_3} = 500$ GeV, $s^2_\sigma = 0.001$ and $v_s = v$. Left: $\lambda = 0.1$, $\Delta_t = 85$ GeV. Right: $\lambda = 0.8$, $\Delta_t = 75$ GeV. Orange and blue regions as in figure 5.8. The red and dark red regions are excluded by LEP direct searches for $h_2 \to b\bar{b}$ and $h_2 \to$ hadrons respectively.

Part IV

A comparison of precision tests

Chapter 6

What next? Higgs vs. electroweak observables

In this thesis, we have considered models of EWSB satisfying all the existing bounds and able to give sizeable effects at future experiments. It has been shown however that the MCHM, MSSM and NMSSM have to face a certain degree of fine-tuning raised by the null results coming from the first run of the LHC.

In fact, despite the hope that some of the models described in this thesis will manifest themselves at the LHC, it should be said that the results of the first LHC phase, as partly already hinted by previous experiments as well [150], have shown that the proposed natural models do not work in the way they were originally thought. Here we take the view that it will be in any case crucial for the entire field to push as high as possible the sensitivity to the signs of "quasi-natural" theories of EWSB, as they may now be called.

In the concluding part of this thesis we would like to comment on the information that might come from indirect searches in precision measurements. Such measurements could play a leading role in a sufficiently long period of time, after a relatively early stage of the new LHC phase, whatever its findings will be, and before the advent of a needed higher energy hadron collider. Specifically we have in mind the measurements of the Higgs boson couplings at the LHC and the improvements in the EWPTs that could be done at a new Z factory, like at an ILC or at TLEP. A different opportunity is offered by flavour physics experiments, as discussed, for example, in chapter 3 for the CHM case.

In order to try to have a sufficiently broad view of the possible outcomes we discuss all the three models encountered so far in this thesis. Also in view of the current bounds, they models provide a significant representation of quasi-natural models of EWSB, even though different specific realizations are possible, that can give rise to different features. The early results of the LHC in its second phase might clearly point to one of them, perhaps with some needed integration, or could keep them all as open possibilities.

This chapter relies on [6].

6.1 A "composite" Higgs boson

The simplified model of composite Higgs boson that we consider is defined by the Lagrangian [18]

$$\mathcal{L} = \frac{1}{2}(D_\mu \Phi)^2 - \lambda(\Phi^2 - f_0^2)^2 - V(\varphi, \varphi_5), \tag{6.1}$$

where Φ is a five-plet of real scalar fields, D_μ is the covariant derivative with respect to the SM gauge group and $V(\varphi, \varphi_5)$ is a potential that breaks explicitly the $SO(5)$ symmetry of the λ-dependent term down to $SO(4)$. Under this $SO(4)$ $\Phi = \varphi + \varphi_5$ where φ is quartet, or a complex doublet under $SU(2)_L \times U(1)_Y$, and φ_5 is a SM singlet.

In a non-linearly realized $SO(5)/SO(4)$ σ-model, as introduced in section 2.2, the λ-term is replaced by $\delta(\Phi^2 - f^2)$, where f is the decay constant of the (pseudo)-Goldstone boson field φ. Here we keep a finite coupling λ to increase the calculability of the model.

With a specific choice of the potential V, e.g. [151]

$$V(\varphi, \varphi_5) = \alpha f_0^2 \varphi^2 - \beta \varphi^2 \varphi_5^2, \tag{6.2}$$

one can compute the vacuum expectation values of φ and φ_5

$$\langle \varphi \rangle^2 = \frac{2 f_0^2 (\alpha - \beta)\lambda}{\beta(\beta - 4\lambda)} = v^2 = (246 \text{ GeV})^2, \tag{6.3}$$

$$\langle \varphi_5 \rangle^2 = \frac{f_0^2(\alpha(\beta - 2\lambda) - 2\beta\lambda)}{\beta(\beta - 4\lambda)}, \tag{6.4}$$

as well as the mass and composition of the two physical scalars in Φ. Let us define

$$\langle \varphi \rangle^2 + \langle \varphi_5 \rangle^2 = f_0^2 \frac{4\lambda - \alpha}{4\lambda - \beta} \equiv f^2, \tag{6.5}$$

so that, when $\lambda \to \infty$, then $f_0 \to f$ to recover the non-linear σ-model description. Let us also define the mass eigenstates (h, σ) by

$$h = \cos\theta \varphi + \sin\theta \varphi_5, \quad \sigma = -\sin\theta \varphi + \cos\theta \varphi_5, \tag{6.6}$$

where we maintain the same notation φ for its only physical component. If one insists that the parameters of the breaking potential, α, β, remain limited as λ grows, the parameters α, β, λ and f_0 can be traded for the more physical parameters v, f and the masses m_h, m_σ in a unique way, e.g.

$$\lambda = \frac{m_\sigma^2 + m_h^2}{8 f^2}. \tag{6.7}$$

In this way the mixing angle is also uniquely determined by

$$\sin 2\theta = -2\sqrt{\xi(1-\xi)} \frac{m_\sigma^2 + m_h^2}{m_\sigma^2 - m_h^2} \sqrt{1 - \frac{m_h^2 m_\sigma^2}{(m_\sigma^2 + m_h^2)^2 (1-\xi)\xi}}, \tag{6.8}$$

where we define as customary

$$\xi = \frac{v^2}{f^2}. \tag{6.9}$$

For large m_σ^2/m_h^2 we have

$$\sin^2\theta = \xi - \frac{m_h^2}{m_\sigma^2} + O(\xi \frac{m_h^2}{m_\sigma^2}). \tag{6.10}$$

Had we considered a different $SO(5)$-breaking potential than (6.2), e.g. $V = \alpha f_0^3 \varphi_5 - \beta f_0^2 \varphi^2$ [18], we would have obtained a similar expression except for a factor of 2 in front of the m_h^2/m_σ^2 correction.[1]

The mixing angle (6.8) is the main parameter that determines both the modified Higgs couplings to the gauge bosons, $V = W, Z$, as well as the corrections to the ε-parameters of the EWPT [12]. For the Higgs couplings, normalized to the SM one has,[2]

$$\frac{g_{hVV}}{g_{hVV}^{\rm SM}} = \cos\theta, \qquad \frac{g_{hhVV}}{g_{hhVV}^{\rm SM}} = \cos^2\theta \tag{6.11}$$

and, for those ones of the σ field,

$$\frac{g_{\sigma VV}}{g_{hVV}^{\rm SM}} = -\sin\theta, \qquad \frac{g_{\sigma\sigma VV}}{g_{hhVV}^{\rm SM}} = \sin^2\theta. \tag{6.12}$$

As a consequence, for the $\varepsilon_i, i = 1, 2, 3$

$$\varepsilon_i = \varepsilon_i^{\rm SM,\not h} + \cos^2\theta \bar\varepsilon_i(m_h) + \sin^2\theta \bar\varepsilon_i(m_\sigma), \tag{6.13}$$

where $\varepsilon_i^{\rm SM,\not h}$ are the total SM contributions but the Higgs exchanges, while $\bar\varepsilon_i$ are the pure Higgs contributions to the ε-parameters in the SM. We do not consider modifications of the Higgs-fermions couplings nor the virtual effect of any extra particle other than the σ-scalar itself.

In the large m_σ limit, for the deviations from the SM values $\Delta\varepsilon_i \equiv \varepsilon_i - \varepsilon_i^{\rm SM}$, one gets

$$\Delta\varepsilon_1 = -\sin^2\theta \frac{3\alpha}{8\pi c_w^2}\left[\log\frac{m_\sigma}{m_h} + c_1(m_h) + O(\frac{m_Z^2}{m_\sigma^2})\right], \tag{6.14}$$

$$\Delta\varepsilon_2 = \sin^2\theta \frac{\alpha}{4\pi c_w^2}\left[c_2(m_h) + O(\frac{m_Z^2}{m_\sigma^2})\right], \tag{6.15}$$

$$\Delta\varepsilon_3 = \sin^2\theta \frac{\alpha}{24\pi s_w^2}\left[\log\frac{m_\sigma}{m_h} + c_3(m_h) + O(\frac{m_Z^2}{m_\sigma^2})\right], \tag{6.16}$$

where numerically for $m_h = 125$ GeV

$$c_1 = -0.57, \qquad c_2 = 0.10, \qquad c_3 = 0.62. \tag{6.17}$$

As noticed in [153], to obtain the values of the finite terms c_i, one has to include the correct dependence of the ε_i on m_h, which is not only contained in the vacuum polarization amplitudes entering the usual parameters S, T, U [15] (see section 1.1 in chapter 1).

The outcome of these considerations is represented in figure 6.1, where we show the relative deviation of g_{hVV} from the SM and the value of $\Delta\varepsilon_1$ as a most representative quantity in the EWPT. In all of the (m_σ, f) plane, λ is below 3, i.e. in a semi-perturbative regime, with $\Gamma_\sigma < m_\sigma$. At LHC the 1σ attainable precision on g_{hVV} is expected to be around 5% after

[1] The potential (6.2) can be viewed as the linearized version of MCHM$_{5,10}$ [47], whereas $V = \alpha f_0^3 \varphi_5 - \beta f_0^2 \varphi^2$ represents the linearized version of MCHM$_4$ [45].

[2] One can show that, in the $m_\sigma \to \infty$ limit, scattering amplitudes sensitive to the couplings in eq.(6.11) (e.g. $VV \to VV, hh$) agree with those of the non-linear σ-model [152].

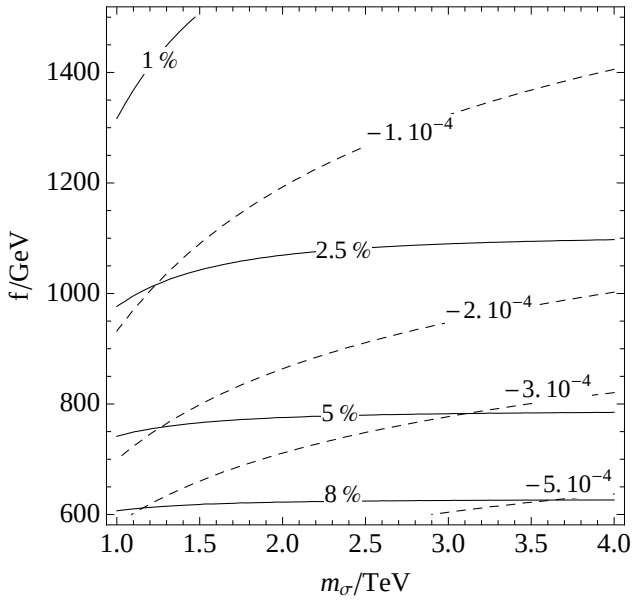

Figure 6.1. "Composite" Higgs model. Isoline of $|\delta g_{hVV}|$ (solid) and $\Delta\varepsilon_1$ (dashed).

300 fb^{-1} and it might be lowered by a factor of about 2 in the High Luminosity configuration (HL-LHC) [154,155] with a corresponding reduction of the theory uncertainties[3]. A precision below 1% is expected on the other hand in a Higgs factory at an e^+e^- collider [157]. About the EWPT, the error on the parameter $\Delta\varepsilon_1$, currently of $(5 \div 8)10^{-4}$ depending on the assumptions of the fit [16, 17], might be reduced by more than one order of magnitude at TLEP [157–159].

6.2 NMSSM

As a relevant representative of a weakly coupled theory, we consider, as in chapter 5, the NMSSM with s-partners heavy enough that their virtual exchanges do not affect in a significant way the precision observables of interest here. More specifically we focus on the H decoupled case of section 5.4 which allows for a formal connection with the model discussed in the previous section. Indeed, in the limit where the extra scalar doublet orthogonal to the observed states (the Goldstone and the Higgs bosons) is also decoupled, the two residual physical scalars are again an admixture of an $SU(2)$ doublet and a real singlet S.[4] This admixture is controlled by the rotation of an angle γ that diagonalizes the scalar mass matrix

$$\mathcal{M} = \begin{pmatrix} m_Z^2 (\frac{1-\tan^2\beta}{1+\tan^2\beta})^2 + \frac{2\tan^2\beta}{(1+\tan^2\beta)^2}\lambda^2 v^2 + \Delta_t^2 & \lambda v M \\ \lambda v M & m_S^2 \end{pmatrix}, \tag{6.18}$$

[3] See [156] for a recent detailed analysis.

[4] The pseudo-scalar component of the complex singlet is decoupled from the system in presence of CP conservation.

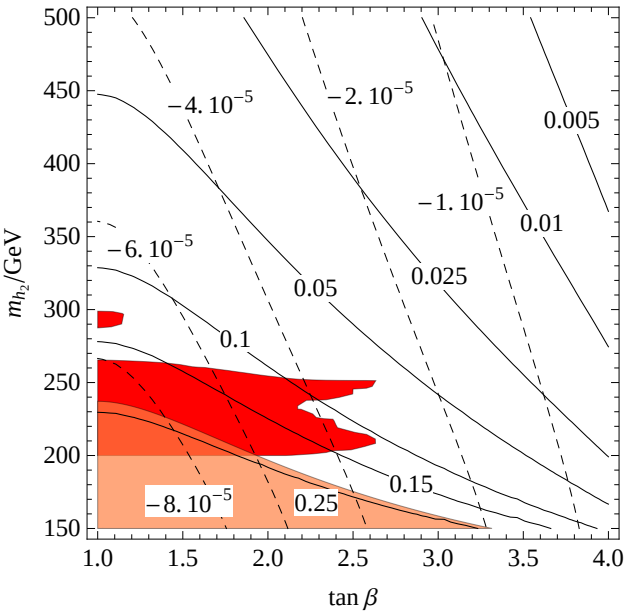

Figure 6.2. NMSSM at $\lambda = 0.8$ and $\Delta_t = 75$ GeV. Isolines of $\sin^2\gamma$ (solid) and $\Delta\varepsilon_1$ (dashed). The orange region is excluded at 95%C.L. by the experimental data for the signal strengths of h. The red region is excluded by direct searches for $h_2 \to ZZ$ [149]. This exclusion above the threshold $h_2 \to hh$ depends on the vacuum expectation value of S. Here we take $\langle S\rangle = 2v$.

where λ is the usual supersymmetric Yukawa coupling of the NMSSM and Δ_t lumps the main radiative correction effects that do no decouple in the heavy s-partner limit. The diagonalization of this matrix, trading M and m_S for the physical masses in the order $m_h < m_{h_2}$, gives the mixing angle of eq. (5.14),

$$\sin^2\gamma = \frac{1}{m_{h_2}^2 - m_h^2}\left[\frac{2\tan^2\beta}{(1+\tan^2\beta)^2}\lambda^2 v^2 + \Delta_t^2 + m_Z^2\left(\frac{1-\tan^2\beta}{1+\tan^2\beta}\right)^2 - m_h^2\right]. \tag{6.19}$$

The formal analogy with the previous model makes it such that eq.s (6.11-6.17) are also valid here with the replacements $\theta \to \gamma$ and $\sigma \to h_2$. The important difference with the composite Higgs model is that in the NMSSM not only the couplings g_{hVV} but also the couplings to all the fermions, $g_{hf\bar{f}}$, are rescaled by a universal factor $\cos\gamma$ relative to the SM ones.

The impact of all this on the precision observables is shown in figure 6.2 for $\lambda = 0.8$, at the upper border for perturbativity up to the Grand Unified Scale [126, 128], and $\Delta_t = 75$ GeV, compatible with stop masses above 700 GeV. How changes in these parameters would affect figure 6.2 is clear from eq. (6.19). In the same figure we also show the currently excluded regions from the measurements of the Higgs couplings and from the direct search of $h_2 \to ZZ$ [149].

At LHC a universal rescaling by $\cos\gamma$ of all the Higgs couplings manifests itself in the signal strengths as an effective branching ratio in invisible channels. The current limit at 95% C.L., $\sin^2\gamma < 0.24$, should be reduced to $\sin^2\gamma < 0.15$ after 300 fb^{-1} of the next LHC phase, whereas $\sin^2\gamma \lesssim 0.05$ might be attainable at HL-LHC [154, 155]. An absolute measurement at TLEP of the hZ cross section could increase the sensitivity to $\sin^2\gamma$ at the 1% level or

less [157]. Figure 6.2 makes clear that the EWPT would have a relatively limited impact on the NMSSM, at least in the configuration that we have considered.

6.3 MSSM

The MSSM has been analysed in chapter 4. However, for ease of the reader we reproduce here some of the relevant formulae. Referring to the mass matrix (4.13), the two mass eigenstate h and H, taken in the order $m_h < m_H$, are given by

$$h = \cos\delta\ h_v - \sin\delta\ h_v^\perp, \qquad H = \cos\delta\ h_v^\perp + \sin\delta\ h_v. \tag{6.20}$$

An expression, accurate for $m_H \gtrsim 400$ GeV and any value of $\tan\beta$, is

$$\sin\delta = -\frac{m_h^2}{\tan\beta m_H^2} + \frac{1-\tan^2\beta}{1+\tan^2\beta}\frac{m_Z^2}{\tan\beta m_H^2} + O(\frac{1}{m_H^4}). \tag{6.21}$$

From eq. (6.20) and the fixed form of the supersymmetric Yukawa couplings, all the Higgs couplings are

$$\frac{g_{hu\bar{u}}}{g_{hu\bar{u}}^{\rm SM}} = \cos\delta + \frac{\sin\delta}{\tan\beta}, \quad \frac{g_{hd\bar{d}}}{g_{hd\bar{d}}^{\rm SM}} = \cos\delta - \tan\beta\sin\delta, \quad \frac{g_{hVV}}{g_{hVV}^{\rm SM}} = \cos\delta. \tag{6.22}$$

$$\frac{g_{Hu\bar{u}}}{g_{hu\bar{u}}^{\rm SM}} = \sin\delta - \frac{\cos\delta}{\tan\beta}, \quad \frac{g_{Hd\bar{d}}}{g_{hd\bar{d}}^{\rm SM}} = \sin\delta + \tan\beta\cos\delta, \quad \frac{g_{HVV}}{g_{hVV}^{\rm SM}} = \sin\delta. \tag{6.23}$$

The isolines of $\sin\delta$ in the $(\tan\beta, m_H)$ are shown in figure 5.8, together with the currently excluded regions, at 95%C.L. and within the given assumptions, from the fit of the Higgs couplings and from the search for $A, H \to \tau\bar{\tau}$ [118].

To determine the sensitivity to $\sin\delta$ in the next LHC phase after 300 fb^{-1} of integrated luminosity we use the projected uncertainties of the measurements of the signal strengths of the Higgs boson by ATLAS [160] and CMS [161] given in table 6.1. The corresponding 95%C.L. exclusion line with SM central values is also shown in figure 6.3.

	ATLAS	CMS
$h \to \gamma\gamma$	0.16	0.15
$h \to ZZ$	0.15	0.11
$h \to WW$	0.30	0.14
$Vh \to Vb\bar{b}$	–	0.17
$h \to \tau\tau$	0.24	0.11
$h \to \mu\mu$	0.52	–

Table 6.1. Projected uncertainties of the measurements of the signal strengths of h at the 14 TeV LHC with 300 fb^{-1}.

The EWPT observables receive contributions from the complete Higgs system, determined in terms of $\sin\delta$ and the masses of all the physical states $m_h, m_H, m_A, m_{H^\pm}$. In the

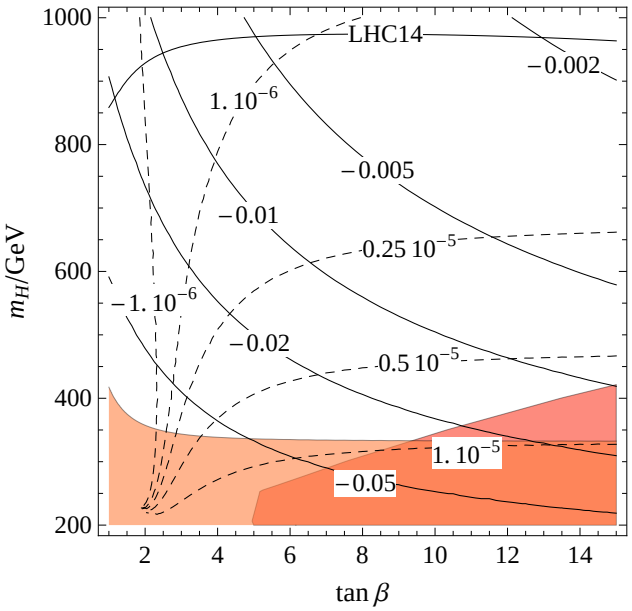

Figure 6.3. MSSM. Isolines of $\sin\delta$ (solid) and $\Delta\epsilon_1$ (dashed). The line LHC14 gives the 95%C.L. projected exclusion from the sensitivity on the signal strengths of h at ATLAS and CMS with 300 fb^{-1}. The orange region is excluded at 95%C.L. by current data for the signal strengths of h. The red region is excluded by CMS direct searches for $A, H \to \tau^+\tau^-$ [118].

formal limit of large $m_H, m_A, m_{H^\pm}$ at fixed $\sin\delta$ one would obtain the usual "infrared" logarithms of the same form as in eq.s (6.16). However, as seen in eq. (6.21), $\sin^2\delta$ vanishes as $1/m_H^4$. As a consequence the EWPT observables, at $m_H \gtrsim 400$ GeV, are not dominated by the mixing effect, as in the previous cases, but by the non-degeneracy of the $H, A, H^\pm$ states, which gives effects scaling like $1/m_H^2$. The explicit expressions of the $\Delta\varepsilon_i$ at leading order in $1/m_H^2$. To make this statement more precise, each Δe_i which defines $\Delta\varepsilon_i$ as in (1.10) is the sum of two contributions,

$$\Delta e_i = \sin^2\delta\big[\bar{e}_i(m_H) - \bar{e}_i(m_h)\big] + \delta e_i, \tag{6.24}$$

where the first is the usual term due to modified Higgs couplings with subtracted SM terms, whereas the second comes mainly from diagrams with exchange of the $H, A, H^\pm$ scalars, which are sensitive to their splittings. Notice that δe_i is not vanishing when $\sin\delta = 0$. As an example of this consider that, at tree-level, $m^2_{H^\pm} = m_A^2 + m_W^2$ independently of $\sin\delta$. This kind of splitting can be traced back to quartic terms in the scalar potential which feel the EWSB. In the decoupling limit (6.21) the first term of (6.24) is of order $1/m_H^4$. Therefore only δe_i gives the leading $O(1/m_H^2)$ contribution to the electro-weak parameters.

From an explicit computation of all the relevant diagrams, we find for the MSSM

$$\Delta e_1 = \frac{\alpha}{48\pi s_w^2}\frac{m_W^2 - \Delta m^2}{m_H^2} + O(\frac{m_W^4}{m_H^4}), \tag{6.25}$$

$$\Delta e_2 = -\frac{\alpha}{240\pi c_w^2}\frac{m_W^2}{m_H^2} + O(\frac{m_W^4}{m_H^4}), \tag{6.26}$$

$$\Delta e_3 = \frac{\alpha}{96\pi s_w^2}\frac{\Delta m^2 - 2m_W^2}{m_H^2} + O(\frac{m_W^4}{m_H^4}), \tag{6.27}$$

$$\Delta e_4 = \frac{\alpha}{120\pi c_w^2}\frac{m_W^2}{m_H^2} + O(\frac{m_W^4}{m_H^4}), \tag{6.28}$$

$$\Delta e_5 = \frac{\alpha(1+t_w^4)}{240\pi s_w^2}\frac{m_W^2}{m_H^2} + O(\frac{m_W^4}{m_H^4}), \tag{6.29}$$

where we have defined Δm^2 as the $O(1/m_H^2)$ splitting between m_A^2 and m_H^2

$$\Delta m^2 = \frac{m_h^2}{\tan^2\beta} + \frac{m_Z^2(3\tan^2\beta - 1)}{\tan^2\beta(1+\tan^2\beta)}, \tag{6.30}$$

as one can check diagonalizing (4.13).

Two main conclusions stem from the above formulae. First, notice that the leading contribution to $\Delta e_{1,3}$ comes from the Δm^2 splitting, whereas Δe_2 is not sensitive to it and vanishing in the custodial limit, *i.e.* Δe_2 (or U) feels Δm^2 only at $O(1/m_H^4)$ [162]. Second, the size of $\Delta e_{4,5}$ is comparable with that of $\Delta e_{1,2,3}$, *i.e.* with the Peskin-Takeuchi parameters. Differently from the case of the singlet here also Δe_4 is relevant in the computation of $\varepsilon_{2,3}$ because of the presence of $H^\pm$. The asymptotic formulae (6.25)-(6.29) are well justified in most of the parameter space of figure 6.3, where, however, $\Delta\varepsilon_1$ is computed without making the large-m_H approximation.

Numerically one sees the EWPTs play a marginal role for this configuration of the MSSM.

6.4 Discussion

Although with differences in the different cases, the main conclusion that we can draw, as emerging from figures 6.1,6.2 and 6.3, is that the precision measurements will have something significant to say for relevant configurations of every model that we have examined. This is particularly the case for the measurements of the Higgs couplings which will always be able to explore a significant portion of the different parameter spaces. On the contrary the role of precision measurements of the EW observables, even pushed at a dedicated Z-factory, appears mostly limited to the case of a "composite" Higgs boson.

Coming to the individual cases, the key feature that makes the CHM particularly sensitive to precision measurements, both of the Higgs couplings and of the EW observables, as shown in figure 6.1, is the possible separation between the symmetry breaking scale f and the mass of the "composite" resonances, represented in the linear model by the σ-particle. In spite of the crudeness of the model, adopted for its calculability, the relation of the scale f with the strength of the linear Higgs couplings to the vectors is not subject to significant model-dependent corrections [46]. More model dependent in a truly strongly interacting Higgs

boson are the EW observables, as also discussed in our description of indirect constraints on composite resonances (see section 3.3). Nevertheless the "infrared logarithms", which are the main feature in figure 6.1, will anyhow be there [18]. In turn this makes at least highly unlikely that an improved measurement of, say, the ε_1 parameter, at the level necessary to see an effect like in figure 6.1, could end up being consistent with the SM value.

As in the linear σ-model also the NMSSM can show a mixing of the Higgs boson with an $SU(2)$-singlet scalar, with two important, although formal, differences. One is that the mixing is controlled by the single heavier scale, i.e. the mass of the extra scalar. (See eq. (6.19)). The other difference is that this same mixing suppresses all the couplings of the Higgs boson to the vectors and to the fermions in the same way. These differences are at the origin of the relatively weaker explorative power in figure 6.2, with respect to figure 6.1, by the precision measurements. An absolute measurement of the invisible Higgs width would be the key here, as possible at an e^+e^- collider [157]. Another possibility is offered by the measurements of the triple Higgs coupling, with conceivable deviations of relative order unity from the SM [4], against a 30% 1σ accuracy foreseen at HL-LHC.

The third case that we have examined is the MSSM with s-particles sufficiently heavy that their virtual exchange does not influence the precision measurements and with the extra scalars, although heavier than the observed Higgs state, that could be the lightest new particles around. In this case the key features that makes powerful the measurements of the Higgs couplings are: i) their distortion by the mixing between h_v and $h_v^\perp$, different for vectors, the top quark or the bottom/τ; ii) the dependence of the mixing angle δ on m_H and $\tan\beta$ given in eq. (6.21) and shown in figure 6.3.

Given the configuration of the models that we are considering, the competitor of the precision measurements is the direct search for extra scalars, be they new Higgs particles or some strongly interacting new states. This is manifest, for example, in figures 6.2 and 6.3, where exclusion regions due to direct heavy Higgs searches are already present. It would be interesting to know as reliably as possible the future sensitivity of the LHC, including the high luminosity phase, in the parameter spaces at least of the MSSM and the NMSSM, i.e. in the planes of figures 6.2 and 6.3, where in fact the properties of the extra scalars are precisely defined. It appears, however, that the precision measurements will anyhow play an important complementary role.

Summary and conclusions

Following the naturalness principle as a guideline for addressing the Hierarchy Problem we have considered a series of motivated models for the Fermi scale. We have shown that in order to have a natural Higgs boson, the SM should undergo some important deformations which generally predict physics at the TeV scale. The beautiful (and robust) connection between naturalness and physics at the TeV scale has been under challenge since the LEP era and the null results from the first run of the LHC have put it in a quite uncomfortable situation. Nevertheless, it does not seem to us yet the right moment to shift towards more radical approaches, some of which have been discussed in the introductory chapter. Indeed, as this thesis work should have shown, reasonably natural scenarios for the weak scale are still allowed by direct and indirect constraints, with LHC14 ready to probe a large part of their parameter spaces.

While detailed conclusions have been already discussed in the ending sections of chapters 2, 3, 4, 5 and 6, here we summarize again some of the most relevant points. Probably one of the most interesting (general) conclusions that can be drawn is that natural extensions of the SM can be still both weakly or strongly-coupled, despite the fact that the increasing amount of precision data (last but not least the Higgs couplings themselves) might have led to quickly exclude the latter.

In chapter 2 we outlined the basic concepts of the Composite Higgs paradigm. Relying on naive dimensional analysis we estimated the size of the Higgs mass and the corresponding tuning in different models based on several representations of the composite fermions. In general the most conservative way to achieve acceptable levels of tuning is to disentangle the scale of bosonic, m_ρ, and fermionic, m_ψ, scales. If the overall fermionic scale is low, *i.e.* close to f, the tuning is minimal and light composite fermions are expected below the TeV scale (with a scale f saturating the lower bound from indirect searches). Allowing for more fine-tuning two possibilities emerged. The first one is offered by models with double tuning with fermions in **5**, **10** or **4** of SO(5). They provide a 125 GeV Higgs even for an overall heavy fermionic scale $m_\psi \sim 5f$ if at least one top partner is light. The second is obtained with fermions in **14** and a composite t_R. In this case the Higgs mass can be light even *without* light partners, with 125 GeV obtained just by tuning.

Motivated by the fact that natural CHMs predict light top partners, in chapter 3 we analysed the constraints on such scenario coming from precision measurements. We focused on the class of doubly tuned models with light composite fermions in the **5**, **10** or **4** of SO(5) and with different flavour structures: $U(3)^3$, $U(2)^3$ and anarchy as introduced in chapter 1.

Models with fermions in the **4** are highly constrained by EWPTs, most notably the distortion of the $Zb\bar{b}$ coupling, and they are disfavoured irrespectively of the flavour structure. Anarchic models suffer severe bounds from flavour, especially in the Kaon sector. Only assuming that some coefficients, in principle of order unity, are sufficiently small, they can be reconciled with existing bounds. A $U(3)^3$ flavour symmetry with significantly composite left-handed quarks is disfavoured by EWPTs, while in the opposite case, with composite right-handed quarks, dijet constraints from LHC are already probing the natural parameter space. Instead, a minimally broken $U(2)^3$ symmetry has flavour bounds milder than $U(3)^3$ and negligible constraints from EWPTs given the different degree of compositeness of the first two and the third generation of quarks.

In chapter 4 we introduced Natural Superymmetry. Despite the amount of tuning of the MSSM, we studied its phenomenology in light of the Higgs mass and BRs measurements. It turned out that the Higgs sector of the MSSM can be meaningfully constrained by the Higgs coupling fit. Over the full range of $\tan\beta$ a heavy extra Higgs lighter than 350 GeV is excluded at 95% CL, at least for the configuration we have considered. However, the possibility of an extra CP-even Higgs below 125 GeV is still allowed by current data, although in a squeezed region of the parameter space.

The NMSSM as a motivated option for natural SUSY has been discussed in chapter 5. After a brief general discussion, we quantified the impact of Higgs couplings on the NMSSM extended Higgs sector. With some simplifying assumptions we focused on spectra with only two light CP-even scalars and the third one decoupled. Contrary to the case where the doublet-like state is light, the case with a light singlet-like state (dubbed H-decoupled scenario) is poorly constrained by the fit to the Higgs couplings. The H decoupled case can be probed by direct searches, with hh and ZZ as two prominent decay channels for the heavy extra Higgs. Also the possible enhancement of the triple Higgs coupling could be a signature of this scenario. Both the S and H decoupled cases allow for an extra scalar lighter than 125 GeV in regions not excluded by LHC and LEP.

In the final chapter we have discussed a comparison of precision tests in specific examples of models presented in this thesis. We studied the overall impact of Higgs and EW observables on a few fully calculable models. Both existing data and projections of future experiments have been used, such as LHC14 at 300/fb and also HL-LHC and TLEP. In all the models under consideration, the Higgs couplings will have a significant impact regardless of the weakly or strongly-coupled nature of the model, while EWPTs seem particularly relevant only for the latter.

Bibliography

[1] M. Redi and A. Tesi, JHEP **1210**, 166 (2012), 1205.0232.

[2] G. Panico, M. Redi, A. Tesi, and A. Wulzer, JHEP **1303**, 051 (2013), 1210.7114.

[3] R. Barbieri, D. Buttazzo, F. Sala, D. M. Straub, and A. Tesi, JHEP **1305**, 069 (2013), 1211.5085.

[4] R. Barbieri, D. Buttazzo, K. Kannike, F. Sala, and A. Tesi, Phys.Rev. **D87**, 115018 (2013), 1304.3670.

[5] R. Barbieri, D. Buttazzo, K. Kannike, F. Sala, and A. Tesi, Phys. Rev. D 88, **055011** (2013), 1307.4937.

[6] R. Barbieri and A. Tesi, Phys. Rev. D **89**, 055019 (2014).

[7] ATLAS Collaboration, G. Aad *et al.*, Phys.Lett. **B716**, 1 (2012), 1207.7214.

[8] CMS Collaboration, S. Chatrchyan *et al.*, Phys.Lett. **B716**, 30 (2012), 1207.7235.

[9] F. Englert and R. Brout, Phys.Rev.Lett. **13**, 321 (1964).

[10] P. W. Higgs, Phys.Rev.Lett. **13**, 508 (1964).

[11] ALEPH Collaboration, DELPHI Collaboration, L3 Collaboration, OPAL Collaboration, SLD Collaboration, LEP Electroweak Working Group, SLD Electroweak Group, SLD Heavy Flavour Group, S. Schael *et al.*, Phys.Rept. **427**, 257 (2006), hep-ex/0509008.

[12] G. Altarelli and R. Barbieri, Phys.Lett. **B253**, 161 (1991).

[13] R. Barbieri, M. Frigeni, and F. Caravaglios, Phys.Lett. **B279**, 169 (1992).

[14] R. Barbieri, A. Pomarol, R. Rattazzi, and A. Strumia, Nucl.Phys. **B703**, 127 (2004), hep-ph/0405040.

[15] M. E. Peskin and T. Takeuchi, Phys.Rev. **D46**, 381 (1992).

[16] M. Baak *et al.*, Eur.Phys.J. **C72**, 2205 (2012), 1209.2716.

[17] M. Ciuchini, E. Franco, S. Mishima, and L. Silvestrini, JHEP **1308**, 106 (2013), 1306.4644.

[18] R. Barbieri, B. Bellazzini, V. S. Rychkov, and A. Varagnolo, Phys.Rev. **D76**, 115008 (2007), 0706.0432.

[19] N. Cabibbo, Phys.Rev.Lett. **10**, 531 (1963).

[20] M. Kobayashi and T. Maskawa, Prog.Theor.Phys. **49**, 652 (1973).

[21] L. Wolfenstein, Phys.Rev.Lett. **51**, 1945 (1983).

[22] R. Barbieri, D. Buttazzo, F. Sala, and D. M. Straub, (2014), 1402.6677.

[23] S. Aoki *et al.*, (2013), 1310.8555.

[24] CKMfitter Collaboration, (2012).

[25] W. Buchmuller and D. Wyler, Nucl.Phys. **B268**, 621 (1986).

[26] G. Isidori, Y. Nir, and G. Perez, Ann.Rev.Nucl.Part.Sci. **60**, 355 (2010), 1002.0900.

[27] R. Barbieri, G. Isidori, J. Jones-Perez, P. Lodone, and D. M. Straub, Eur.Phys.J. **C71**, 1725 (2011), 1105.2296.

[28] R. Barbieri, D. Buttazzo, F. Sala, and D. M. Straub, JHEP **1207**, 181 (2012), 1203.4218.

[29] P. P. Giardino, K. Kannike, I. Masina, M. Raidal, and A. Strumia, (2013), 1303.3570.

[30] A. Falkowski, F. Riva, and A. Urbano, JHEP **1311**, 111 (2013), 1303.1812.

[31] B. Grinstein, C. W. Murphy, D. Pirtskhalava, and P. Uttayarat, (2013), 1401.0070.

[32] D. Buttazzo *et al.*, JHEP **1312**, 089 (2013), 1307.3536.

[33] A. Sakharov, Pisma Zh.Eksp.Teor.Fiz. **5**, 32 (1967).

[34] A. V. Manohar, (1996), hep-ph/9606222.

[35] D. B. Kaplan, (1995), nucl-th/9506035.

[36] S. R. Coleman and E. J. Weinberg, Phys.Rev. **D7**, 1888 (1973).

[37] M. Farina, D. Pappadopulo, and A. Strumia, JHEP **1308**, 022 (2013), 1303.7244.

[38] S. Weinberg, Phys.Rev.Lett. **59**, 2607 (1987).

[39] S. Weinberg, Rev.Mod.Phys. **61**, 1 (1989).

[40] V. Agrawal, S. M. Barr, J. F. Donoghue, and D. Seckel, Phys.Rev. **D57**, 5480 (1998), hep-ph/9707380.

[41] D. B. Kaplan and H. Georgi, Phys.Lett. **B136**, 183 (1984).

[42] H. Georgi and D. B. Kaplan, Phys.Lett. **B145**, 216 (1984).

[43] S. R. Coleman, J. Wess, and B. Zumino, Phys.Rev. **177**, 2239 (1969).

[44] J. Callan, Curtis G., S. R. Coleman, J. Wess, and B. Zumino, Phys.Rev. **177**, 2247 (1969).

[45] K. Agashe, R. Contino, and A. Pomarol, Nucl.Phys. **B719**, 165 (2005), hep-ph/0412089.

[46] G. Giudice, C. Grojean, A. Pomarol, and R. Rattazzi, JHEP **0706**, 045 (2007), hep-ph/0703164.

[47] R. Contino, L. Da Rold, and A. Pomarol, Phys.Rev. **D75**, 055014 (2007), hep-ph/0612048.

[48] A. Pomarol and F. Riva, JHEP **1208**, 135 (2012), 1205.6434.

[49] D. B. Kaplan, Nucl.Phys. **B365**, 259 (1991).

[50] R. Contino, T. Kramer, M. Son, and R. Sundrum, JHEP **0705**, 074 (2007), hep-ph/0612180.

[51] O. Matsedonskyi, G. Panico, and A. Wulzer, JHEP **1301**, 164 (2013), 1204.6333.

[52] J. Mrazek *et al.*, Nucl.Phys. **B853**, 1 (2011), 1105.5403.

[53] G. Panico and A. Wulzer, JHEP **1109**, 135 (2011), 1106.2719.

[54] D. Marzocca, M. Serone, and J. Shu, JHEP **1208**, 013 (2012), 1205.0770.

[55] L. Randall and R. Sundrum, Phys.Rev.Lett. **83**, 3370 (1999), hep-ph/9905221.

[56] N. Arkani-Hamed, M. Porrati, and L. Randall, JHEP **0108**, 017 (2001), hep-th/0012148.

[57] R. Rattazzi and A. Zaffaroni, JHEP **0104**, 021 (2001), hep-th/0012248.

[58] G. Panico, M. Serone, and A. Wulzer, Nucl.Phys. **B762**, 189 (2007), hep-ph/0605292.

[59] G. Panico, E. Ponton, J. Santiago, and M. Serone, Phys.Rev. **D77**, 115012 (2008), 0801.1645.

[60] C. Csaki, A. Falkowski, and A. Weiler, JHEP **0809**, 008 (2008), 0804.1954.

[61] N. Arkani-Hamed, A. G. Cohen, and H. Georgi, Phys.Lett. **B513**, 232 (2001), hep-ph/0105239.

[62] M. Piai, A. Pierce, and J. G. Wacker, (2004), hep-ph/0405242.

[63] H.-C. Cheng, J. Thaler, and L.-T. Wang, JHEP **0609**, 003 (2006), hep-ph/0607205.

[64] S. De Curtis, M. Redi, and A. Tesi, JHEP **1204**, 042 (2012), 1110.1613.

[65] T. Das, G. Guralnik, V. Mathur, F. Low, and J. Young, Phys.Rev.Lett. **18**, 759 (1967).

[66] R. Contino, (2010), 1005.4269.

[67] R. Barbieri and G. Giudice, Nucl.Phys. **B306**, 63 (1988).

[68] CERN Report No. ATLAS-CONF-2012-130, 2012 (unpublished).

[69] CERN Report No. CMS-PAS-B2G-12-003, 2012 (unpublished).

[70] A. De Simone, O. Matsedonskyi, R. Rattazzi, and A. Wulzer, JHEP **1304**, 004 (2013), 1211.5663.

[71] Y. Grossman and M. Neubert, Phys.Lett. **B474**, 361 (2000), hep-ph/9912408.

[72] S. J. Huber and Q. Shafi, Phys.Lett. **B498**, 256 (2001), hep-ph/0010195.

[73] T. Gherghetta and A. Pomarol, Nucl.Phys. **B586**, 141 (2000), hep-ph/0003129.

[74] K. Agashe, G. Perez, and A. Soni, Phys.Rev. **D71**, 016002 (2005), hep-ph/0408134.

[75] M. Blanke, A. J. Buras, B. Duling, S. Gori, and A. Weiler, JHEP **0903**, 001 (2009), 0809.1073.

[76] M. Bauer, S. Casagrande, U. Haisch, and M. Neubert, JHEP **1009**, 017 (2010), 0912.1625.

[77] B. Keren-Zur *et al.*, Nucl.Phys. **B867**, 429 (2013), 1205.5803.

[78] G. Cacciapaglia *et al.*, JHEP **0804**, 006 (2008), 0709.1714.

[79] R. Barbieri, G. Isidori, and D. Pappadopulo, JHEP **0902**, 029 (2009), 0811.2888.

[80] M. Redi and A. Weiler, JHEP **1111**, 108 (2011), 1106.6357.

[81] K. Agashe, R. Contino, L. Da Rold, and A. Pomarol, Phys.Lett. **B641**, 62 (2006), hep-ph/0605341.

[82] N. Vignaroli, Phys.Rev. **D86**, 115011 (2012), 1204.0478.

[83] W. Altmannshofer and D. M. Straub, JHEP **1208**, 121 (2012), 1206.0273.

[84] G. Isidori, J. F. Kamenik, Z. Ligeti, and G. Perez, Phys.Lett. **B711**, 46 (2012), 1111.4987.

[85] L. Calibbi, Z. Lalak, S. Pokorski, and R. Ziegler, JHEP **1207**, 004 (2012), 1204.1275.

[86] A. J. Buras, C. Grojean, S. Pokorski, and R. Ziegler, JHEP **1108**, 028 (2011), 1105.3725.

[87] K. Agashe, A. Azatov, and L. Zhu, Phys.Rev. **D79**, 056006 (2009), 0810.1016.

[88] O. Gedalia, G. Isidori, and G. Perez, Phys.Lett. **B682**, 200 (2009), 0905.3264.

[89] R. Barbieri, D. Buttazzo, F. Sala, and D. M. Straub, JHEP **1210**, 040 (2012), 1206.1327.

[90] CERN Report No. ATLAS-CONF-2012-088, 2012 (unpublished).

[91] Report No. CMS-PAS-EXO-12-016, 2012 (unpublished).

[92] M. Redi, Eur.Phys.J. **C72**, 2030 (2012), 1203.4220.

[93] O. Domenech, A. Pomarol, and J. Serra, Phys.Rev. **D85**, 074030 (2012), 1201.6510.

[94] W. Altmannshofer *et al.*, JHEP **0901**, 019 (2009), 0811.1214.

[95] S. P. Martin, (1997), hep-ph/9709356.

[96] M. Papucci, J. T. Ruderman, and A. Weiler, JHEP **1209**, 035 (2012), 1110.6926.

[97] S. Dimopoulos and G. Giudice, Phys.Lett. **B357**, 573 (1995), hep-ph/9507282.

[98] A. G. Cohen, D. Kaplan, and A. Nelson, Phys.Lett. **B388**, 588 (1996), hep-ph/9607394.

[99] R. Barbieri and D. Pappadopulo, JHEP **0910**, 061 (2009), 0906.4546.

[100] CERN Report No. ATLAS-CONF-2013-047, 2013 (unpublished).

[101] M. S. Carena, J. Espinosa, M. Quiros, and C. Wagner, Phys.Lett. **B355**, 209 (1995), hep-ph/9504316.

[102] A. Djouadi, Phys.Rept. **459**, 1 (2008), hep-ph/0503173.

[103] R. T. D'Agnolo, E. Kuflik, and M. Zanetti, JHEP **1303**, 043 (2013), 1212.1165.

[104] R. S. Gupta, M. Montull, and F. Riva, (2012), 1212.5240.

[105] ATLAS Collaboration, F. Hubaut. Talk at the Moriond 2013 EW session.
ATLAS Collaboration, E. Mountricha. Talk at the Moriond 2013 QCD session.
ATLAS Collaboration, V. Martin. Talk at the Moriond 2013 EW session.
ATLAS Collaboration, ATLAS-CONF-2013-009.
ATLAS Collaboration, ATLAS-CONF-2013-010.
ATLAS Collaboration, ATLAS-CONF-2013-011.
ATLAS Collaboration, ATLAS-CONF-2013-012.
ATLAS Collaboration, ATLAS-CONF-2013-013.
ATLAS Collaboration, ATLAS-CONF-2013-014.
ATLAS Collaboration, ATLAS-CONF-2013-030.

[106] CMS Collaboration, G. Gomez-Ceballos. Talk at the Moriond 2013 EW session.
CMS Collaboration, M. Shen. Talk at the Moriond 2013 QCD session.
CMS Collaboration, B. Mansoulie. Talk at the Moriond 2013 EW session.
CMS Collaboration, V. Dutta. Talk at the Moriond 2013 EW session.
CMS Collaboration, CMS-PAS-HIG-13-001.
CMS Collaboration, CMS-PAS-HIG-13-002.
CMS Collaboration, CMS-PAS-HIG-13-003.
CMS Collaboration, CMS-PAS-HIG-13-004.
CMS Collaboration, CMS-PAS-HIG-13-006.
CMS Collaboration, CMS-PAS-HIG-13-009.

[107] CDF and D0 Collaborations, L. Živković, Talk at the Moriond 2013 EW session.

[108] A. Djouadi and J. Quevillon, (2013), 1304.1787.

[109] L. Maiani, A. Polosa, and V. Riquer, Phys.Lett. **B718**, 465 (2012), 1209.4816.

[110] C. Cheung, S. D. McDermott, and K. M. Zurek, JHEP **1304**, 074 (2013), 1302.0314.

[111] A. Azatov and J. Galloway, Int.J.Mod.Phys. **A28**, 1330004 (2013), 1212.1380.

[112] D. Carmi, A. Falkowski, E. Kuflik, T. Volansky, and J. Zupan, JHEP **1210**, 196 (2012), 1207.1718.

[113] LHC Higgs Cross Section Working Group, S. Dittmaier *et al.*, (2011), 1101.0593, Updates on https://twiki.cern.ch/twiki/bin/view/LHCPhysics/CrossSections.

[114] C. Anastasiou, S. Bucherer, and Z. Kunszt, JHEP **0910**, 068 (2009), 0907.2362.

[115] M. Spira, A. Djouadi, D. Graudenz, and P. Zerwas, Nucl.Phys. **B453**, 17 (1995), hep-ph/9504378.

[116] M. Spira, (1995), hep-ph/9510347.

[117] A. Arbey, M. Battaglia, and F. Mahmoudi, Phys.Rev. **D88**, 015007 (2013), 1303.7450.

[118] CMS Collaboration, (2012), CMS-PAS-HIG-12-050.

[119] LEP Higgs Working Group for Higgs boson searches, (2001), hep-ex/0107034.

[120] P. Fayet, Nucl.Phys. **B90**, 104 (1975).

[121] U. Ellwanger, C. Hugonie, and A. M. Teixeira, Phys.Rept. **496**, 1 (2010), 0910.1785.

[122] R. Barbieri, L. J. Hall, Y. Nomura, and V. S. Rychkov, Phys.Rev. **D75**, 035007 (2007), hep-ph/0607332.

[123] L. J. Hall, D. Pinner, and J. T. Ruderman, JHEP **1204**, 131 (2012), 1112.2703.

[124] K. Agashe, Y. Cui, and R. Franceschini, JHEP **1302**, 031 (2013), 1209.2115.

[125] T. Gherghetta, B. von Harling, A. D. Medina, and M. A. Schmidt, JHEP **1302**, 032 (2013), 1212.5243.

[126] J. Espinosa and M. Quiros, Phys.Lett. **B279**, 92 (1992).

[127] M. Masip, R. Munoz-Tapia, and A. Pomarol, Phys.Rev. **D57**, R5340 (1998), hep-ph/9801437.

[128] R. Barbieri, L. J. Hall, A. Y. Papaioannou, D. Pappadopulo, and V. S. Rychkov, JHEP **0803**, 005 (2008), 0712.2903.

[129] R. Harnik, G. D. Kribs, D. T. Larson, and H. Murayama, Phys.Rev. **D70**, 015002 (2004), hep-ph/0311349.

[130] S. Chang, C. Kilic, and R. Mahbubani, Phys.Rev. **D71**, 015003 (2005), hep-ph/0405267.

[131] A. Birkedal, Z. Chacko, and Y. Nomura, Phys.Rev. **D71**, 015006 (2005), hep-ph/0408329.

[132] A. Delgado and T. M. Tait, JHEP **0507**, 023 (2005), hep-ph/0504224.

[133] T. Gherghetta, B. von Harling, and N. Setzer, JHEP **1107**, 011 (2011), 1104.3171.

[134] N. Craig, D. Stolarski, and J. Thaler, JHEP **1111**, 145 (2011), 1106.2164.

[135] C. Csaki, Y. Shirman, and J. Terning, Phys.Rev. **D84**, 095011 (2011), 1106.3074.

[136] E. Hardy, J. March-Russell, and J. Unwin, JHEP **1210**, 072 (2012), 1207.1435.

[137] K. Choi, S. H. Im, K. S. Jeong, and M. Yamaguchi, JHEP **1302**, 090 (2013), 1211.0875.

[138] J. Baglio *et al.*, JHEP **1304**, 151 (2013), 1212.5581.

[139] ALEPH Collaboration, DELPHI Collaboration, L3 Collaboration, OPAL Collaboration, LEP Working Group for Higgs Boson Searches, S. Schael *et al.*, Eur.Phys.J. **C47**, 547 (2006), hep-ex/0602042.

[140] M. J. Dolan, C. Englert, and M. Spannowsky, JHEP **1210**, 112 (2012), 1206.5001.

[141] (2012), **ATLAS Collaboration**, ATL-PHYS-PUB-2012-004.

[142] F. Goertz, A. Papaefstathiou, L. L. Yang, and J. Zurita, JHEP **1306**, 016 (2013), 1301.3492.

[143] M. Misiak *et al.*, Phys.Rev.Lett. **98**, 022002 (2007), hep-ph/0609232.

[144] M. Badziak, M. Olechowski, and S. Pokorski, JHEP **1306**, 043 (2013), 1304.5437.

[145] CMS Collaboration, CMS-PAS-HIG-13-016.

[146] M. Gouzevitch *et al.*, JHEP **1307**, 148 (2013), 1303.6636.

[147] CMS Collaboration, S. Chatrchyan *et al.*, Eur.Phys.J. **C73**, 2469 (2013), 1304.0213.

[148] CMS Collaboration, CERN Report No. CMS-PAS-HIG-13-032, 2014 (unpublished).

[149] CMS Collaboration, S. Chatrchyan *et al.*, Phys.Rev. **D89**, 092007 (2014), 1312.5353.

[150] R. Barbieri and A. Strumia, (2000), hep-ph/0007265.

[151] R. Contino, D. Marzocca, D. Pappadopulo, and R. Rattazzi, JHEP **1110**, 081 (2011), 1109.1570.

[152] R. Contino, C. Grojean, D. Pappadopulo, R. Rattazzi, and A. Thamm, JHEP **1402**, 006 (2014), 1309.7038.

[153] A. Orgogozo and S. Rychkov, JHEP **1306**, 014 (2013), 1211.5543.

[154] ATLAS, ATL-PHYS-PUB-2013-014 (2013).

[155] CMS Collaboration, (2013), 1307.7135.

[156] L. G. Almeida, S. J. Lee, S. Pokorski, and J. D. Wells, Phys.Rev. **D89**, 033006 (2014), 1311.6721.

[157] TLEP Design Study Working Group, M. Bicer *et al.*, JHEP **1401**, 164 (2014), 1308.6176.

[158] S. Mishima, talk at the 6th TLEP worskhop .

[159] M. Ciuchini, E. Franco, S. Mishima, and L. Silvestrini, in preparation .

[160] T. ATLAS-Collaboration, CERN Report No. ATL-PHYS-PUB-2012-001, 2012 (unpublished).

[161] CMS Collaboration, CERN Report No. CMS-NOTE-2012-006. CERN-CMS-NOTE-2012-006, 2012 (unpublished).

[162] H. E. Haber and D. O'Neil, Phys.Rev. **D83**, 055017 (2011), 1011.6188.